

Batch and repeated-batch oil production by microalgae

Giulia Benvenuti

Thesis committee

Promotor

Prof. Dr R.H. Wijffels
Professor of Bioprocess Engineering
Wageningen University

Co-promotors

Dr R. Bosma
AlgaePARC operational manager, Bioprocess Engineering
Wageningen University

Dr M.J. Barbosa
Associate professor, Bioprocess Engineering
Wageningen University

Other members

Prof. Dr V. Fogliano, Wageningen University
Dr P. Uronen, Neste, Provo, Finland
Prof. M.R. Tredici, Florence University, Italy
Dr I.M. van der Meer, Wageningen University

This research was conducted under the auspices of the Graduate School VLAG (Advanced studies in Food Technology, Agrobiotechnology, Nutrition and Health Sciences).

Batch and repeated-batch oil production by microalgae

Giulia Benvenuti

Thesis

submitted in fulfilment of the requirements for the degree of doctor
at Wageningen University

by the authority of the Rector Magnificus

Prof. Dr. A.P.J. Mol

in the presence of the

Thesis Committee appointed by the Academic Board

to be defended in public

on Friday 4 March 2016

at 1:30 p.m. in the Aula.

G. Benvenuti

Batch and repeated-batch oil production by microalgae,
150 pages.

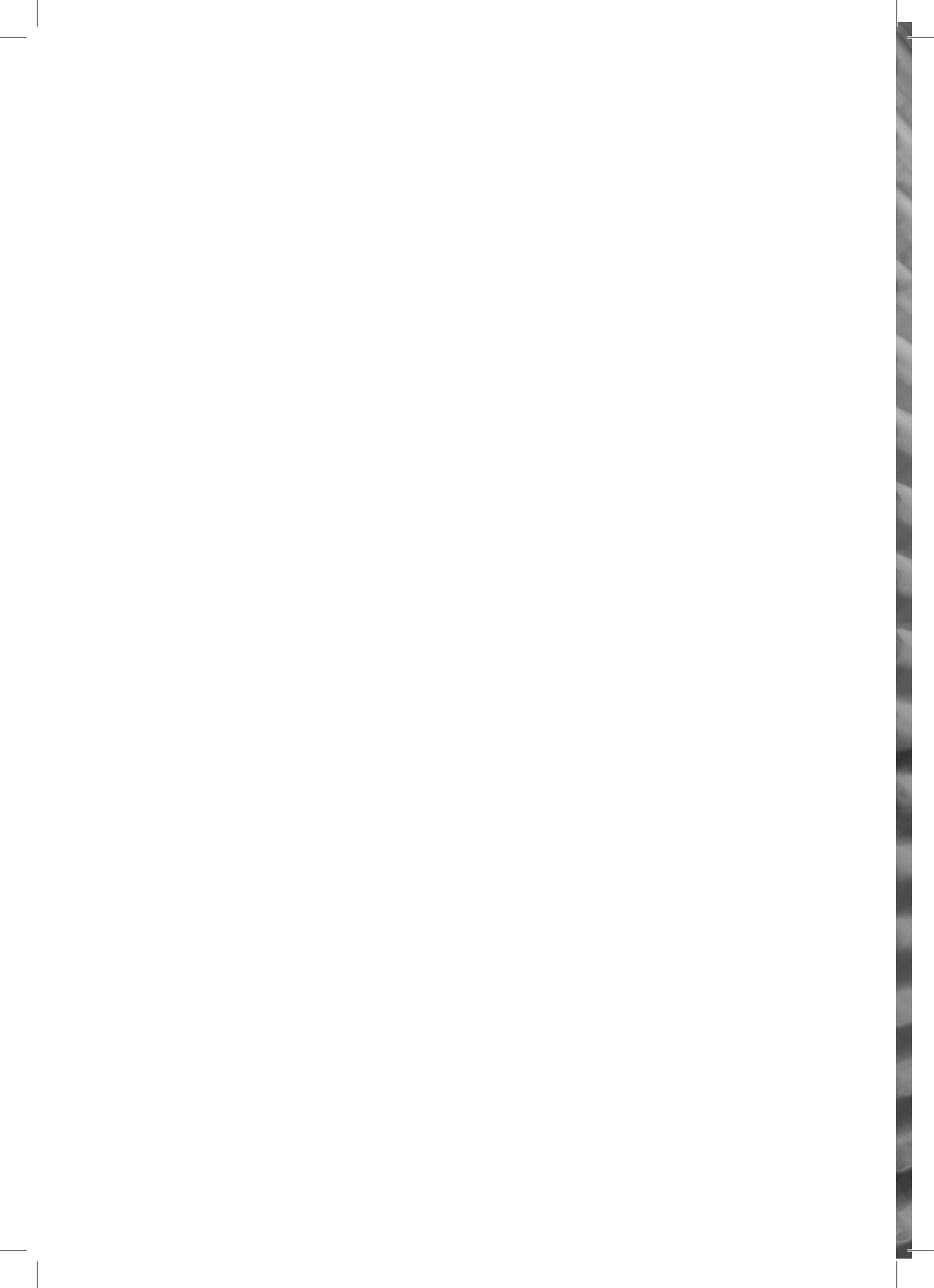
PhD thesis, Wageningen University, Wageningen, NL (2016)
With references, with summary in English

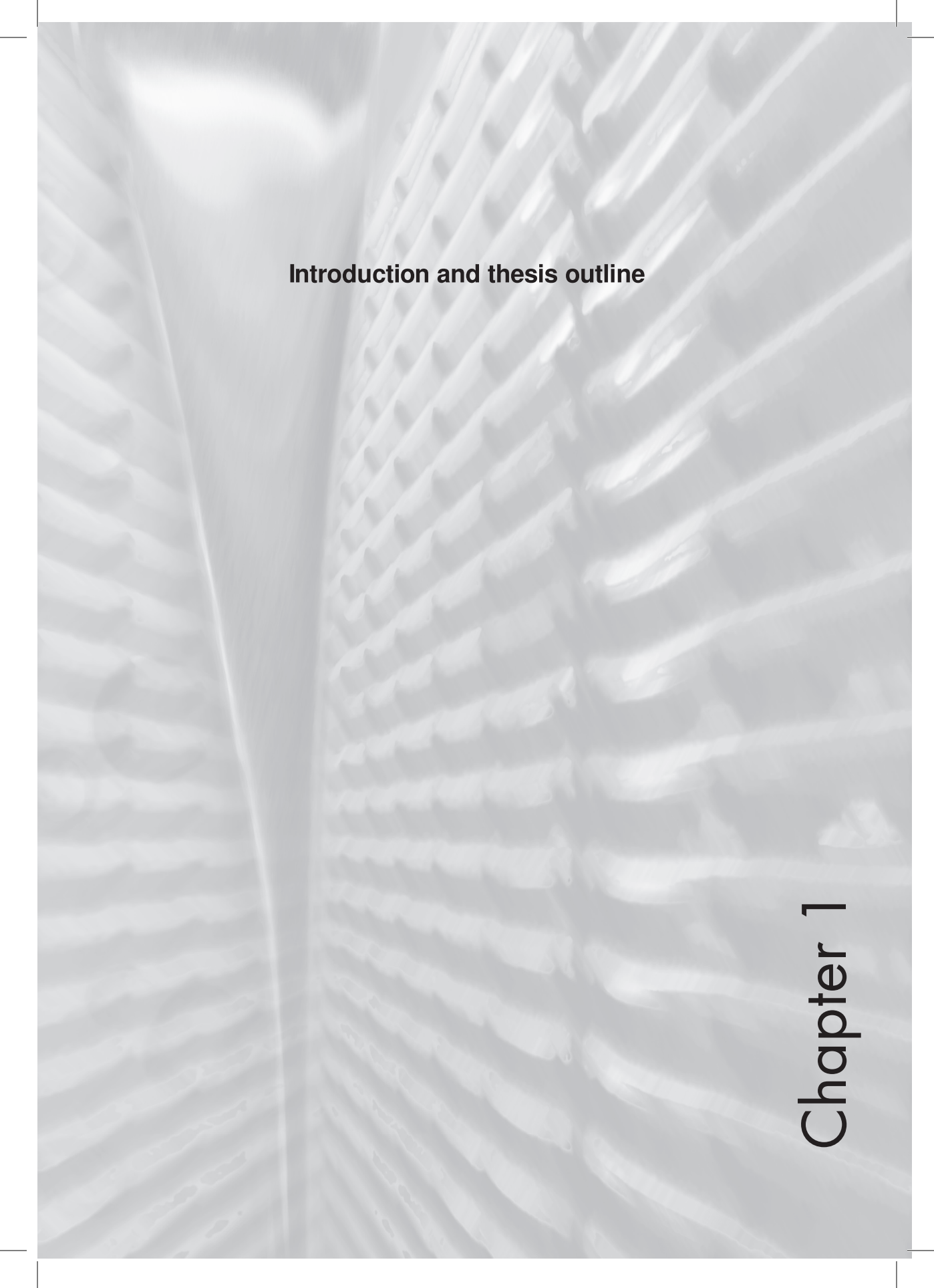
ISBN 978-94-6257-658-2

Se fu vista da tanti così bella
il merito è d' Omero

- Alekos Panagoulis -

Chapter 1	9
Introduction and thesis outline	
<hr/>	
Chapter 2	17
Selecting microalgae with high lipid productivity and photosynthetic activity under nitrogen-starvation	
<hr/>	
Chapter 3	35
Microalgal triglyceride production in outdoor batch-operated tubular PBRs	
<hr/>	
Chapter 4	55
Batch and repeated-batch microalgal triglyceride production in lab-scale and outdoor photobioreactors	
<hr/>	
Chapter 5	75
Microalgal TAG production strategies: why batch beats repeated-batch	
<hr/>	
Chapter 6	115
General discussion	
<hr/>	
References	131
Summary	139
Acknowledgements	143
About the author	147
List of publications	148
Overview of completed training activities	149





Introduction and thesis outline

Chapter 1

I.1 Commercial applications of microalgae

Microalgae are eukaryotic unicellular organisms (Fig. 1.1) capable to convert light energy into chemical energy through photosynthesis. Microalgae produce a wide range of metabolites (e.g. proteins, lipids, carbohydrates, pigments and/or vitamins) that have a broad range of potential applications. Currently, microalgae are used as aquaculture feed and for the production of high-value products for human health and cosmetics (Table 1.1), thus being limited to low market volumes. No commercial applications of microalgae can be found yet for the production of bulk commodities (i.e. chemicals, food and fuels).

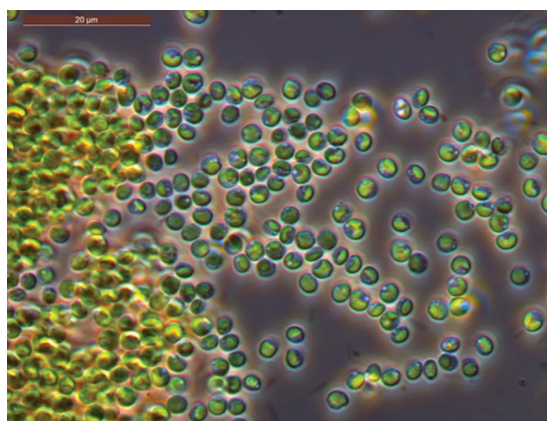


Figure 1.1 Microscopy photograph of the microalga *Nannochloropsis* sp..

Table 1.1 Commercial applications of microalgae and cyanobacteria. From Spolaore et al. (2006).

Species	Product/Activity	Application(s)
Anabena	N ₂ fixation	Biofertilizers, growth promoting substances
Arthrospira platensis	Proteins, PUFAs, vitamins, phycocyanin	Human health, animal feed additive, cosmetics
Chaetoceros muelleri	PUFAs	Aquaculture feed
Chlorella spp.	Proteins, PUFAs, β-1, 3-glucans	Human health, animal feed additive, cosmetics
Dunaliella salina	β-carotene	Human health, aquaculture feed, cosmetics
Haematococcus pluvialis	Astaxanthin	Human health, aquaculture feed
Isochrysis	PUFAs	Aquaculture feed
Nannochloropsis spp.	PUFAs	Aquaculture feed, cosmetics
Nostoc	Vitamin B12, auxins, N ₂ fixation	Biofertilizers, growth promoting substances
Phaeodactylum	PUFAs	Aquaculture feed
Thalassiosira pseudonana	PUFAs	Aquaculture feed
Tetraselmis suecica	Proteins	Aquaculture feed

1.2 Microalgal triacylglycerides as sustainable and renewable feedstock for the commodity industries

Triacylglycerides (TAGs) are a class of glycerol lipids constituted of three fatty acyl groups attached to a glycerol backbone. TAGs are largely used by the petro-, oleo-chemical and food industries in a wide range of applications (e.g. detergents, lubricants, solvents, biodiesel, food structure and taste) (Royal Dutch Shell Group 1983; German 1999; Rupilius and Ahmad 2007). These TAGs are commonly derived from fossil reserves and terrestrial crops (e.g. palm, soybean, rapeseed, jatropha). However, the oscillations in crude-oil price and the limited availability of arable lands have determined a renewed interest in the development of sustainable alternative production platforms. Microalgal TAGs have drawn much attention from industry as potential supplement or replacement for the current commodity feedstocks (Chisti 2007; Draaisma et al. 2013). In addition, higher areal productivities may be achieved with microalgae compared to terrestrial plants (Mata et al. 2010). The reason is that most of the microalgal biomass can be used (e.g. no roots, leaves etc.) compared to terrestrial plants, thus allowing higher land coverage (Tredici 2010). Furthermore, as microalgae are cultivated in photobioreactors, they do not require arable lands and can be grown in seawater, brackish or wastewater.

Despite the potential advantages offered by microalgal TAGs, these are not yet economically feasible for the commodity industries due to the high production costs (Griffiths and Harrison 2009; Wijffels and Barbosa 2010; Norsker et al. 2011; Ación et al. 2012). In order to reduce the production costs, microalgal TAG productivity should be further increased (Griffiths and Harrison 2009; Wijffels and Barbosa 2010; Norsker et al. 2011; Ación et al. 2012). Higher productivities would indeed result in a higher production per unit of time on the same ground area. To achieve high TAG productivities, cultivation parameters such as production strain and operational strategy need to be optimized.

1.3 Species-specific photosynthetic activity under nitrogen starvation

TAGs are accumulated in microalgae under unbalanced growth conditions, such as nutrient starvation/limitation (Klok et al. 2013; Benvenuti et al. 2014; San Pedro et al. 2014), high pH (Santos et al. 2012), high light intensities and high medium salinities (Pal et al. 2011). Nitrogen (N) starvation is the most common and straightforward strategy to induce TAG accumulation in microalgae (Rodolfi et al. 2009; Griffiths et al. 2011) and it was adopted also for this thesis.

Under unbalanced growth conditions (e.g. nitrogen starvation), microalgae adapt photosynthesis to meet their metabolic demands (Foyer et al. 1990). During N-starvation, microalgae decrease their energy intake by reducing their pigmentation, activity of the photosystems and number of photosynthetic membranes (Simionato et al. 2013). Additionally, part of the absorbed photons is dissipated as heat or fluorescence (Klok et al. 2013). Therefore, TAG accumulation is always accompanied by a reduction in photosynthetic activity. The remaining photosynthetic activity dictates the amount of photons directed towards the synthesis of TAGs, and thus the TAG productivity.

The ability of retaining a high photosynthetic activity during N-starvation is expected to be species-dependent and to represent the biggest contributor to the observed differences in reported TAG productivities (Griffiths and Harrison 2009). Therefore, the selection of microalgal species that maintain a high photosynthetic activity during N-starvation represents a key biological parameter for achieving high TAG productivities (Wijffels and Barbosa 2010).

1.4 Cultivation strategies for optimized TAG production

The cultivation strategy (i.e. batch, semi-continuous, continuous) is expected to have an impact on TAG productivity. As already mentioned, nitrogen (N) starvation is the most applied and effective method to produce TAGs. N-starvation can be applied in batch and semi-continuous (e.g. repeated-batch) processes. In a batch-process (Fig. 1.2A), biomass is initially produced under N-replete conditions (“growth phase”), and subsequently subjected to N-starvation to trigger TAG accumulation (“stress phase”). In a production facility, this implies that a fraction of the facility area is used to produce the inoculum for the “stress reactor”, rather than being allocated to actual TAG production. Consequently, the total TAG productivity is reduced.

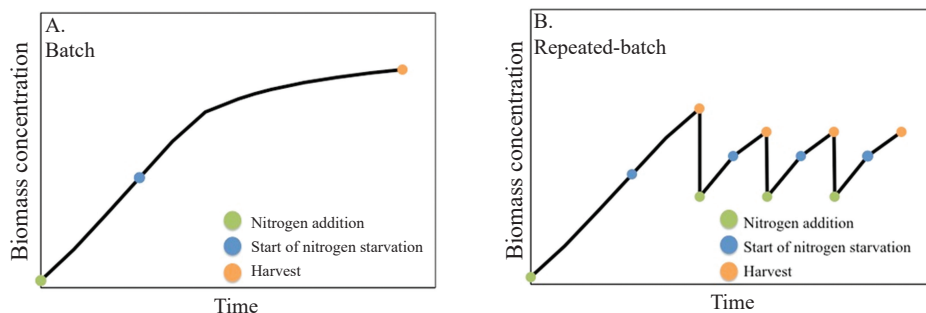


Figure 1.2 Schematic representation of batch and repeated-batch processes.

In repeated-batch processes (i.e. culture is partly harvested and the remaining fraction is resupplied with nutrients; Fig.1.2B), both biomass and TAG production occur in the same reactor, thus minimizing the area of the facility that is allocated to inoculum production. Additionally, in repeated-batch cultivations, nutrients are periodically resupplied, which could allow recovery of photosynthetic activity. Therefore, by repeatedly harvesting the culture at short time intervals, higher residual photosynthetic efficiencies could be maintained and thus higher total TAG productivities could possibly be achieved compared to a batch process.

1.5 Lab-scale and outdoor microalgal TAG production

Lab-scale research under well-defined conditions is essential to understand the effects of biological and process parameters on TAG productivity (Fig. 1.3A-B). However, it should always be validated whether lab-scale results can be translated to outdoor cultivations (Fig. 1.3C-D). Outdoors, cells have to continuously adapt to changing light and temperature conditions and therefore, lower productivities may be expected. Likewise, when bottlenecks are encountered outdoors, these should be further investigated and optimized at lab-scale before being tested again outdoors.

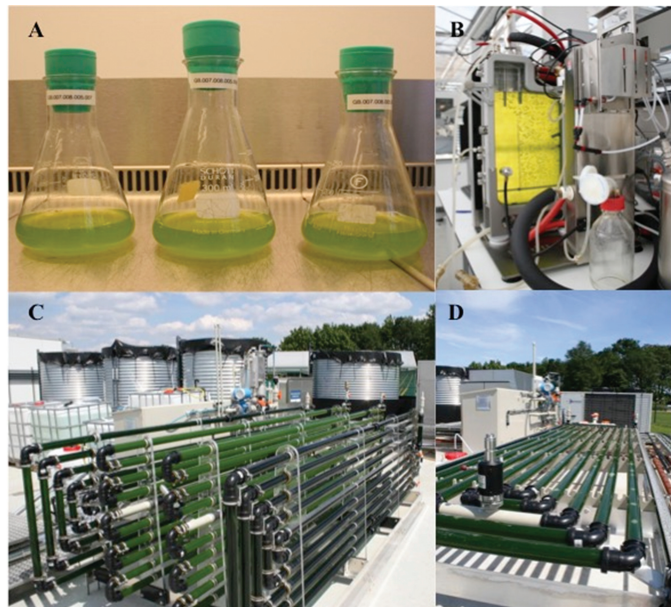


Figure 1.3 Cultivation systems used in this thesis. **A)** Erlenmeyer flasks. **B)** Lab-scale flat panel photobioreactor. **C)** Vertically stacked tubular reactors. **D)** Horizontally stacked tubular reactor.

In general, more experience with outdoor TAG production is required. This is essential to fill the gap between lab-scale research and commercial production. At pilot-scale, possible process and technology bottlenecks (e.g. light gradients due to reactor mutual shading, temperature and pH control, mixing) should be tackled before scaling-up.

1.6 Thesis aim and outline

The aim of the research presented in this thesis is to increase microalgal TAG productivity by investigating the effect of biological and engineering parameters, such as the production strain and the operational strategy.

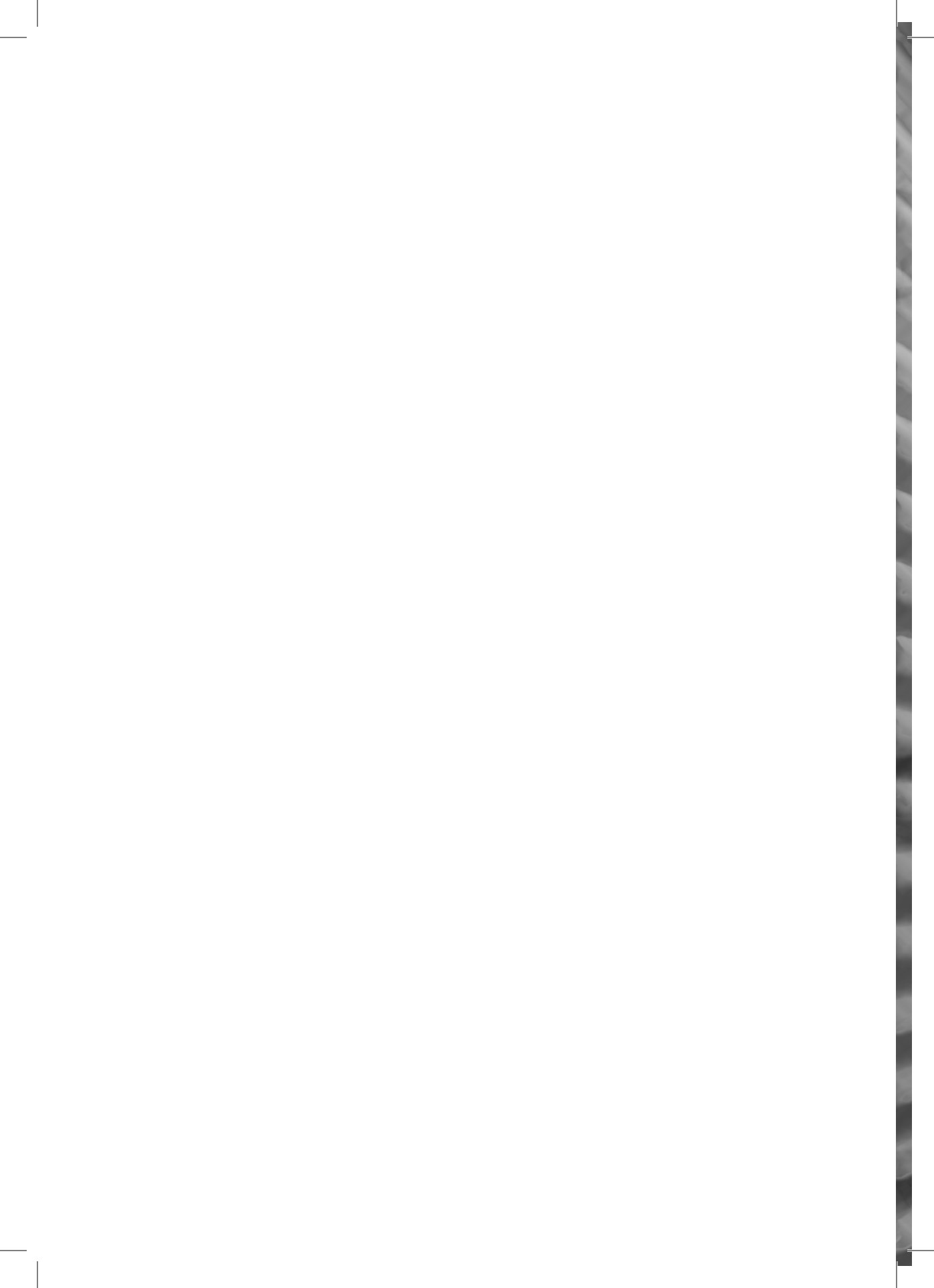
Chapter 2 aims at selecting a marine species with high TAG productivity. Seven species were screened performing nitrogen (N) run-out experiments. *Nannochloropsis* sp. was selected as the most suitable species for lipid production because it retained the highest photosynthetic efficiency during N- starvation, and thus achieved the highest TAG productivity. *Nannochloropsis* sp. was therefore used in all subsequent research performed in this thesis.

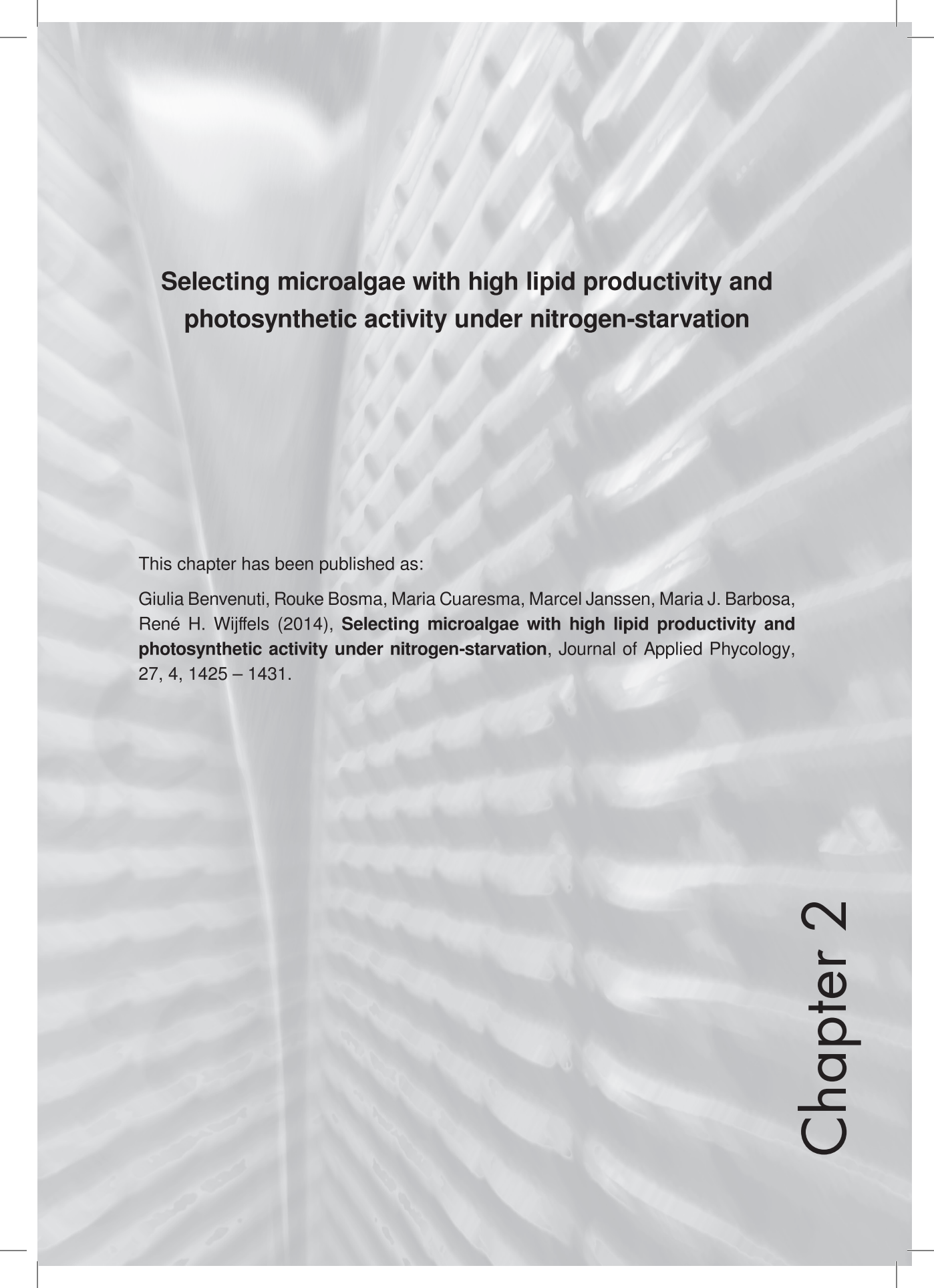
Besides the selection of highly productive strains, process design has a great impact on the TAG productivity. This thesis highlights several contributing factors, which are mainly related to the applied stress pressure. In **chapter 3** the effect of the initial-biomass-specific (IBS) light availability (i.e. ratio of light impinging on reactor ground area divided by initial biomass concentration per ground area) is investigated for batch outdoor cultivations of *Nannochloropsis* sp. cultivated in two different tubular reactors (horizontal and vertically stacked) at different initial biomass concentrations at the start of the TAG accumulation phase, during two distinct seasons. Based on the observed trends, optimal initial biomass concentrations are suggested to achieve high areal TAG productivities for each reactor configuration and season.

The research performed for **chapter 4** aimed at researching a different operational strategy to further increase TAG productivity. For this, repeated-batch cultivations were tested and compared to batch cultivations both at lab-scale and in two identical, simultaneously operated, outdoor vertically stacked tubular PBRs over different seasons. Although at lab-scale, batch and repeated-batch cultivations yielded similar TAG productivities, outdoors the batch process always outcompeted the repeated-batch strategy. It was concluded that repeated-batch TAG production required further optimization and that a full understanding of the physiological responses underlying a process is essential to pursue process optimization and thus, process comparison. In **chapter 5**, the physiological responses of *Nannochloropsis* sp. to N-starvation and N-replenishment were determined in lab scale batch and repeated-

batch cultivations. These physiological insights were condensed into a mechanistic model describing both batch and repeated-batch TAG production processes in flat panel PBRs. Scenarios for improved TAG yields on light were simulated and, based on the optimized yields, a comparison of the two processes was performed. It was concluded that under continuous light, an optimized batch process will always result in higher TAG productivities than an optimized repeated-batch process.

In **chapter 6** an outlook on the research needed to further increase TAG productivity and assess the economic viability of microalgal TAG production is needed. Furthermore, a two-step TAG production process (i.e. growth reactors are operated in continuous mode such that multiple batch-operated stress reactors are inoculated and sequentially harvested ensuring a daily harvest of TAG-enriched biomass) is proposed for a hypothetical 100 ha-scale plant in southern Spain. Photosynthetic efficiencies based on outdoor pilot data are used as model input to conduct a techno-economic analysis. The production cost of TAG-enriched biomass is presented based on current process technology. Finally, a sensitivity analysis is performed and a scenario with reduced production cost is identified.



A grayscale, high-magnification photograph of a plant stem, likely a leaf or stem, showing a clear pattern of vascular bundles. The bundles are arranged in a regular, repeating pattern, with each bundle containing a central vascular cylinder surrounded by sclerenchyma sheaths. The overall appearance is that of a well-developed, vascularized plant tissue.

Selecting microalgae with high lipid productivity and photosynthetic activity under nitrogen-starvation

This chapter has been published as:

Giulia Benvenuti, Rouke Bosma, Maria Cuaresma, Marcel Janssen, Maria J. Barbosa, René H. Wijffels (2014), **Selecting microalgae with high lipid productivity and photosynthetic activity under nitrogen-starvation**, *Journal of Applied Phycology*, 27, 4, 1425 – 1431.

Abstract

An economically feasible microalgal lipid industry heavily relies on the selection of suitable strains. Because microalgal lipid content increases under a range of adverse conditions (e.g. nutrient deprivation, high light intensity), photosynthetic activity is usually strongly reduced. As a consequence, lipid productivity rapidly declines over time, after reaching a maximum within the first days of cultivation. The microalgae *Chlorella vulgaris*, *Chlorococcum littorale*, *Nannochloropsis oculata*, *Nannochloropsis* sp., *Neochloris oleoabundans*, *Stichococcus bacillaris* and *Tetraselmis suecica* were compared on fatty acid content and productivity, but also on photosynthetic activity under nitrogen (N)-starvation. Cultures in N-replete conditions were used as reference. Photosystem II (PSII) maximum efficiency was followed during the experiment, as proxy for the change in photosynthetic activity of the cells. Strains with a high capacity for both lipid accumulation as well as high photosynthetic activity under N-starvation, exhibited a high lipid productivity over time.

Among the tested strains, *Nannochloropsis* sp. showed highest fatty acid content (45% w/w) and productivity (238 mg L⁻¹ d⁻¹) as well as PSII maximum efficiency, demonstrating to be the most suitable strain, of those tested, for lipid production.

This study highlights that for microalgae, maintaining a high photosynthetic efficiency during stress is key to maintain high fatty acid productivities over time and should be considered when selecting strains for microalgal lipid production.

Keywords: Microalgae; nitrogen-starvation; lipid productivity; photosynthetic activity.

2.1 Introduction

Microalgae can offer an important contribution to the transition to a bio-based economy. They can use residual carbon dioxide and nutrient-rich effluents and, through photosynthesis, produce bulk materials (e.g. proteins, fatty acids) for the fuel, chemical, feed and food industry. Microalgal lipids have drawn particular interest from industry due to their wide range of applications; they can serve as supplement in human and animal nutrition (Tredici et al., 2009), or as source of biodiesel (Schenk et al. 2008) and bioplastics (Hempel et al. 2011). Although a large-scale microalgal lipid production is technically feasible, production costs need to be drastically decreased to become economically viable (Wijffels and Barbosa 2010). Currently, biomass productivity, lipid content and lipid productivity are important bottlenecks preventing commercial production (Pienkos and Darzins 2009; Griffiths and Harrison 2009).

Cellular accumulation of lipids can be enhanced by applying factors that limit or prohibit normal cell replication such as nutrient limitation/deprivation and high light intensities (Solovchenko et al. 2007; Rodolfi et al. 2009; Griffiths et al. 2011). Such conditions are often referred to as environmental stress conditions. In particular, nitrogen (N)-limitation/starvation represents one of the most common and effective strategies to trigger lipid accumulation in microalgae (Rodolfi et al. 2009). Usually nitrogen stress in microalgae is accompanied by a reduction of photosynthetic capacity (Berges et al. 1996; Berges and Falkowski 1998; Parkhill et al. 2001). Possibly, lipid productivity suffers due to this reduction in photosynthetic energy supply (Klok et al. 2013) as it generally decreases over time after reaching an optimum within the first hours/days of starvation (Breuer et al. 2012).

Strains with a high capacity for both lipid accumulation and high photosynthetic efficiency under N-starvation are expected to exhibit high lipid productivity over time, representing suitable candidate for industrial applications.

Pulse-Amplitude Modulated (PAM) fluorimeters have been widely accepted as a non-invasive tool to assess photosynthetic responses to changes in nutrient availability of microalgae and cyanobacteria (White et al. 2011; Schreiber et al. 2012; San Pedro et al. 2013; Ramanna et al. 2014).

In this study, photosystem II maximum efficiency of N-starved cells was followed by means of chlorophyll fluorescence and considered as screening-parameter, together with fatty acid content and productivity, for selecting suitable strains for lipid production.

2.2 Materials and methods

2.2.1 Experimental approach

The microalgae *Chlorella vulgaris* UTEX 259 (Cv), *Chlorococcum littorale* NBRC 102761(Cl), *Nannochloropsis oculata* UTEX 2164 (Noc), *Nannochloropsis* sp. CCAP 211/78 (Nsp), *Neochloris oleoabundans* UTEX 1185 (Nol), *Tetraselmis suecica* CCAP 6614 (Ts) and *Stichococcus bacillaris* UTEX B176 (Sb) were screened for their growth characteristics, lipid content and photosynthetic efficiency under nitrogen (N)-starvation. The strains were cultivated under identical controlled conditions in 250-mL Erlenmeyer flasks (150 mL of culture) either in NO_3^- -containing (N-replete) or NO_3^- -free (N-depleted) medium. The standard culture medium was designed for comparison purposes and contained (in mM unless otherwise indicated): NaCl, 420; $\text{MgSO}_4 \cdot 7\text{H}_2\text{O}$, 5; Na_2SO_4 , 3.5; $\text{CaCl}_2 \cdot 2\text{H}_2\text{O}$, 2.5; NaNO_3 , 70; KH_2PO_4 , 0.88; K_2HPO_4 , 2.3; NaHCO_3 , 10; 2-[4-(2-hydroxyethyl)piperazinonitrogen-1-yl]ethanesulfonic acid (HEPES), 100; EDTA-Fe(III)-Na-salt, 0.11; $\text{Na}_2\text{EDTA} \cdot 2\text{H}_2\text{O}$, 0.18; $\text{ZnSO}_4 \cdot 7\text{H}_2\text{O}$, 4 μM ; $\text{CoCl}_2 \cdot 6\text{H}_2\text{O}$, 1.2 μM ; $\text{MnCl}_2 \cdot 2\text{H}_2\text{O}$, 15.5 μM ; $\text{CuSO}_4 \cdot 5\text{H}_2\text{O}$, 1.3 μM ; biotin, 0.1 μM , vitamin B1, 3.7 μM , vitamin B12, 0.1 μM . NaCl concentration was increased up to 490 mM in the N-depleted medium (0 mM NaNO_3) to maintain the same salinity in both media. The pH was adjusted at 7.5 and monitored throughout the cultivation period.

Each strain was initially grown in four replicate flasks inoculated at an optical density of 0.5 at 750 nm in N-replete medium. Flasks were placed in an orbital shaker incubator (Multitron, Infors HT, Switzerland) at 120 rpm, 70 % humidity and 25 °C. The flasks were continuously illuminated at a light intensity of 190 $\mu\text{mol m}^{-2} \text{s}^{-1}$ supplied by fluorescent lamps (TL-D Reflex 36 W/840, Philips, the Netherlands). To avoid carbon limitation the CO_2 level in the headspace was maintained at 5% v/v. When a biomass dry weight of 2 g L^{-1} was reached, replicate flasks were pooled together, divided in a N-replete (N^+) pool and a N-depleted (N^-) pool and centrifuged (780 g, 5 minutes). Once the supernatant was discharged, the cells were washed with either N-replete or N-depleted medium and centrifuged again to eliminate remaining nitrate. Finally, cells were re-suspended in 150 mL of either N-replete or N-depleted medium. The moment of re-suspension was considered as beginning of the lipid accumulation phase ($t = 0$). Duplicate flasks were incubated for 14 days under the same conditions as previously described.

2.2.2 Biomass dry weight

Samples were firstly diluted in ammonium formate (0.5 M) and then filtered over pre-dried and pre-weighed glass fiber filters (Whatman, Ø 55 mm, pore size 0.7 µm). The filters containing the samples were rinsed three times with ammonium formate, dried (95 °C, 24 hours) and then cooled in a desiccator for at least two hours before being weighted again. Biomass dry weight (C_x , g L⁻¹) was determined using the difference between the weights of the blank filters and the ones containing the samples.

2.2.3 Fatty acid analysis

Biomass fatty acid content (f_{FA} , g g⁻¹) and profile were determined by a series of mechanical cell disruption, solvent based lipid extraction and trans-esterification of fatty acids to fatty acid methyl esters (FAMES). Pentadecanoic acid (C15:0; Sigma–Aldric) was added to each sample as internal standard. FAMES were determined using gas chromatography (GC-FID) according to the procedure described by Breuer et al. (2013). Total fatty acid content was calculated as the sum of individual fatty acids.

2.2.4 Dry weight-specific absorption coefficient

Light absorption by the microalgae cells in the range 400-750 nm was measured in a specialized spectrophotometer set-up. It includes an integrating sphere placed behind the sample cuvette to minimize the effect of light scattering on the absorption measurement. The wavelength-dependent dry weight specific absorption coefficient (a_λ , m² g⁻¹) was determined following the procedure described by Vejrazka et al. (2011) and averaged over the PAR range (400-700 nm) to obtain the dry weight-specific absorption coefficient (a_x , m² g⁻¹).

2.2.5 Maximum photosystem II quantum yield

Photosystem II (PSII) maximum quantum yield (F_v/F_m) was determined at several time points during the experiment (day 0, 1, 2, 3, 4, 6, 9, 14) by means of chlorophyll fluorescence in a portable pulse-amplitude modulated fluorimeter (AquaPen-C AP-C 100, Photon Systems Instruments, Czech Republic; emission peak: 620 nm, saturating light pulse: 2100 µmol m⁻² s⁻¹). Beforehand, F_v/F_m was measured for a range of sample concentrations at optical densities (750 nm) between 0.05 and 0.4 and at three saturating light pulses (1500, 2100 and 3000 µmol m⁻² s⁻¹). Results of three independent measurements showed no substantial difference in F_v/F_m values obtained with the different settings (data not shown).

After 10 minutes of dark adaptation at room temperature, fluorescence of microalgal samples at optical density (750 nm) between 0.2 and 0.4 was measured using the PAM fluorimeter previously described.

The parameter F_v/F_m reflects the maximum quantum yield of photosystem II and it is calculated from the minimum level of fluorescence of dark-acclimated cells (F_0) after exposure to a non-actinic beam, and the maximum fluorescence (F_m) following a short but strong actinic light pulse (Eq. 2.1).

$$(F_v / F_m) = (F_m - F_0) / F_m \quad \text{Equation 2.1}$$

2.2.6 Calculations

The cultivation time-averaged volumetric productivity (P) was calculated by dividing the amount of product formed (i.e. biomass, total fatty acids) per culture volume during the 14-day-experiment by the cultivation time according to Eq. 2.2.

$$P_i = c_i(t_{end}) - c_i(t_0) / (t_{end} - t_0) \quad (\text{g L}^{-1} \text{d}^{-1}) \quad \text{Equation. 2.2}$$

The maximum daily volumetric productivity ($P_{i,max}$) observed between two consecutive sampling points was calculated according to Eq. 2.3.

$$P_{i,max} = \max [(c_i(t_{j+1}) - c_i(t_j)) / (t_{j+1} - t_j)] \quad (\text{g L}^{-1} \text{d}^{-1}) \quad \text{Equation. 2.3}$$

Where c_i is the concentration of the component i (biomass or fatty acid concentration) and t is the time.

2.3 Results and Discussion

2.3.1 Biomass growth and productivity

In all experiments an increase in dry weight concentration under both nitrogen (N)-replete and N-depleted conditions was observed. However, the maximum increase in N-depleted cultures was always lower than in the N-replete ones (Table 2.1). Under N-starvation, the maximum increase was achieved at the end of the experiment (day 14), except for *Neochloris oleoabundans* (day 3), *Chlorella vulgaris* (day 11) and *Tetraselmis suecica* (day 4). *Nannochloropsis* sp. displayed the highest relative increase compared to the initial concentration under both N-replete (9.6 ± 0.5 -fold) and N-depleted growth conditions (5.8 ± 0.1 -fold).

As an example, the time-evolution of biomass concentration and fatty acid content of N-depleted cultures of *Neochloris oleoabundans* and *Nannochloropsis* sp. are shown in Figure 2.1. These two strains were chosen as example because, besides their high fatty acid content, they showed very different growth behavior under N-starvation. The data for the others strains are reported in Supplementary material 2.1. *Neochloris oleoabundans* increased in dry weight until day 3, whereas *Nannochloropsis* sp., despite a slow initial pace, increased in biomass concentration until the last day of the experiment.

Table 2.1 Maximum fold-increase in biomass concentration (relative to initial dry weight, 1 fold-increase), maximum biomass productivity ($P_{x, max}$), fatty acid content at the end of the cultivation ($f_{FA, day14}$) and cultivation time-averaged volumetric fatty acid productivity (P_{FA}) for nitrogen-replete (N⁺) and nitrogen-depleted (N⁻) cultures of *Chlorella vulgaris* (Cv), *Chlorococcum littorale* (Cl), *Nannochloropsis oculata* (Noc), *Nannochloropsis* sp. (Nsp), *Neochloris oleoabundans* (Nol), *Stichococcus bacillaris* (Sb) and *Tetraselmis suecica* (Ts).

Strain	Max fold-increase in C_x	$P_{x, max}$ (g L ⁻¹ d ⁻¹)	$f_{FA, day14}$ (g g ⁻¹)	P_{FA} (mg L ⁻¹ d ⁻¹)
Cv N ⁺	6.7	2.2	0.13	73
Cv N ⁻	3.4	2.4	0.39	87
Cl N ⁺	9.1	2.4	0.11	78
Cl N ⁻	4.1	2.5	0.35	126
Noc N ⁺	6.0	0.7	0.16	76
Noc N ⁻	1.8	0.4	0.30	36
Nsp N ⁺	9.6	1.2	0.16	128
Nsp N ⁻	5.8	0.6	0.45	238
Nol N ⁺	7.5	3.4	0.14	84
Nol N ⁻	3.4	3.5	0.35	88
Sb N ⁺	5.9	0.8	0.11	45
Sb N ⁻	2.6	0.5	0.37	69
Ts N ⁺	5.7	2.8	0.11	50
Ts N ⁻	2.8	2.5	0.17	26

An initial increase in dry weight under N-starvation was also observed in previous studies (Li et al. 2008; Breuer et al. 2012; Van Vooren et al. 2012). This can be attributed to the fact that novel biomass is produced in the absence of nitrogen, showing that cells remain photosynthetically active to some extent. The example of *Neochloris oleoabundans* and *Nannochloropsis* sp. shows that the duration of the period in which photosynthetic efficiency is retained is highly species-specific.

During the first three days of cultivation in both N-replete and N-depleted cultures, all strains showed similar biomass concentrations (Supplementary material 2.1), and thus productivities. Thereafter, N-depleted cultures exhibited lower biomass productivities than the N-replete ones, or even negative productivities (*Neochloris oleoabundans*, *Chlorella vulgaris* and *Tetraselmis suecica*).

Maximum daily biomass productivities are often achieved in the first days of N-starvation (Griffiths et al. 2011). In our experiment, maximum productivities (Eq. 2.3) were achieved in the first day of N-starvation, with the exception of *Nannochloropsis oculata*, *Stichococcus bacillaris* and *Nannochloropsis* sp. (Table 2.1). The initial high productivities could be related to the sudden exposure to higher light per cell after re-inoculation. Under N-starvation, the highest maximum daily productivities were observed for *Neochloris oleoabundans* (3.5 g L⁻¹ d⁻¹), *Chlorococcum littorale* (2.5 g L⁻¹ d⁻¹) and *Tetraselmis suecica* (2.5 g L⁻¹ d⁻¹).

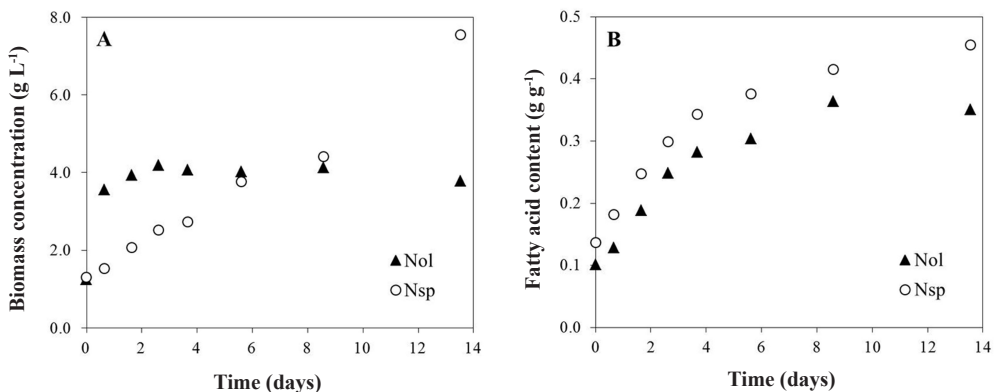


Figure 2.1 Time-evolution of biomass concentration (A) and fatty acid content (B) in nitrogen-depleted cultures of *Nannochloropsis* sp. (Nsp) and *Neochloris oleoabundans* (NoI).

Cultivation time-averaged biomass volumetric productivities (Table 2.1) were calculated over the 14-day-experiment (Eq. 2.2). Because of the steady time-increase in biomass concentration, the highest biomass productivity was observed for *Nannochloropsis* sp. (0.8 and 0.5 g L⁻¹ d⁻¹ for N-replete and N-depleted cultures, respectively).

2.3.2 Fatty acid content and productivity

Under nitrogen (N)-replete conditions, fatty acid content was constant over the entire cultivation period for all tested strains (Supplementary material 2.1). On the contrary, N-depleted conditions led to considerable fatty acid accumulation (more than two-fold) in most strains by the end of the cultivation period. At day 14, fatty acid contents ranged between 35% and 45% w/w. An exception was *Tetraselmis suecica* which did not exhibit high lipid accumulation (only 1.4-fold increase) in response to N-starvation, as was reported before by Bondioli et al. (2012). The highest final fatty acid content was found in *Nannochloropsis* sp. (45% w/w).

Lipid productivity has been proposed as the most suitable parameter when comparing microalgal strains for lipid production (Griffiths and Harrison 2009).

Under N-starvation, the highest productivities were achieved within the first 2-3 days of cultivation. However, productivity rapidly dropped in time because biomass growth was heavily impaired for most strains. An exception was *Nannochloropsis* sp., which exhibited high daily fatty acid productivities until the end of the cultivation period. Moreover, *Nannochloropsis* sp. and *Chlorococcum littorale* always exhibited higher daily fatty acid productivities under N-depleted conditions than under N-replete conditions (Fig. 2.2).

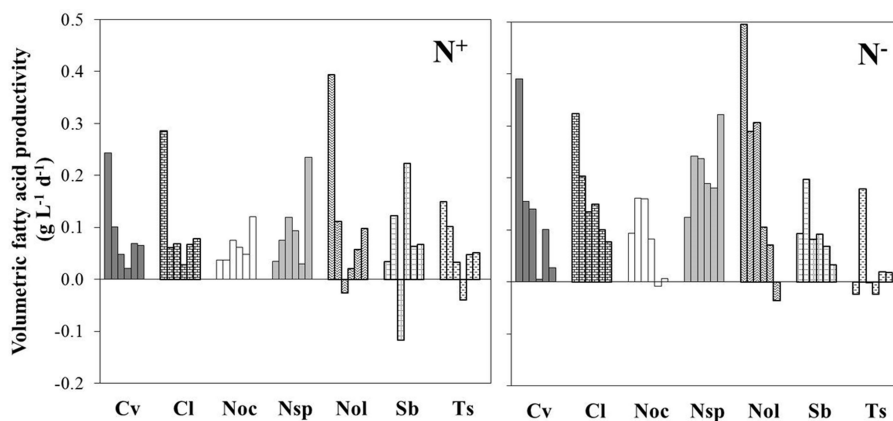


Figure 2.2 Daily volumetric fatty acid productivity for nitrogen-replete (N^+) and nitrogen-depleted (N^-) cultures of *Chlorella vulgaris* (Cv), *Chlorococcum littorale* (Cl), *Nannochloropsis oculata* (Noc), *Nannochloropsis* sp. (Nsp), *Neochloris oleoabundans* (Nol), *Stichococcus bacillaris* (Sb) and *Tetraselmis suecica* (Ts) at day 1, 2, 3, 4, 9 and 14 of cultivation.

In general, cultivation time-averaged fatty acid productivities were higher under N-depleted conditions than under N-replete ones (Table 2.1). Under N-starvation, *Nannochloropsis* sp. in the first place, and *Chlorococcum littorale* in the second place, almost doubled their cultivation time-averaged fatty acid productivity.

Overall, the best balance between fatty acid content and growth was retained by *Nannochloropsis* sp. that showed the highest daily fatty acid productivities, except for the first two days (Fig. 2.2), and the highest cultivation time-averaged fatty acid productivity (Table 2.1).

2.3.3 Fatty acid profile

To investigate the potential application of the microalgal lipids, fatty acid profiles under nitrogen (N)-replete and N-depleted conditions were analyzed for the entire cultivation period (Supplementary material 2.2). When cultivating strains under N-replete conditions the fatty acid profile of all strains did not change significantly. In N-replete cultures of *Nannochloropsis* sp. and *Nannochloropsis oculata*, EPA was the most abundant fatty acid and it accounted for 35% w/w of total fatty acids. Thereby, these strains are promising species for production of EPA as alternative to fish oil. The most abundant fatty acids in N-replete cultures of the other strains were C18:2 and C18:3. Overall, the high abundance of unsaturated fatty acids found in N-replete cultures makes all seven strains a suitable source of nutraceuticals and aquaculture feed (Tredici et al. 2009).

Under N-starvation the overall degree of unsaturation decreased for all strains. N-starvation led to a three-fold decrease in EPA content for the two *Nannochloropsis*

strains. Major changes in fatty acid profile regarded the increase primarily of C18:0 and C18:1 content in Chlorophyceae, and of C16:0 in *Nannochloropsis oculata*, *Nannochloropsis* sp., *Stichococcus bacillaris* and *Tetraselmis suecica*. Our results are consistent with other studies (Griffiths et al. 2011; Simionato et al. 2013) who observed similar trends.

2.3.4 Light absorption and maximum photosystem II quantum yield under nitrogen-starvation

When screening microalgae for lipid productivity, it is important to know the photosynthetic capacity under stress conditions. For that reason we measured light absorption and the efficiency of light utilization over time.

The specific absorption coefficient (a_x) is a direct measure for cell-specific light absorption and an indirect measure for cellular pigmentation. A time-increase in the specific absorption coefficient was observed for nitrogen (N)-replete cultures (data not shown). In fact, given the high cell densities achieved by N-replete cultures, this increase can be explained as a result of an augmented degree of cell self-shading. Because the cultures suffered light limitation, the amount of chlorophylls likely increased to compensate for the reduced amount of light per cell. This phenomenon is a component of the photoacclimatory response (Falkowski and Owens 1980).

A reduced ability to absorb light was found in the N-depleted cultures of all strains. This decrease in absorption coefficient (a_x) is related to a decrease in photosynthetic pigment content that is often observed under N-starvation (Geider et al. 1998a; Pruvost et al. 2009; Van Vooren et al. 2012; Solovchenko et al. 2013). Figure 2.3 (white bars) shows the fold-decrease in a_x observed at the end of the cultivation (day 14) relative to the initial a_x value (day 0) for N-starved cultures. The highest fold-decrease in a_x was observed for *Nannochloropsis* sp., suggesting a strong down-regulation of the photosynthetic pigments for this strain.

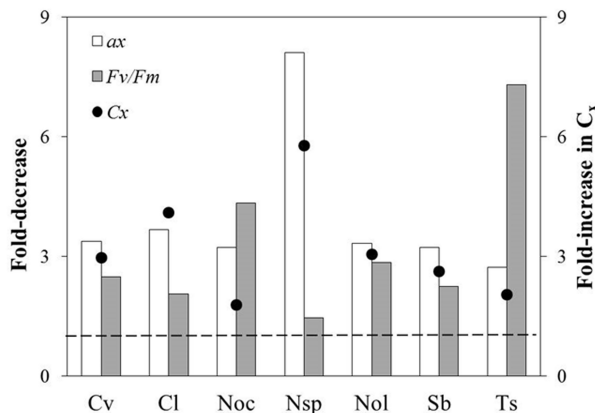


Figure 2.3 Fold-decrease in specific absorption coefficient (a_x ; white bars) and PSII maximum quantum yield (F_v/F_m ; grey bars) and fold-increase in biomass concentration (dots) for nitrogen-depleted cultures of *Chlorella vulgaris* (Cv), *Chlorococcum littorale* (Cl), *Nannochloropsis oculata* (Noc), *Nannochloropsis* sp. (Nsp), *Neochloris oleoabundans* (Nol), *Stichococcus bacillaris* (Sb) and *Tetraselmis suecica* (Ts) at the end of the cultivation (day 14). Initial values (day 0) are 1 fold-decrease/increase.

The maximum quantum yield (F_v/F_m) of photosystem II (PSII) was assessed during the experiment (Supplementary material 2.3) and used as a proxy to monitor the efficiency of light utilization by the seven strains. Photosystem II (PSII) has been suggested as one of the major targets of N-starvation (Berges et al. 1996). In fact, because of reduced protein synthesis, PSII proteins with a high turnover rate are the first ones to be affected by the lack of an inorganic nitrogen supply (Geider et al. 1993). F_v/F_m values around 0.6-0.7 are expected for healthy microalgal cells, whereas lower values are observed if cells have been exposed to biotic or abiotic stress (Young and Beardall 2003). In our study, F_v/F_m of cultures cultivated in nitrogen (N)-replete conditions did not change over time (data not shown). This confirmed the findings of Parkhill et al. (2001) according to which PSII maximum quantum yield is independent of growth irradiance, as long as nutrients are not limiting and cells are fully photo-acclimated. On the contrary, N-starvation led to a strong decrease in F_v/F_m for all strains, as shown in Fig. 2.3 (grey bars) which represents the fold-decrease in F_v/F_m observed at the end of the cultivation (day 14) relative to the initial F_v/F_m value (day 0) for N-starved cultures. The decrease in F_v/F_m indicates that N-starvation diminished the efficiency of photon utilization by PSII and thus, of linear electron transport. In this respect, Klok et al. (2013) observed a decreased photosynthetic efficiency and an increased energy dissipation that was reflected in a strongly reduced yield of biomass on light and productivity in N-limited *Neochloris oleoabundans*.

In our experiments, the effect of N-starvation on photosynthetic efficiency was most severe in *Tetraselmis suecica* (7.3 fold-decrease), whereas the other strains showed a 1.4-4.3 fold-decrease in F_v/F_m (Fig. 2.3). Altogether, our data confirm that photosystem II photochemistry was impaired by N-starvation, although the extent of impairment was highly strain-dependent.

Under N-starvation, light absorption and photosynthetic efficiency seemed to be inversely related (Fig. 2.3). Strains which exhibited a strong reduction in light absorption (i.e. a_x), showed a smaller reduction in photosynthetic efficiency (F_v/F_m) compared to the others. A decrease in light absorption could be attributed to the lower light requirement of N-starved cells. This down-regulation could compensate for the impaired metabolic demand for growth, thus limiting the over-reduction of the photosynthetic machinery (Geider et al. 1993; Sauer et al. 2001). As a consequence, the efficiency of light utilization remained high. Apparently, these two factors resulted in the highest increase in biomass concentration (Fig. 2.3, dots) enhancing fatty acid productivity. This is best represented by *Nannochloropsis* sp. that exhibited the strongest decrease in a_x , the smallest decrease in F_v/F_m and the highest increase in biomass concentration and fatty acid productivity under N-starvation. This observation is in accordance with the findings of Simionato et al. (2013), according to which *Nannochloropsis* largely retains its photosynthetic capacity and cell duplication under nitrogen-starvation due to the rearrangement of its photosynthetic apparatus.

2.4 Conclusions

In this study, a positive relation between high PSII maximum quantum yield and high fatty acid productivity was found for certain strains, highlighting the importance of aiming for an alga that accumulates large amounts of lipids while maintaining its photosynthetic capacity under nitrogen (N)-starvation to ensure high lipid productivities over time.

Among the tested strains, *Nannochloropsis* sp. showed highest fatty acid content (45% w/w) and productivity ($238 \text{ mg L}^{-1} \text{ d}^{-1}$) as well as PSII maximum quantum yield over time demonstrating to be the most suitable strain, of those tested, for lipid production.

2

Acknowledgements

The authors would like to thank the Ministry of Economic Affairs, Agriculture and Innovation and Province of Gelderland, and Biosolar Cells, BASF, BioOils, Cellulac, Drie Wilgen Development, DSM, Exxon Mobil, GEA Westfalia Separator, Heliae, Neste, Nijhuis, Paques, Proviron, Roquette, SABIC, Simris Alg, Staatsolie Suriname, Synthetic Genomics, TOTAL and Unilever for financially supporting the AlgaePARC research program. Thanks to Christa Heryanto for performing the analysis of the fatty acid samples.

Supplementary material

Supplementary material 2.1 Time-evolution of biomass concentration (C_x) and fatty acid content (f_{FA}) in nitrogen (N)-replete (N⁺) and N-depleted (N⁻) cultures of *Chlorella vulgaris*, *Chlorococcum littorale*, *Nannochloropsis oculata*, *Nannochloropsis* sp., *Neochloris oleoabundans*, *Stichococcus bacillaris* and *Tetraselmis suecica* for the duplicate cultures (A, B).

<i>Chlorella vulgaris</i> (N ⁺)					<i>Chlorococcum littorale</i> (N ⁺)			
Time (days)	C_x (g L ⁻¹)		f_{FA} (g g ⁻¹)		C_x (g L ⁻¹)		f_{FA} (g g ⁻¹)	
	A	B	A	B	A	B	A	B
0	1.31	1.31	0.13	0.13	1.24	1.26	0.11	0.11
1	2.75	2.75	0.12	0.12	2.93	2.76	0.11	0.12
2	3.27	3.41	0.14	0.12	3.80	3.93	0.10	0.10
3	3.93	4.16	0.12	0.11	4.72	4.50	0.10	0.10
4	4.07	4.33	0.12	0.12	4.85	4.75	0.10	0.10
6	4.92	4.97	0.13	0.12	5.56	6.29	0.11	0.11
9	7.14	6.66	0.12	0.12	8.22	8.22	0.11	0.09
14	8.77	8.61	0.13	0.13	11.37	11.30	0.11	0.10

<i>Chlorella vulgaris</i> (N ⁻)					<i>Chlorococcum littorale</i> (N ⁻)			
Time (days)	C_x (g L ⁻¹)		f_{FA} (g g ⁻¹)		C_x (g L ⁻¹)		f_{FA} (g g ⁻¹)	
	A	B	A	B	A	B	A	B
0	1.15	1.12	0.13	0.13	1.32	1.30	0.11	0.11
1	2.55	2.91	0.15	0.15	3.01	2.90	0.13	0.12
2	2.85	3.06	0.19	0.19	3.71	3.76	0.14	0.16
3	3.16	3.20	0.22	0.22	3.81	3.69	0.19	0.18
4	3.11	3.07	0.23	0.22	4.29	3.95	0.20	0.21
6	3.06	3.07	0.31	0.29	4.40	4.54	0.25	0.23
9	3.77	3.42	0.33	0.34	4.70	4.85	0.30	0.32
14	3.32	3.42	0.37	0.41	5.31	5.41	0.36	0.34

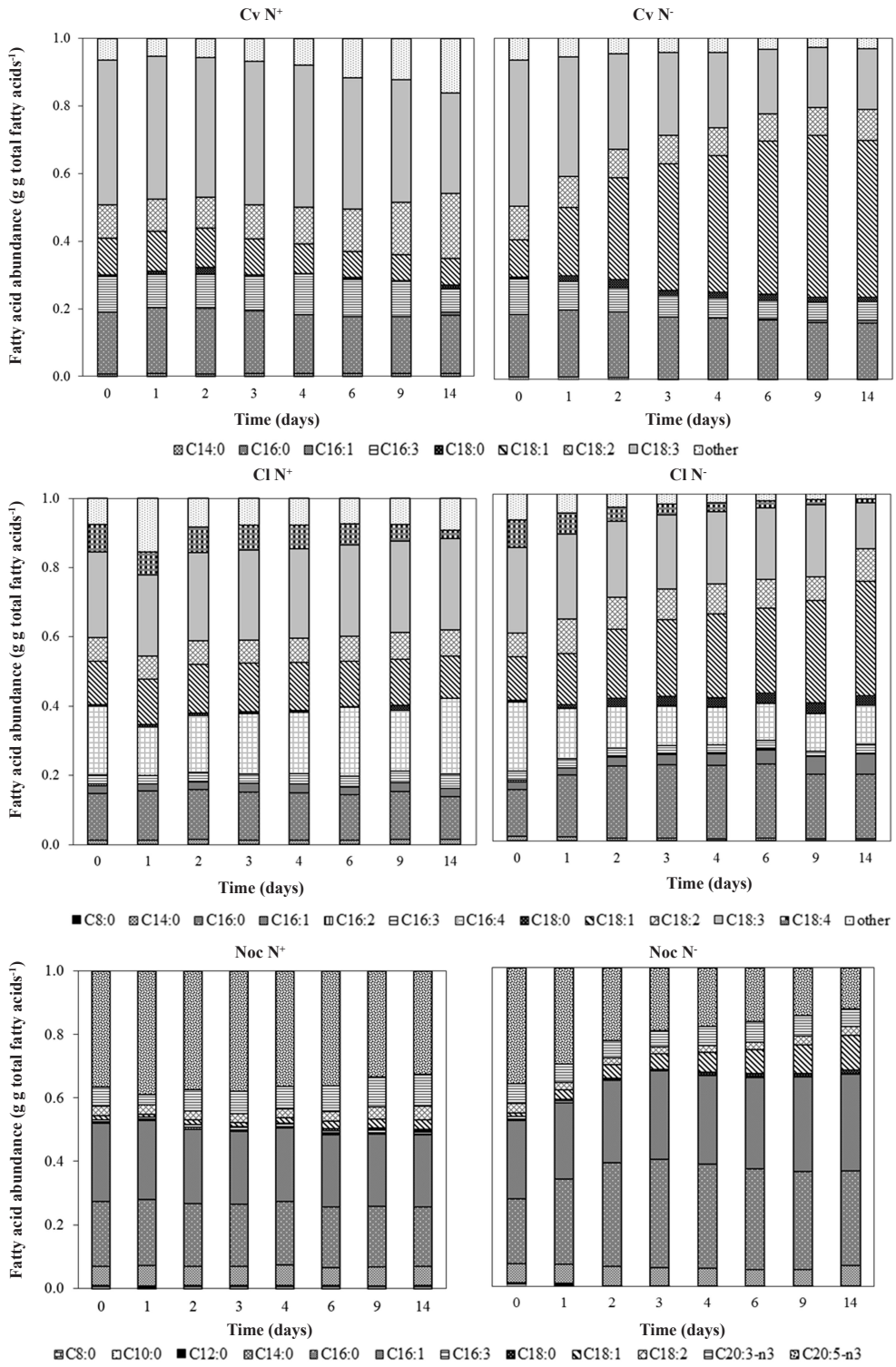
<i>Nannochloropsis oculata</i> (N ⁺)					<i>Nannochloropsis</i> sp. (N ⁺)			
Time (days)	C_x (g L ⁻¹)		f_{FA} (g g ⁻¹)		C_x (g L ⁻¹)		f_{FA} (g g ⁻¹)	
	A	B	A	B	A	B	A	B
0	1.30	1.34	0.15	0.15	1.26	1.26	0.14	0.14
1	1.35	1.39	0.17	0.17	1.40	1.39	0.15	0.14
2	1.79	1.52	0.16	0.16	1.79	1.80	0.16	0.15
3	2.32	2.08	0.16	0.15	2.77	2.70	0.15	0.14
4	2.68	2.40	0.16	0.16	3.28	3.20	0.15	0.15
6	3.39	3.15	0.15	0.15	4.70	4.39	0.15	0.14
9	4.61	4.30	0.14	0.15	6.25	5.68	0.12	0.14
14	8.15	7.73	0.16	0.16	12.57	11.67	0.15	0.16

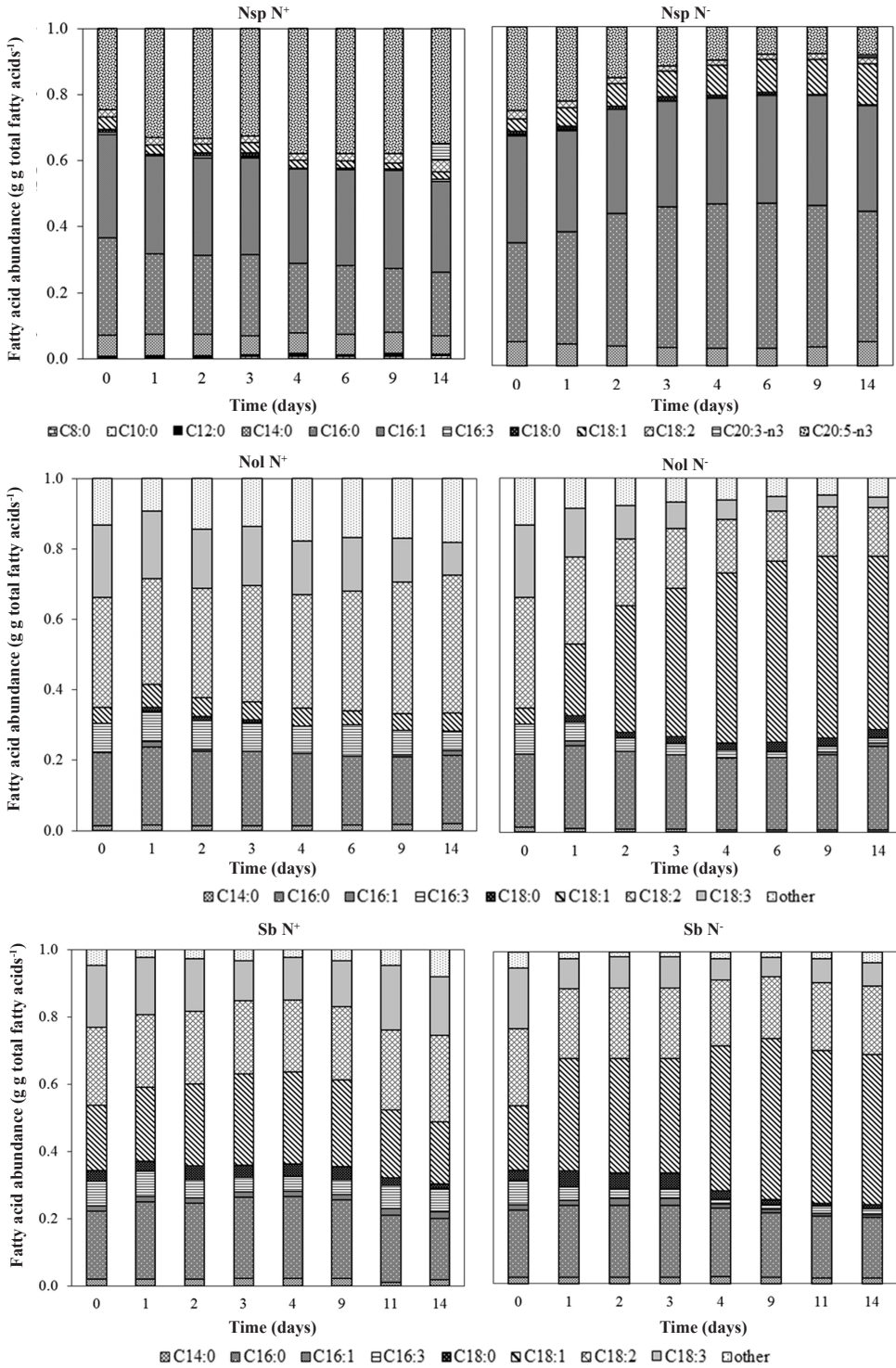
<i>Nannochloropsis oculata</i> (N [*])					<i>Nannochloropsis</i> sp. (N [*])			
Time (days)	C_x (g L ⁻¹)		f_{FA} (g g ⁻¹)		C_x (g L ⁻¹)		f_{FA} (g g ⁻¹)	
	A	B	A	B	A	B	A	B
0	1.23	1.23	0.15	0.15	1.31	1.31	0.14	0.14
1	1.12	1.33	0.22	0.21	1.50	1.54	0.18	0.18
2	1.34	1.62	0.30	0.27	2.04	2.11	0.25	0.24
3	1.73	2.03	0.31	0.31	2.47	2.58	0.28	0.32
4	1.87	2.25	0.32	0.32	2.70	2.75	0.34	0.35
6	1.91	2.27	0.33	0.32	3.73	3.80	0.38	0.37
9	1.82	2.31	0.30	0.29	4.36	4.45	0.43	0.40
14	1.96	2.41	0.29	0.30	7.49	7.62	0.45	0.46

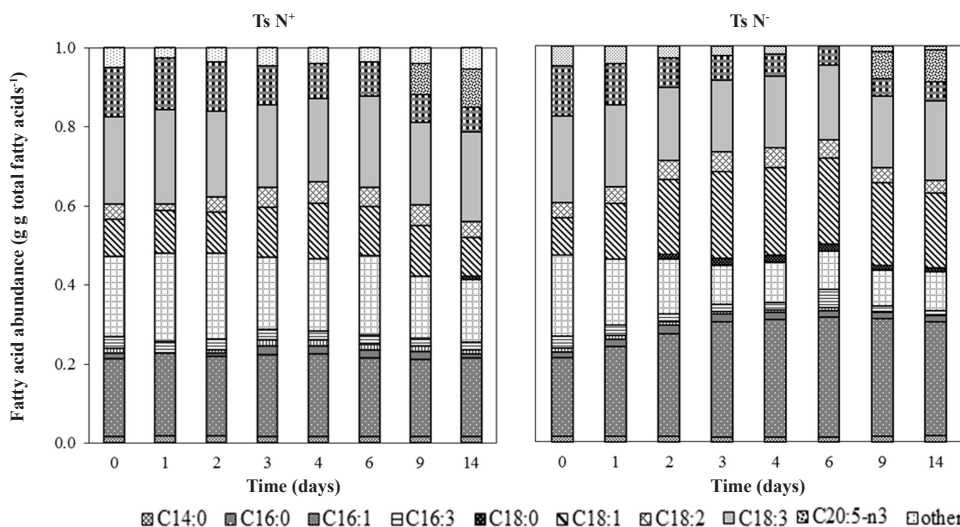
<i>Neochloris oleoabundans</i> (N [*])					<i>Tetraselmis suecica</i> (N [*])			
Time (days)	C_x (g L ⁻¹)		f_{FA} (g g ⁻¹)		C_x (g L ⁻¹)		f_{FA} (g g ⁻¹)	
	A	B	A	B	A	B	A	B
0	1.18	1.20	0.10	0.10	1.47	1.35	0.12	0.12
1	3.38	3.53	0.11	0.11	2.98	3.57	0.10	0.07
2	3.97	4.04	0.12	0.13	3.33	3.19	0.11	0.12
3	4.18	4.17	0.11	0.11	3.49	3.45	0.11	0.13
4	4.31	4.34	0.11	0.12	3.81	3.76	0.10	0.09
6	4.71	5.02	0.13	0.12	4.83	4.63	0.10	0.11
9	6.56	6.63	0.12	0.12	6.76	6.20	0.09	0.09
14	8.86	9.08	0.14	0.14	8.31	7.80	0.10	0.11

<i>Neochloris oleoabundans</i> (N [*])					<i>Tetraselmis suecica</i> (N [*])			
Time (days)	C_x (g L ⁻¹)		f_{FA} (g g ⁻¹)		C_x (g L ⁻¹)		f_{FA} (g g ⁻¹)	
	A	B	A	B	A	B	A	B
0	1.24	1.24	0.10	0.10	1.40	1.40	0.12	0.12
1	3.53	3.59	0.13	0.13	3.04	3.07	0.10	0.09
2	3.86	3.99	0.19	0.19	3.75	3.78	0.09	0.09
3	4.19	4.17	0.25	0.25	3.87	3.92	0.07	0.09
4	4.07	4.06	0.28	0.29	3.93	3.94	0.07	0.08
6	3.94	4.08	0.33	0.28	3.79	3.78	0.08	0.10
9	4.17	4.06	0.35	0.38	3.60	3.57	0.11	0.11
14	3.83	3.72	0.35	0.35	2.90	2.80	0.16	0.17

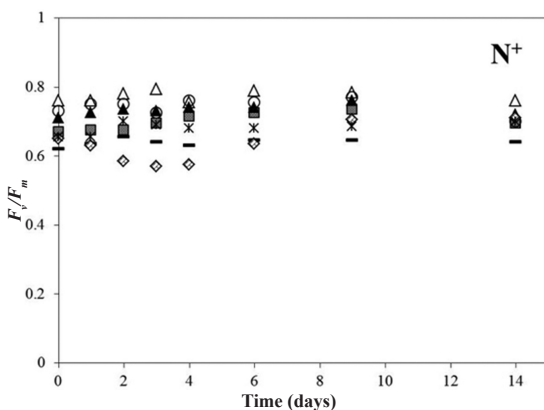
<i>Stichococcus bacillaris</i> (N [*])					<i>Stichococcus bacillaris</i> (N [*])			
Time (days)	C_x (g L ⁻¹)		f_{FA} (g g ⁻¹)		C_x (g L ⁻¹)		f_{FA} (g g ⁻¹)	
	A	B	A	B	A	B	A	B
0	1.12	1.12	0.10	0.10	1.12	1.12	0.10	0.10
1	1.41	1.43	0.10	0.10	1.40	1.65	0.12	0.14
2	1.96	2.03	0.13	0.14	1.81	2.24	0.18	0.21
3	2.46	2.43	0.11	0.11	2.38	2.27	0.20	0.21
4	3.45	2.84	0.11	0.12	2.60	2.46	0.24	0.21
9	3.52	3.61	0.11	0.12	2.68	2.80	0.33	0.34
14	6.46	6.66	0.11	0.11	2.92	2.94	0.36	0.37



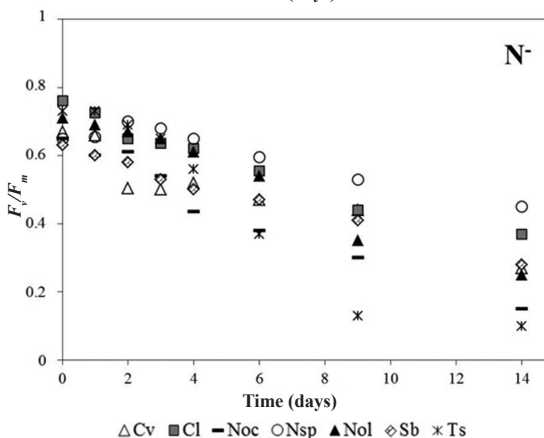


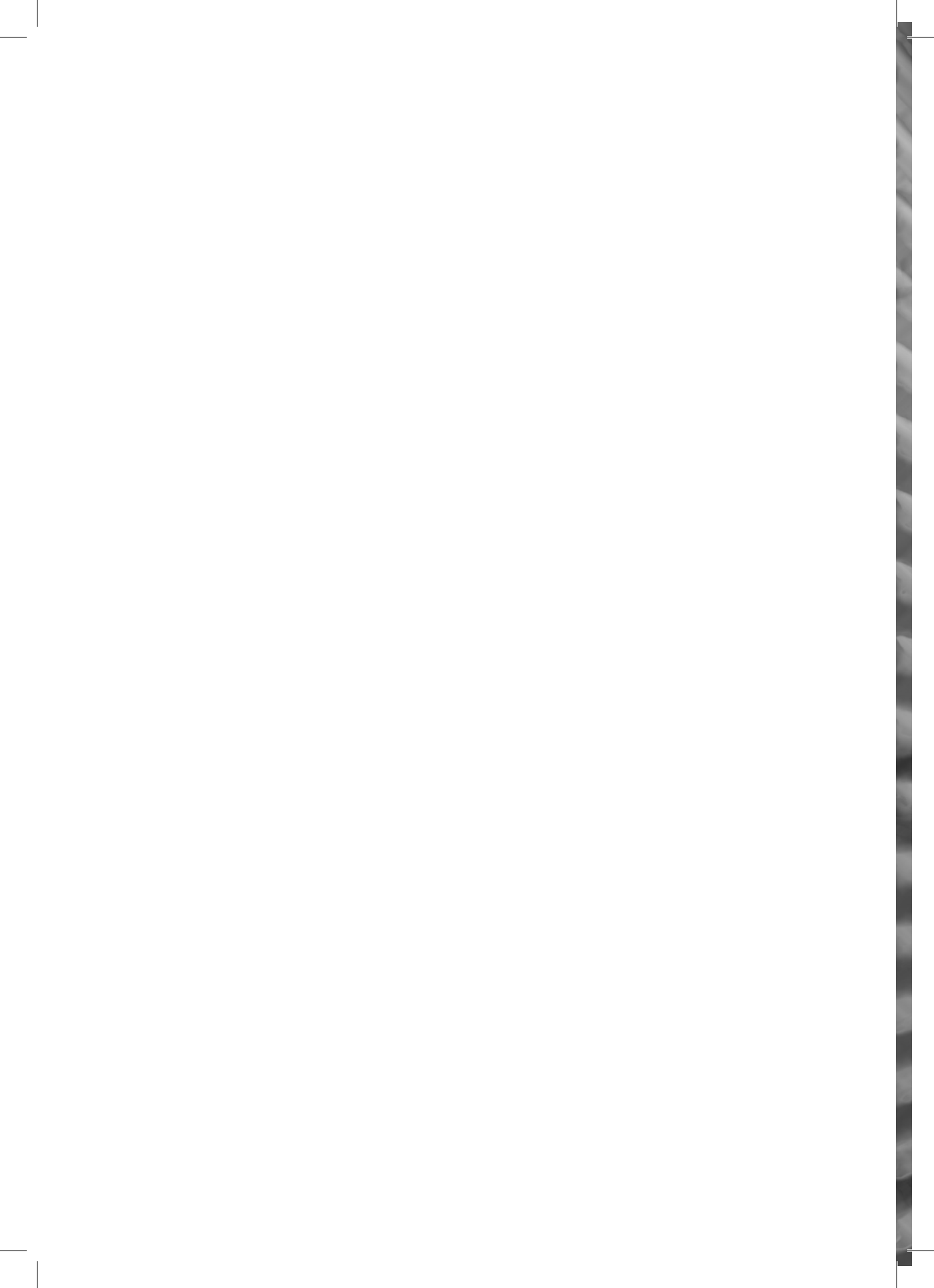


Supplementary material 2.2 Time-evolution of fatty acid abundance in nitrogen (N)-replete (N⁺) and N-depleted (N⁻) cultures of *Chlorella vulgaris* (Cv), *Chlorococcum littorale* (Cl), *Nannochloropsis oculata* (Noc), *Nannochloropsis* sp. (Nsp), *Neochloris oleoabundans* (Nol), *Stichococcus bacillaris* (Sb) and *Tetraselmis suecica* (Ts).



Supplementary material 2.3 Time-evolution of maximum quantum yield of photosystem II (F_v/F_m) for nitrogen (N)-replete (N⁺) and N-depleted (N⁻) cultures of *Chlorella vulgaris* (Cv), *Chlorococcum littorale* (Cl), *Nannochloropsis oculata* (Noc), *Nannochloropsis* sp. (Nsp), *Neochloris oleoabundans* (Nol), *Stichococcus bacillaris* (Sb) and *Tetraselmis suecica* (Ts).





A grayscale photograph of a large-scale microalgal cultivation system. The image shows a dense array of vertical, cylindrical tubular photobioreactors (PBRs) arranged in rows. The tubules are filled with a light-colored, turbid liquid, likely a microalgal culture. The perspective is from a low angle, looking up the length of the tubules, creating a strong sense of depth and repetition. The lighting is bright, highlighting the texture of the liquid and the structure of the tubules.

Microalgal triglyceride production in outdoor batch-operated tubular PBRs

This chapter has been published as:

Giulia Benvenuti, Rouke Bosma, Anne J. Klok, Fang Ji, Packo P. Lamers, Maria J. Barbosa, René H. Wijffels (2015), **Microalgal triacylglycerides production in outdoor batch-operated tubular PBRs**, *Biotechnology for Biofuels* 8, 100.

Background: Microalgal triglycerides (TAGs) are a promising sustainable feedstock for the biofuel, chemical and food industry. However, industrial production of microalgal products for commodity markets is not yet economically viable, largely because of low microalgal productivity. The latter is strictly dependent on initial-biomass-specific (IBS) light availability (i.e. ratio of light impinging on reactor ground area divided by initial biomass concentration per ground area). This study investigates the effect of IBS-light availability on batch TAG production for *Nannochloropsis* sp. cultivated in two outdoor tubular reactors (i.e. vertical and horizontal) at different initial biomass concentrations for the TAG accumulation phase, during two distinct seasons (i.e. high and low light conditions).

Results: Increasing IBS-light availability led to both a higher IBS-TAG production rate and TAG content at the end of the batch, whereas biomass yield on light decreased. As a result, an optimum IBS-light availability was determined for the TAG productivity obtained at the end of the batch and several guidelines could be established. The vertical reactor (VR) should be operated at an initial biomass concentration of 1.5 g L⁻¹ to achieve high TAG productivities (1.9 and 3.2 g m⁻² d⁻¹ under low and high light, respectively). Instead, the horizontal reactor (HR) should be operated at 2.5 g L⁻¹ under high light (2.6 g m⁻² d⁻¹), and at 1.5 g L⁻¹ under low light (1.4 g m⁻² d⁻¹).

Conclusions: From this study, the great importance of IBS-light availability on TAG production can be deduced. Although maintaining high light availabilities in the reactor is key to reach high TAG contents at the end of the batch, considerable losses in TAG productivity were observed for the two reactors regardless of light condition, when not operated at optimal initial biomass concentrations (15–40% for VR and 30–60% for HR).

Keywords: Microalgae; TAG productivity; outdoor; pilot-scale; light availability.

3.1 Background

Microalgal triglycerides (TAGs) are a promising sustainable feedstock for the food, chemical and biofuel industry, as an alternative to traditional feedstocks that are typically derived from fossil or vegetable oil. Although high value products from microalgae are already commercially available, industrial production of microalgal products for commodity markets is not yet economically viable, largely because of low microalgal productivity (Pienkos and Darzins 2009). In this respect, outdoor pilot-scale research, in addition to mechanistic studies under controlled laboratory conditions, is essential to fully investigate the potential of the selected microalga for high outdoor productivities and to foster process scale-up.

In both laboratory and outdoor studies, the important role of light availability (i.e. ratio of light impinging on the reactor surface divided by biomass concentration in the reactor) on lipid production has been highlighted (Su et al. 2010; Münkkel et al. 2013). In such cases, light availability was varied by varying initial biomass concentrations at the start of the lipid accumulation phase. Higher lipid content was obtained by increasing light availability, whereas an opposite trend was observed for TAG productivity at the end of the batch cultivation.

However, in outdoor cultivations, light availability, besides being influenced by total irradiance, is also determined by reactor configuration (vertical or horizontal) and design. When operated at the same total irradiance and (volumetric) biomass concentration, a lower light availability is expected in a vertical reactor because more biomass is present per ground area, compared to a horizontal one.

Experimental data that quantify the effect of light availability (i.e. biomass concentration, total irradiance and reactor configuration) on TAG production are therefore essential for process optimization.

This study assesses the effect of initial-biomass-specific (IBS) light availability (i.e. ratio of light impinging on reactor ground area divided by the initial biomass concentration per ground area) on batch TAG production in *Nannochloropsis* sp. CCAP 211/78. N-starved cultivations were carried out at AlgaePARC pilot facilities in Wageningen, the Netherlands (N 51°59'45.88", 5°39'28.15"). IBS-light availability was varied by setting different initial biomass concentrations (1 g L⁻¹, 1.5 g L⁻¹ and 2.5 g L⁻¹) at the start of the TAG-accumulation phase in a vertical and in horizontal tubular pilot-scale reactors, which were simultaneously operated. Each initial biomass concentration was tested under two seasons, resulting in two distinct light conditions (14 ± 3 and 36 ± 2 mol m⁻² d⁻¹ average light intensity).

Based on the trends observed in this study, several guidelines for optimization of outdoor batch TAG production are proposed.

3.2 Results

The time-evolution of biomass concentration, TAG, intracellular nitrogen and carbohydrate contents, as well as the TAG productivity, are shown in Fig. 3.1 for the run inoculated at 1.5 g L^{-1} in the vertical reactor under low light conditions. This run is shown as a typical example, and the parameters for all runs are given in Supplementary material 3.1.

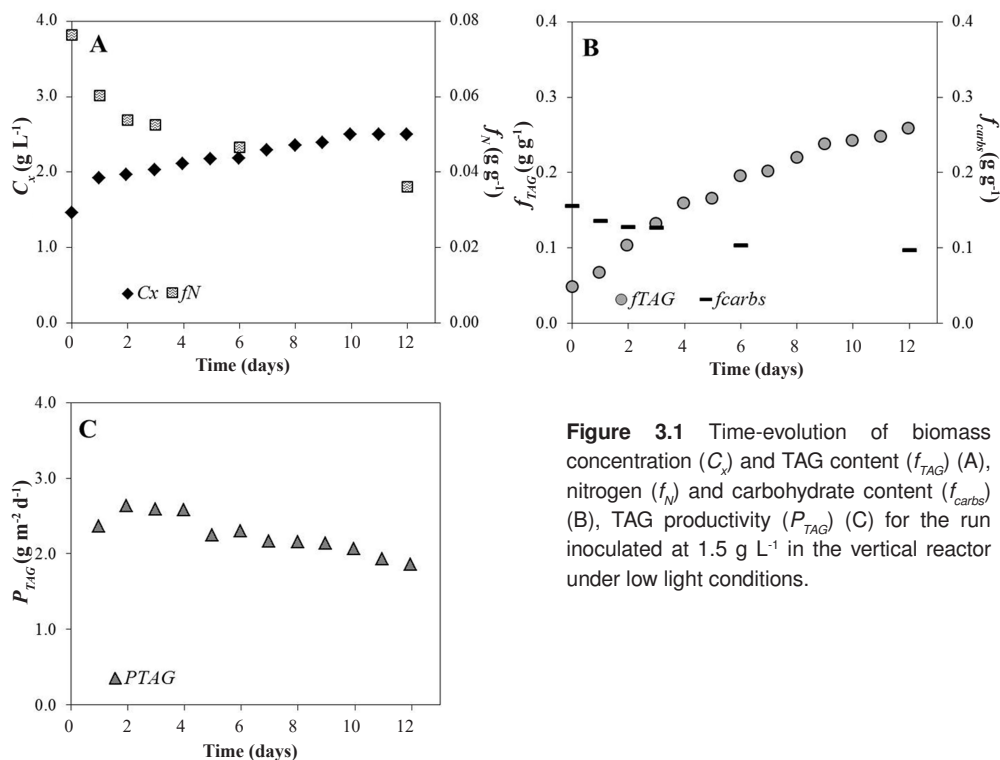


Figure 3.1 Time-evolution of biomass concentration (C_x) and TAG content (f_{TAG}) (A), nitrogen (f_N) and carbohydrate content (f_{carbs}) (B), TAG productivity (P_{TAG}) (C) for the run inoculated at 1.5 g L^{-1} in the vertical reactor under low light conditions.

Under nitrogen (N)-starvation, biomass concentration increased, though at a low pace, while the intracellular nitrogen content exhibited a constant decline over time (Fig. 3.1A). As a response to N-starvation, TAG content promptly increased (Fig. 3.1B), while carbohydrate content decreased over time (Fig. 3.1B), suggesting that TAGs represent the main storage compound for N-starved cells of *Nannochloropsis* sp..

During a batch process, TAG productivity and content are inversely correlated because those conditions (e.g. N-starvation) which enhance massive TAG accumulation typically impair biomass production (Benvenuti et al. 2014). As a result, TAG productivity (P_{TAG}) declined over time, after reaching a maximum in the early N-starvation phase (Fig. 3.1C).

3.2.1 Batch TAG content

In general, at the end of the batch, TAG content ($f_{TAG, batch}$) was similar for both vertical (VR) and horizontal (HR) reactors, under both light conditions (Table 3.1). An exception was the run inoculated at 2.5 g L⁻¹ under high light conditions. In this case, HR showed a much higher $f_{TAG, batch}$ than VR (16% in VR, 25% in HR).

The highest $f_{TAG, batch}$ of this study were found under high light conditions for the runs inoculated at 1 and 1.5 g L⁻¹ (32-34% w/w) (Table 3.1). The highest $f_{TAG, batch}$ for the low light conditions were obtained by the runs inoculated at 1 and 1.5 g L⁻¹ (26-31% w/w) (Table 3.1).

3.2.2 TAG productivity

TAG productivities ($P_{TAG}(t)$) achieved under high light conditions were always higher than those found at low light conditions (Table 3.1). For this study, highest TAG productivities at the end of the batch ($P_{TAG, batch}$) were obtained under high light conditions by the runs inoculated at 1.5 g L⁻¹ in VR (3.2 g m⁻² d⁻¹) and at 2.5 g L⁻¹ in the HR (2.6 g m⁻² d⁻¹). For the low light conditions, the highest $P_{TAG, batch}$ was obtained by the runs inoculated at 1.5 g L⁻¹ (1.9 g m⁻² d⁻¹ in VR and 1.4 g m⁻² d⁻¹ in HR).

In general, maximum TAG productivity ($P_{TAG, max}$) was achieved within the first three days of cultivation, regardless of light conditions and reactor configuration, with the exception of the runs inoculated at 2.5 g L⁻¹ under high light conditions. In these cases, a $P_{TAG, max}$ was achieved at day 10 (Table 3.1) in both reactors. Under high light conditions, highest $P_{TAG, max}$ were achieved by the runs inoculated at 1.5 g L⁻¹ (8.3 g m⁻² d⁻¹ in VR and 5.4 g m⁻² d⁻¹ in HR). Under low light conditions, very similar $P_{TAG, max}$ (2.4-2.6 g m⁻² d⁻¹) was found among the different runs and reactors. Only exception was the run inoculated at 1 g L⁻¹ in HR, which resulted in the lowest $P_{TAG, max}$ (1.5 g m⁻² d⁻¹).

3.2.3 TAG yield on light

For both the vertical (VR) and the horizontal (HR) reactors, TAG yield on light ($Y_{TAG, ph}(t)$) showed a maximum within the first three days of cultivation (Table 3.1). Exceptions were the runs inoculated at 2.5 g L⁻¹ under high light conditions, which exhibited a maximum at day 10 (VR) and at day 4 (HR). After reaching maximum, $Y_{TAG, ph}(t)$ decreased, resulting in values as low as 0.5 – 0.11 g mol⁻¹ (VR) and 0.03 – 0.08 g mol⁻¹ (HR).

With the exception of the runs inoculated at 1.5 g L⁻¹, maximum TAG yield on light ($Y_{TAG, ph, max}$) was higher under low light conditions. The highest $Y_{TAG, ph, max}$ (0.29 g mol⁻¹) of this study was found for the run inoculated at 1.5 g L⁻¹ in VR under high light conditions (Table 3.1).

Table 3.1 Batch TAG content ($f_{TAG, batch}$), batch ($P_{TAG, batch}$) and maximum ($P_{TAG, max}$) TAG productivity, and maximum TAG yield on light ($Y_{TAG, ph, max}$) obtained for the different initial biomass concentrations ($C_{x, N=0}$) and average light intensity (I_{av}). In brackets, day at which maximum TAG productivity and TAG yield on light were obtained.

High light conditions ($36 \pm 2 \text{ mol m}^{-2} \text{ d}^{-1}$)					
Vertical reactor					
$C_{x, N=0}$ (g L ⁻¹)	I_{av} (mol m ⁻² d ⁻¹)	$f_{TAG, batch}$ (% w/w)	$P_{TAG, batch}$ (g m ⁻² d ⁻¹)	$P_{TAG, max}$ (g m ⁻² d ⁻¹)	$Y_{TAG, ph, max}$ (g mol ⁻¹)
1	35 ± 12	34	1.9	3.5 (day3)	0.16 (day3)
1.5	35 ± 10	32	3.2	8.3 (day1)	0.29 (day1)
2.5	39 ± 14	16	2.7	2.9 (day10)	0.08 (day10)
Horizontal reactor					
$C_{x, N=0}$ (g L ⁻¹)	I_{av} (mol m ⁻² d ⁻¹)	$f_{TAG, batch}$ (% w/w)	$P_{TAG, batch}$ (g m ⁻² d ⁻¹)	$P_{TAG, max}$ (g m ⁻² d ⁻¹)	$Y_{TAG, ph, max}$ (g mol ⁻¹)
1	35 ± 12	33	1.0	1.7 (day3)	0.08 (day3)
1.5	35 ± 10	32	1.6	5.4 (day1)	0.19 (day1)
2.5	39 ± 14	25	2.6	3.1 (day10)	0.08 (day4)
Low light conditions ($14 \pm 3 \text{ mol m}^{-2} \text{ d}^{-1}$)					
Vertical reactor					
$C_{x, N=0}$ (g L ⁻¹)	I_{av} (mol m ⁻² d ⁻¹)	$f_{TAG, batch}$ (% w/w)	$P_{TAG, batch}$ (g m ⁻² d ⁻¹)	$P_{TAG, max}$ (g m ⁻² d ⁻¹)	$Y_{TAG, ph, max}$ (g mol ⁻¹)
1	17 ± 7	29	1.4	2.6 (day2)	0.13 (day1)
1.5	17 ± 4	26	1.9	2.6 (day2)	0.14 (day2)
2.5	12 ± 5	21	1.6	2.4 (day2)	0.12 (day2)
Horizontal reactor					
$C_{x, N=0}$ (g L ⁻¹)	I_{av} (mol m ⁻² d ⁻¹)	$f_{TAG, batch}$ (% w/w)	$P_{TAG, batch}$ (g m ⁻² d ⁻¹)	$P_{TAG, max}$ (g m ⁻² d ⁻¹)	$Y_{TAG, ph, max}$ (g mol ⁻¹)
1	17 ± 7	28	0.6	1.5 (day2)	0.07 (day2)
1.5	17 ± 4	31	1.4	2.6 (day1)	0.13 (day1)
2.5	12 ± 5	22	1.0	2.4 (day1)	0.11 (day1)

3.3 Discussion

3.3.1 Effect of initial-biomass-specific light availability on TAG production

With initial-biomass-specific (IBS) light availability (I_{IBS}), it is possible to account for both initial biomass concentration and total irradiance received. With this parameter, it is possible to isolate the effect of light on TAG production, independently of initial biomass concentration and solar conditions. Due to their designs and different areal biomass concentrations, a larger fraction of the light impinging on the ground area was intercepted by the vertical reactor, than by the horizontal one. Therefore, trends for each reactor were considered separately.

At higher IBS-light availabilities ($I_{IBS, batch}$), biomass yield on light ($Y_{x, ph, batch}$; Fig. 3.2A) decreased, whereas TAG content at the end of the batch ($f_{TAG, batch}$; Fig. 3.2B) increased. These trends are in line with previously reported data (Münkel et al. 2013).

Additionally, a clear positive relation between batch IBS-TAG production rate ($r_{TAG, IBS, batch}$) and $I_{IBS, batch}$ was observed in our study, for both reactor configurations (Fig. 3.2C). This relation clearly indicates that N-starvation alone does not guarantee high TAG production rates, and highlights the enhancing role of light on TAG accumulation (Kandilian et al. 2014).

For biorefinery of the biomass, high TAG contents are desired. Fig. 3.2B shows that higher TAG contents ($f_{TAG, batch}$) can be obtained by increasing $I_{IBS, batch}$. Increasing $I_{IBS, batch}$ can be achieved by reducing biomass concentration. However, the amount of biomass present in the system directly influences TAG productivity ($P_{TAG, batch}$). Under the outdoor conditions of the Netherlands, optima for $P_{TAG, batch}$ were found as functions of $I_{IBS, batch}$ (Fig. 3.2D, Table 3.1). Decreasing the biomass concentration below a certain optimum value led to a loss in biomass productivity, because light was likely largely dissipated as heat rather than used, as also observed in the work of (Klok et al. 2013) for N-limited cultures of *Neochloris oleoabundans*. On the contrary, at lower $I_{IBS, batch}$, biomass productivity was enhanced, but $f_{TAG, batch}$ was not always high enough to enable high $P_{TAG, batch}$. In such cases, the applied energy imbalance was inadequate to ensure a high degree of stress and therefore, high specific $r_{TAG, IBS, batch}$ (Klok et al. 2013).

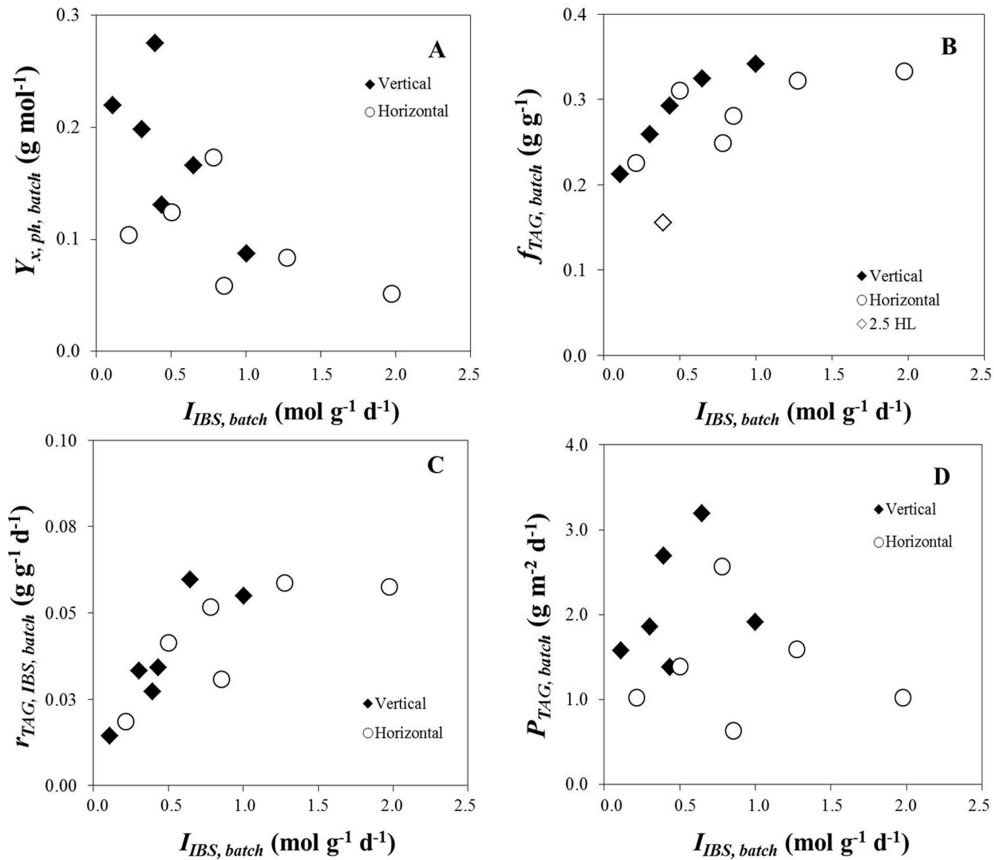


Figure 3.2 Biomass yield on light ($Y_{x, ph, batch}$; **A**), TAG content ($f_{TAG, batch}$; **B**), initial-biomass-specific TAG production rate ($r_{TAG, IBS, batch}$; **C**) and TAG productivity ($P_{TAG, batch}$; **D**) at the end of the batch at increasing initial-biomass-specific light availabilities ($I_{IBS, batch}$) for the different runs in vertical (black diamonds) and horizontal (white circles) reactors.

3.3.2 Optimal settings for outdoor batch TAG production: reactor configuration and initial biomass concentration

As previously discussed, initial-biomass-specific light availability in the system directly influenced both TAG content ($f_{TAG, batch}$) and TAG productivity ($P_{TAG, batch}$) at the end of the batch. As a result, optimal initial biomass concentrations for batch TAG production could be identified for each light condition and reactor configuration.

Regardless of light conditions, an initial biomass concentration of 1.5 g L^{-1} resulted in highest batch TAG contents (32% and 26% w/w at HL and LL, respectively) in VR (Table 3.1). Under these conditions, the trade-off between TAG content and biomass productivity produced highest $P_{TAG, batch}$ ($3.2 \text{ g m}^{-2} \text{d}^{-1}$ and $1.9 \text{ g m}^{-2} \text{d}^{-1}$ at HL and LL, respectively).

Instead, HR, which because of its design receives more direct light, should be operated at higher biomass concentrations to limit photo-saturation and thus, light dissipation under high light conditions. In such a way, the resulting high biomass concentrations (Supplementary material 3.1) will largely compensate for the lower TAG content and TAG production rates.

However, under low light conditions, an intermediate initial biomass concentration (1.5 g L^{-1}) is suggested to reach high $f_{TAG, batch}$ (31% w/w) and $P_{TAG, batch}$ ($1.4 \text{ g m}^{-2} \text{ d}^{-1}$) in HR.

The optima for $P_{TAG, batch}$ as function of initial biomass concentration found within the range of tested initial biomass concentrations, are in contrast with what is reported in literature. In fact, in the studies of Su et al. (2010); Feng et al. (2011); Münkkel et al. (2013), $P_{TAG, batch}$ increased with increasing initial biomass concentration. This discrepancy from the trends observed in our study, could be attributed to different light availabilities due to different reactor designs, light regimes, range of initial biomass concentrations and species (Feng et al. 2011; Münkkel et al. 2013), as well as duration of the nitrogen-starvation period (Su et al. 2010).

We believe that $P_{TAG, batch}$ in HR could be further increased by increasing initial biomass concentration and by optimizing the reactor design. Likely, due to the large distance of the photoactive part from the ground (1 m) and spacing between tubes (0.05 m), a considerable amount of light was lost, thus reducing productivity.

3.3.3 Considerations on outdoor TAG production

The performance of outdoor lipid production processes should be described by productivities and yields calculated on the basis of ground area. Data obtained from a pilot plant can be used for extrapolation to full scale plants if dummy units are included in the pilot to mimic shading effects as if the reactor was placed in a large commercial production facility (Bosma et al. 2014).

Microalgal batch lipid production at pilot-scale has been frequently carried out in flat panel reactors (Feng et al. 2011; Zemke et al. 2013; Münkkel et al. 2013). Those studies were mostly conducted in single panels, without dummies and/or other reactor units. For this reason, productivities/yields obtained with such setups cannot be easily extrapolated to a full-scale plant, in which several reactor units are present and, consequently, reciprocal shadowing is likely to take place. Moreover, because of very different reactor designs, and thus light regimes, it is not possible to compare our results, for tubular reactors, with the ones obtained in flat panels, without falling in misleading assumptions.

To the best of our knowledge, only one data dataset is available for batch lipid production in tubular reactors San Pedro et al. (2014). Table 3.2 shows a comparison of the results obtained by San Pedro et al. (2014) in a vertical tubular reactor with the ones obtained for our run at an initial biomass concentration of 1.5 g L^{-1} in the vertical reactor under high light conditions. Higher TAG content and initial-biomass-specific TAG production rate were obtained in our study suggesting that *Nannochloropsis* sp. is a more suitable alga than *Nannochloropsis gaditana* for TAG production. However, because of the much higher volume-to-ground area ratio for the reactor used by San Pedro et al. (2014), similar TAG productivities were achieved in the two studies.

Table 3.2 Microalga used, initial biomass concentration ($C_{x, N=0}$), duration of the cultivation, reactor type, volume-to-ground area ratio (V/A_{ground}), TAG productivity ($P_{\text{TAG, batch}}$), TAG content ($f_{\text{TAG, batch}}$) and initial-biomass-specific TAG production rate ($r_{\text{TAG, IBS, batch}}$) at the end of the batch are shown for each study. The TAG productivity reported by (San Pedro et al. 2014) was re-calculated using the duration of the actual batch cultivation under N-starvation (i.e. 12 days), neglecting the time necessary to produce inoculum in chemostat-mode.

Microalga	$C_{x, N=0}$ (g L^{-1})	Duration (days)	Reactor type	V/A_{ground} ($\text{m}^3 \text{m}^{-2}$)	$P_{\text{TAG, batch}}$ ($\text{g m}^{-2} \text{d}^{-1}$)	$f_{\text{TAG, batch}}$ (g g^{-1})	$r_{\text{TAG, IBS, batch}}$ ($\text{g g}^{-1} \text{d}^{-1}$)	Ref.
<i>N. gaditana</i>	1.5	12	vertical tubular	0.13	3.1	18	0.02	(San Pedro et al. 2014)
<i>N. sp.</i>	1.5	12	vertical tubular	0.04	3.2	32	0.06	This study

For the *Nannochloropsis* genus, much higher TAG productivities ($4.6\text{-}6.3 \text{ g m}^{-2} \text{d}^{-1}$) and contents (40-48 % w/w) are reported for semi-continuous cultivations in nitrogen-free medium by Rodolfi et al. (2009) and Bondioli et al. (2012). In both cases, a 40% daily culture harvest was applied, resulting in higher light availabilities and therefore corresponding high TAG productivities.

Based on these studies, it seems promising to explore other cultivation modes to increase TAG productivity. Although strategies such as semi-continuous (Rodolfi et al. 2009; Bondioli et al. 2012) or continuous (Klok et al. 2013) cultivations are more complex to operate than a batch, they offer several advantages (Klok et al. 2014). Firstly, process conditions can be adjusted to changing light conditions. Secondly, biomass production and TAG accumulation occur simultaneously. In addition, (semi-) continuous processes require much less downtime than batch processes, which will result in more efficient use of equipment and therefore lower investment costs. Finally, maximum TAG productivities, obtained within the first days of a batch cultivation (Table 3.1), can potentially be maintained for longer periods in optimized (semi-)continuous processes. Overall, these advantages could result in a higher TAG productivity and, by that, reduce land use.

3.4 Conclusions

From this study, the importance of initial-biomass-specific (IBS) light availability on TAG production can be deduced. It was shown that higher TAG contents and IBS-TAG production rates can be achieved by increasing IBS-light availability. Moreover, under the tested outdoor conditions, an optimum for TAG productivity as a function of IBS-light availability was found for each reactor configuration. Based on these trends, an optimal initial biomass concentration for each light condition in the two tested reactor configurations was proposed: under high light, the vertical reactor should be operated at an initial biomass concentration of 1.5 g L^{-1} and the horizontal reactor at 2.5 g L^{-1} . Under low light conditions, an initial biomass concentration of 1.5 g L^{-1} was suggested, regardless of the reactor configuration.

3.5 Materials and methods

3.5.1 Inoculum production

Pre-cultures were maintained in 250 mL Erlenmeyer flasks placed in an orbital shaker incubator (Multitron, Infors HT, The Netherlands) at 120 rpm under 2% CO_2 -enriched headspace, 70% humidity and $50 \mu\text{mol m}^{-2} \text{ s}^{-1}$ continuous light supply.

Subsequently, the flask cultures were used as inoculum for a 4.5 L air-lift flat panel reactor with a 2.5 cm light path. Mass-flow controllers (Brooks Instrument LLC 0254, Hungary) supplied 1.5 L min^{-1} of pressurized air for mixing, as well as CO_2 on demand to keep pH at the set point of 7.5. A culture temperature of $25 \text{ }^\circ\text{C}$ was maintained by a water jacket which was connected to a cryostat (Julabo F12 EH, Germany). For the first cultivation days, the ingoing light intensity was increased daily to keep the outgoing light at about $20 \mu\text{mol m}^{-2} \text{ s}^{-1}$. Thereafter, the ingoing light was set to $1000 \mu\text{mol m}^{-2} \text{ s}^{-1}$.

When the biomass concentration was about 5 g L^{-1} , the culture was used to inoculate an indoor horizontal tubular reactor (280 L). The photoactive part of this reactor was made of eight transparent flexible plastic LDPE tubes (8 m long, \varnothing 0.060 m; Oerlemans Plastics, the Netherlands). The tubes were connected to a manifold, a recirculation pump and a reactor vessel. The liquid velocity was 0.3 m s^{-1} . In the vessel, dissolved oxygen and pH sensors were placed, as well as cooling and heating coil to keep the culture temperature at $25 \text{ }^\circ\text{C}$. The pH was set at 7.5 and controlled by means of on demand CO_2 addition. Since the tubular reactor was located in a greenhouse, it was exposed to natural day/night cycles. However, to achieve higher

biomass productivities, continuous light was supplied by six high-pressure sodium lamps (Hortilux, Schröder, the Netherlands) placed above the tubes. The lamps supplied a light intensity of $350 \mu\text{mol m}^{-2} \text{s}^{-1}$.

In all pre-cultivation steps, cells were grown on filtered natural seawater (obtained from the Oosterschelde, the Netherlands) enriched with (in mM): NaNO_3 , 25; KH_2PO_4 , 1.7; Na_2EDTA , 0.56; $\text{FeSO}_4 \cdot 7\text{H}_2\text{O}$, 0.11; $\text{MnCl}_2 \cdot 2\text{H}_2\text{O}$, 0.01; $\text{ZnSO}_4 \cdot 7\text{H}_2\text{O}$, $2.3 \cdot 10^{-3}$; $\text{Co}(\text{NO}_3)_2 \cdot 6\text{H}_2\text{O}$, $0.24 \cdot 10^{-3}$; $\text{CuSO}_4 \cdot 5\text{H}_2\text{O}$, $0.1 \cdot 10^{-3}$; $\text{Na}_2\text{MoO}_4 \cdot 2\text{H}_2\text{O}$, $1.1 \cdot 10^{-3}$; HEPES (in Erlenmeyer flasks), 20.

3.5.2 Outdoor cultivations under nitrogen-starvation

Right before the onset of nitrogen-depletion, the biomass was harvested from the indoor horizontal tubular reactor and used to inoculate a vertical (VR) and a horizontal (HR) tubular outdoor reactors (Fig. 3.3) in nutrient-enriched, but nitrogen-free, natural seawater. The natural seawater was sterilized by addition of 5 ppm hypochlorite. Once the hypochlorite was removed by an activated carbon filter, the seawater was filtered through cascade filters ($10 \mu\text{m}$, $5 \mu\text{m}$, $1 \mu\text{m}$) and supplied to the reactors. At the beginning of the outdoor experiment (day 0), residual nitrogen (N-NO_3^-) concentration in the medium was negligible ($< 0.10 \text{ mM}$; Supplementary material 3.2).



Figure 3.3 Outdoor tubular reactors used for the nitrogen-starvation regime. Outdoor vertical (A) and horizontal (B) tubular reactors in which the nitrogen-starvation regime was performed.

Each initial biomass concentration (1 g L^{-1} , 1.5 g L^{-1} and 2.5 g L^{-1}) was simultaneously tested in the two outdoor reactors during two seasons. This resulted in two light conditions: high light conditions (HL) refer to an average light intensity on ground area ($I_{\text{ground, av}}$) of $36 \pm 2 \text{ mol m}^{-2} \text{ d}^{-1}$ for the cultivations carried out in May-August 2013; whereas low light conditions (LL) refer to $I_{\text{ground, av}}$ of $14 \pm 3 \text{ mol m}^{-2} \text{ d}^{-1}$ for the cultivations carried out in September-October 2013 and March 2014 (Table 3.3, Supplementary material 3.3).

Both reactors occupied approximately the same ground area (4.4 m² VR, 4.6 m² HR), resulting in an almost two-fold difference in reactor volume: 170 L for VR and 90 L for HR. VR consisted of two interconnected loops, whereas HR had one loop. The photoactive part was made of PMMA tubes (inner \varnothing 0.046 m, outer \varnothing 0.050 m, 0.050 m horizontal and vertical distance between tubes for HR and VR, respectively). To remove oxygen from the culture, strippers (11 L and 22 L for HR and VR, respectively) were installed and air was sparged (1 L min⁻¹) from the bottom through 1 mm holes by air blowers equipped with an air filter (Induvac, MBH series cartridge, 1 μ m). Liquid velocity was set at 0.34 m s⁻¹. To keep the pH at 7.5, CO₂ was added to the culture on demand. A dissolved oxygen sensor was placed at the end of the photoactive part. Partial oxygen pressures never exceeded 300% to prevent oxygen inhibition (Sousa et al. 2012) the specific growth rate was 1.38; 1.36 and 1.06 day⁻¹. Temperature was kept between 20 and 30 °C (Supplementary material 3.4) by means of valves (Proportional Integral Differential regulation) that allowed either warm water (max. 60 °C) or chilled water (8 °C) to move through the double-walled stripper, heating up or cooling down the culture until the set point was reached.

Each reactor was controlled by a PLC (Programmable Logic Controller) connected to a supervisory control and data management system (SCADA). The SCADA was used to control equipment and log online measurements (temperature, pH, liquid/air/CO₂ flows, water). A more detailed description of the systems and equipment is given by Bosma et al. (2014).

3.5.3 Biomass analysis

TAG content and productivity were determined over 12 day-batch cultivation. Every day samples were taken from the reactors at 2:00 p.m., to determine biomass growth (optical density 750 nm and dry weight) and TAG content. Samples for carbohydrate and nitrogen content analysis were taken at day 0, 1, 2, 3, 6 and 12, at the same time of the day. Dry weight was determined as described by Vejrazka et al. (2011) and TAG content of the cells was analyzed as described by Breuer et al. (2013). Carbohydrate content was determined through the Dubois method (1965) using glucose (Sigma-Aldrich G7528) as standard and starch (Fisher Scientific S/7960/53) as positive control. Nitrogen content of the biomass (in %w/w) was determined using a Flash EA 2000 elemental analyzer (ThermoFisher Scientific, USA) at Twente University, the Netherlands.

3.5.4 N-NO₃⁻ analysis

To prevent nitrogen starvation during the inoculum production phase and to verify nitrogen starvation at the start of the outdoor experiments, residual N-NO₃⁻ in the medium was determined with a AQ2 nutrient analyser (Seal Analytical, USA). The method is based on the reduction of nitrate by copperized cadmium to nitrite which reacts with sulphanilamide and N-(1-naphthyl)-ethylenediamide in dilute phosphoric acid to form a reddish-purple azo-dye that can be determined spectrophotometrically at 520 nm (HMSO, 1981; APHA/AWWA/WEF, 4500; USEPA, 19932).

3.5.5 Definitions and calculations

All the parameters calculated according to Eq. 3.1 – 3.7, are expressed as time-averaged functions of cultivation time (i.e. the value at the time point of interest corrected by amount present at time zero and divided by the time from inoculation). “Batch” time-averaged values are obtained at the end of cultivation whereas “maximum” time-averaged values are the peak values encountered during the cultivation. A schematic representation of (time-averaged) ground areal TAG productivity is given in Supplementary material 3.5.

3.5.5.1 Biomass productivity

Biomass productivity at any time point t ($P_x(t)$; g m⁻² d⁻¹) was calculated according to Eq. 3.1;

$$P_x(t) = \frac{C_x(t) - C_{x, N=0}}{t} \cdot \frac{V_R}{A_{ground}} \quad \text{Equation. 3.1}$$

with t as cultivation time (days); C_x as biomass concentration (g L⁻¹); $C_{x, N=0}$ as initial biomass concentration; V_R as reactor volume (L); A_{ground} as ground area (m²).

To extrapolate pilot-plant results to larger scale, A_{ground} was calculated including the empty spaces between the photoactive tubes and half the distance between the photoactive loops and the dummy loops from both sides (Zitelli et al. 2013).

3.5.5.2 Ground areal TAG productivity

TAG productivity at any time point t ($P_{TAG}(t)$; g m² d⁻¹) was calculated according to Eq. 3.2;

$$P_{TAG}(t) = \frac{f_{TAG}(t) \cdot C_x(t) - f_{TAG}(0) \cdot C_{x, N=0}}{t} \cdot \frac{V_R}{A_{ground}} \quad \text{Equation. 3.2}$$

with f_{TAG} as TAG content of biomass (g g⁻¹).

3.5.5.3 *Initial-biomass-specific TAG production rate*

Initial-biomass-specific (IBS) TAG production rate at any time point t ($r_{TAG, IBS}(t)$; $\text{g g}^{-1} \text{d}^{-1}$) indicates the amount of TAG produced per amount of healthy biomass present in the reactor at the start of the cultivation. $r_{TAG, IBS}(t)$ was calculated according to Eq. 3.3;

$$r_{TAG, IBS}(t) = \frac{f_{TAG}(t) \cdot C_x(t) - f_{TAG}(0) \cdot C_{x, N=0}}{C_{x, N=0}} \cdot \frac{1}{t} \quad \text{Equation. 3.3}$$

3.5.5.4 *Light intensity*

Daily light intensity (I_{daily} ; $\text{mol m}^2 \text{d}^{-1}$) was measured by a CaTec Li-Cor LI-190SA sensor. The light impinging on ground area at any time point t ($I(t)$; $\text{mol m}^{-2} \text{d}^{-1}$) was calculated according to Eq. 3.4.

$$I(t) = \frac{\sum_0^t I_{daily}(t)}{t} \quad \text{Equation. 3.4}$$

The average light intensity over the entire cultivation period (I_{av} ; $\text{mol m}^{-2} \text{d}^{-1}$) was calculated according to Eq. 3.4, with $t = 12$ (i.e. last day of batch).

3.5.5.5 *Initial-biomass-specific light availability*

Initial-biomass-specific (IBS) light availability is defined as ratio of light impinging on reactor ground area divided by the initial biomass concentration per ground area. IBS-light availability at any time point t ($I_{IBS}(t)$ $\text{mol g}^{-1} \text{d}^{-1}$) was calculated according to Eq. 3.5;

$$I_{IBS}(t) = \frac{I(t)}{C_{x, N=0} \cdot \frac{V_R}{A_{ground}}} \quad \text{Equation. 3.5}$$

3.5.5.6 *Biomass yield on light*

Biomass yield on light at any time point t ($Y_{x, ph}(t)$; g mol^{-1}) was calculated according to Eq. 3.6.

$$Y_{x, ph}(t) = \frac{P_x(t)}{I(t)} \quad \text{Equation. 3.6}$$

3.5.5.7 *TAG yield on light*

TAG yield on light at any time point t ($Y_{TAG, ph}(t)$; g mol^{-1}) was calculated according to Eq. 3.7.

$$Y_{TAG, ph}(t) = \frac{P_{TAG}(t)}{I(t)} \quad \text{Equation. 3.7}$$

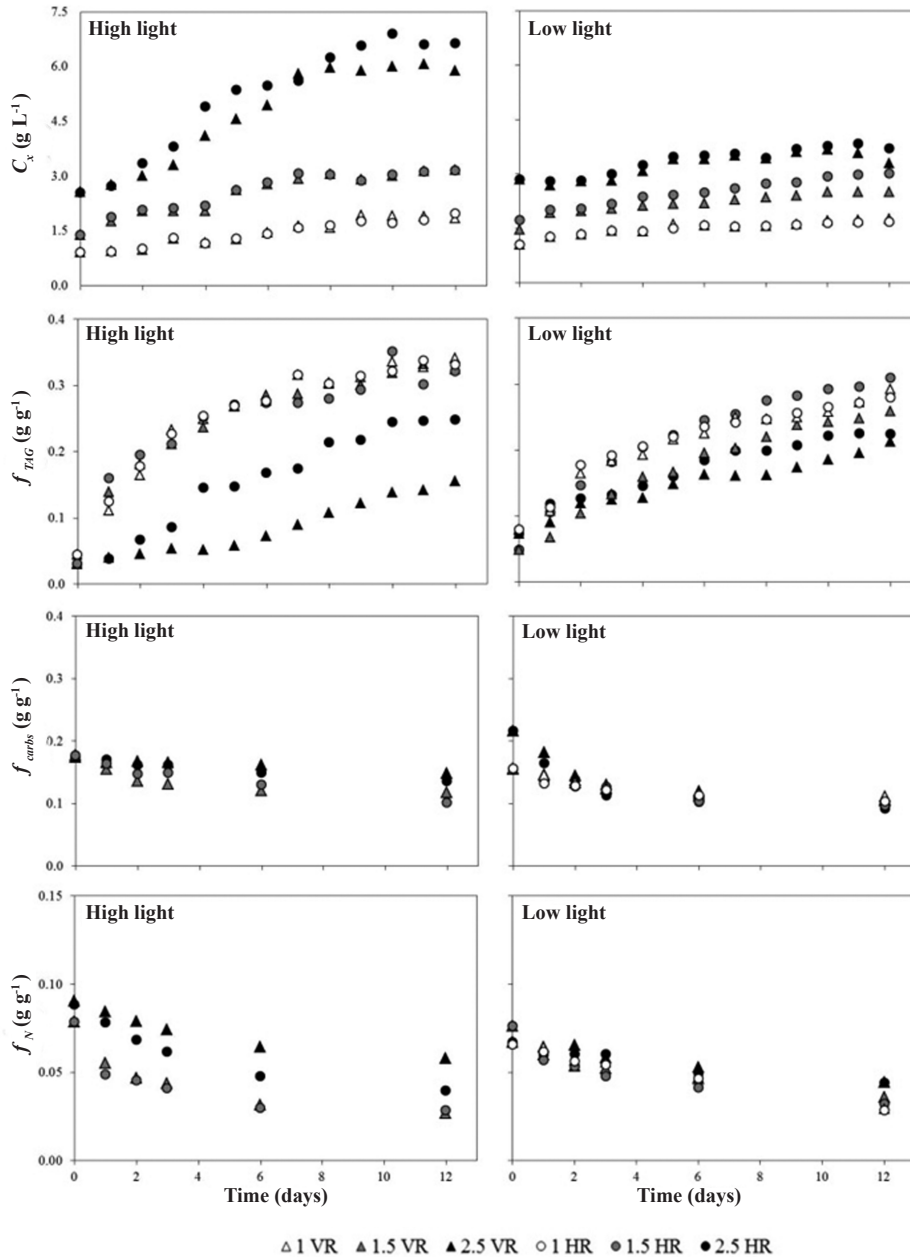
List of symbols and abbreviations

Abbreviation	Description	
HL	High light conditions ($36 \pm 2 \text{ mol m}^{-2} \text{ d}^{-1}$)	
HR	Horizontal (tubular) reactor	
LL	Low light conditions ($14 \pm 3 \text{ mol m}^{-2} \text{ d}^{-1}$)	
VR	Vertical (tubular) reactor	
Symbol	Unit	Description
A_{ground}	m^2	Reactor ground area
$C_x(t)$	g L^{-1}	Biomass concentration at time t
$C_{x, N=0}$	g L^{-1}	Initial biomass concentration
$f_{\text{TAG, batch}}$	g g^{-1}	TAG content at the end of the batch
f_{TAG}	g g^{-1}	TAG content
$I(t)$	$\text{mol m}^{-2} \text{ d}^{-1}$	Time-averaged light intensity at time t
I_{av}	$\text{mol m}^{-2} \text{ d}^{-1}$	Average light intensity
I_{daily}	$\text{mol m}^{-2} \text{ d}^{-1}$	Daily light intensity
$I_{\text{IBS}}(t)$	$\text{mol g}^{-1} \text{ d}^{-1}$	Time-averaged light availability at time t
$I_{\text{IBS, batch}}$	$\text{mol g}^{-1} \text{ d}^{-1}$	Time-averaged initial-biomass-specific light availability at the end of the batch
$P_{\text{TAG}}(t)$	$\text{g m}^{-2} \text{ d}^{-1}$	Time-averaged TAG productivity at time t
$P_{\text{TAG, batch}}$	$\text{g m}^{-2} \text{ d}^{-1}$	Time-averaged TAG productivity at the end of the batch
$P_{\text{TAG, max}}$	$\text{g m}^{-2} \text{ d}^{-1}$	Maximum time-averaged TAG productivity
$P_x(t)$	$\text{g m}^{-2} \text{ d}^{-1}$	Time-averaged biomass productivity at time t
$P_{x, \text{batch}}$	$\text{g m}^{-2} \text{ d}^{-1}$	Time-averaged biomass productivity at the end of the batch
$r_{\text{TAG, IBS}}(t)$	$\text{g g}^{-1} \text{ d}^{-1}$	Time-averaged initial-biomass-specific TAG production rate at time t
$r_{\text{TAG, IBS, batch}}$	$\text{g g}^{-1} \text{ d}^{-1}$	Time-averaged initial-biomass-specific TAG production rate at the end of the batch
V_R	L	Reactor volume
$Y_{\text{TAG, ph}}(t)$	g mol^{-1}	Time-averaged TAG yield on light at time t
$Y_{\text{TAG, ph}^{\text{batch}}}$	g mol^{-1}	Time-averaged TAG yield on light at the end of the batch
$Y_{\text{TAG, ph}^{\text{max}}}$	g mol^{-1}	Maximum time-averaged TAG yield on light
$Y_{x, \text{ph}}(t)$	g mol^{-1}	Time-averaged biomass yield on light at time t
$Y_{x, \text{ph}^{\text{batch}}}$	g mol^{-1}	Time-averaged biomass yield on light at the end of the batch

Acknowledgements

The authors would like to thank the Ministry of Economic Affairs, Agriculture and Innovation and Province of Gelderland, and Biosolar Cells, BASF, BioOils, Drie Wilgen Development, DSM, Exxon Mobil, GEA Westfalia Separator, Heliae, Neste, Nijhuis, Paques, Cellulac, Proviron, Roquette, SABIC, Simris Alg, Staatsolie Suriname, Synthetic Genomics, TOTAL and Unilever for the financial support of the AlgaePARC research program.

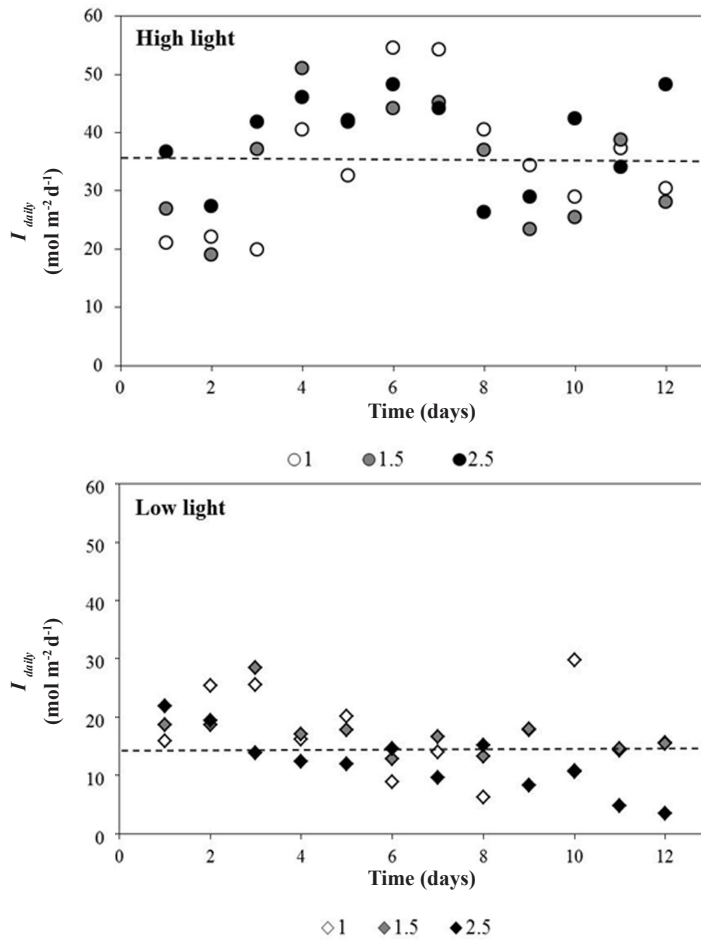
Supplementary material



Supplementary material 3.1 Time-evolution of biomass concentration (C_x), TAG content (f_{TAG}), carbohydrates (f_{carbs}) and nitrogen (f_N) content of the runs at 1, 1.5 and 2.5 g L⁻¹ in the vertical (VR) and horizontal (HR) reactors under high and low light conditions. Nitrogen and carbohydrate content could not be determined for the run inoculated at 1 g L⁻¹ under high light conditions because of small sample volume.

Supplementary material 3.2 Residual N-NO_3^- concentration in the cultivation medium at the start (day 0) of the outdoor runs inoculated at different initial biomass concentrations ($C_{x, N=0}$) under high (HL) and low (LL) light conditions in the vertical (VR) and horizontal (HR) reactors.

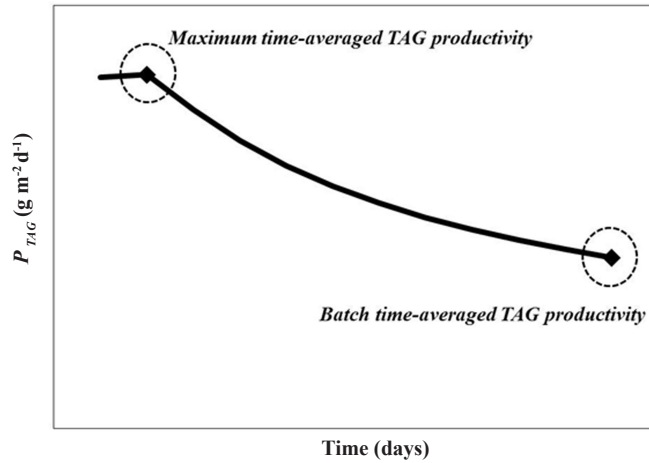
$C_{x, N=0}$ (g L^{-1})	N-NO_3^- (mM)				
	HL		LL		
	VR	HR	VR	HR	HR
1	0.04	0.05	0.10		0.08
1.5	0.02	0.02	0.01		0.03
2.5	0.10	0.10	0.01		0.03



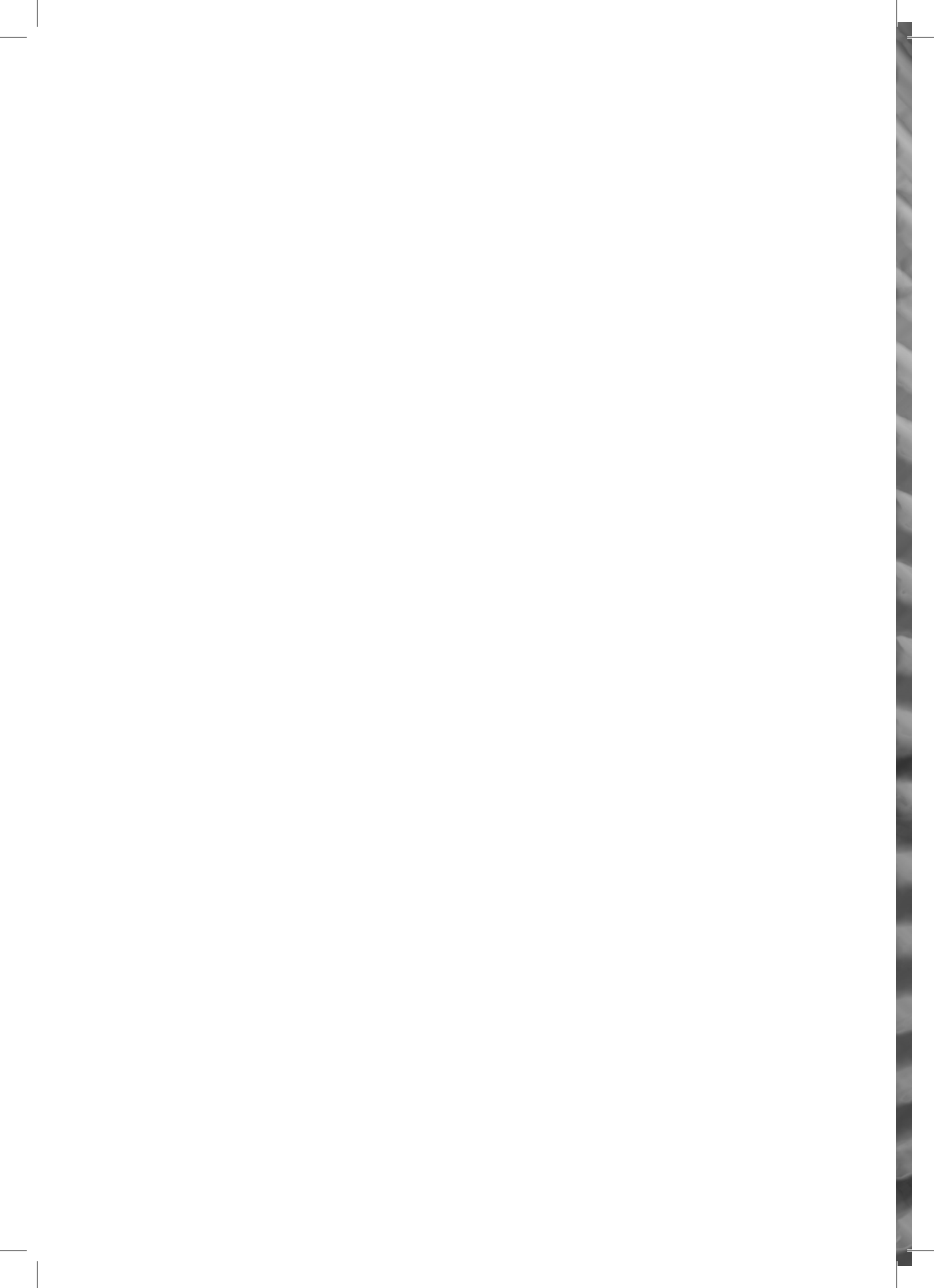
Supplementary material 3.3 Daily light intensity (I_{daily}) for the runs inoculated at 1, 1.5 and 2.5 g L^{-1} . The dotted lines indicate the average light intensity (I_{av}) of 36 ± 2 and 14 ± 3 $\text{mol m}^{-2} \text{d}^{-1}$ for high light (HL) and the high (HL) and the low (LL) light conditions, respectively.

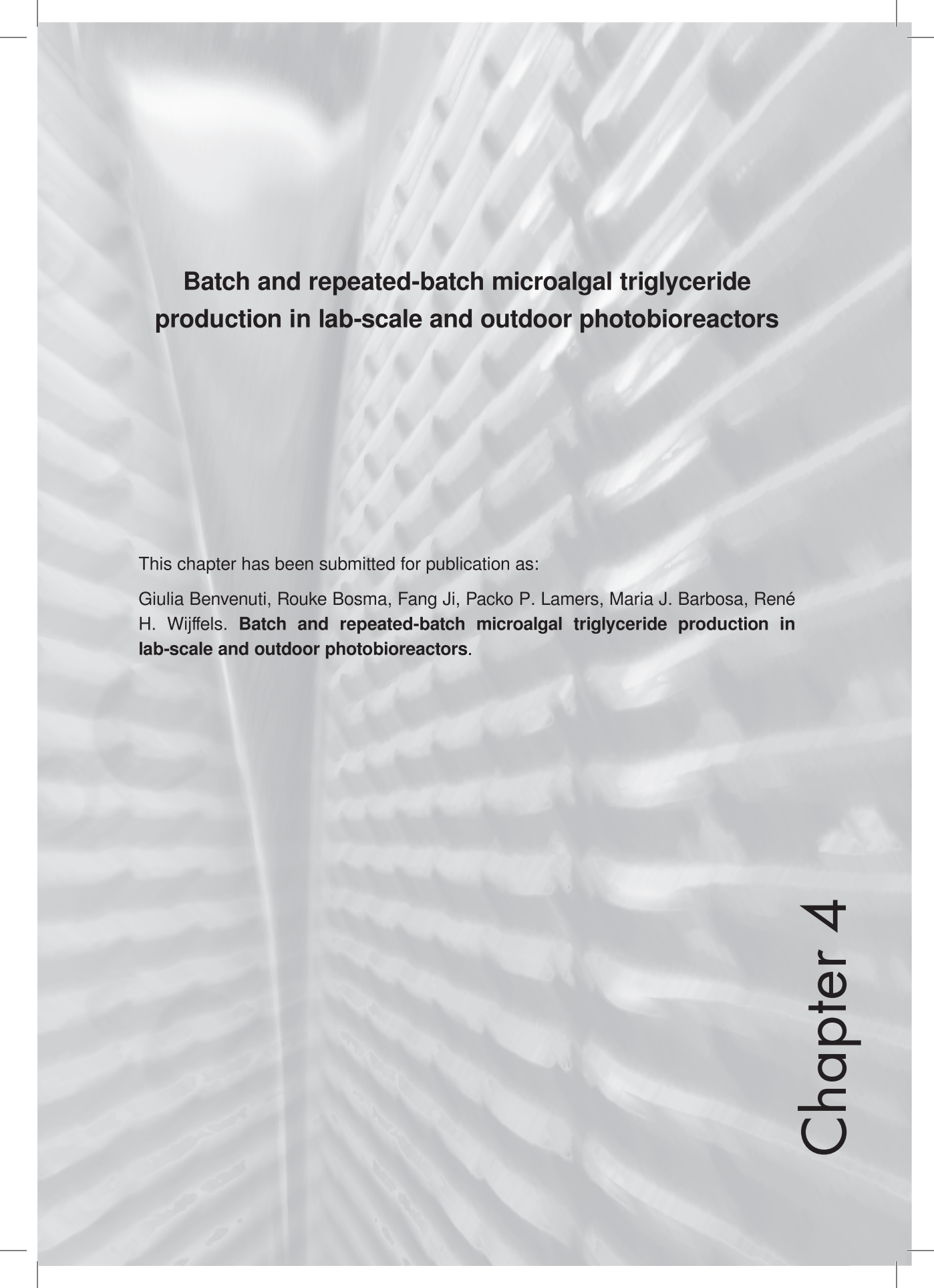
Supplementary material 3.4 Average culture temperature (T_{av}) during the outdoor runs inoculated at different initial biomass concentrations ($C_{x, N=0}$) under high (HL) and low (LL) light conditions in the vertical (VR) and horizontal (HR) reactors.

$C_{x, N=0}$ (g L ⁻¹)	T_{av} (°C)			
	HL		LL	
	VR	HR	VR	HR
1	23	25	22	23
1.5	25	25	23	25
2.5	24	25	21	22



Supplementary material 3.5 Schematic representation of time-evolution of (time-averaged) TAG productivity (P_{TAG}). Maximum and batch time-averaged TAG productivities are highlighted.



A grayscale microscopic image of microalgae cells, showing elongated, rod-shaped structures with internal organelles, arranged in a dense, overlapping pattern. The background is a light, textured surface.

Batch and repeated-batch microalgal triglyceride production in lab-scale and outdoor photobioreactors

This chapter has been submitted for publication as:

Giulia Benvenuti, Rouke Bosma, Fang Ji, Packo P. Lamers, Maria J. Barbosa, René H. Wijffels. **Batch and repeated-batch microalgal triglyceride production in lab-scale and outdoor photobioreactors.**

Abstract

Microalgal triglycerides (TAGs) represent a sustainable feedstock for food, chemical and biofuel industries. Operational strategies (batch, semi-continuous, continuous cultivations) determine TAG productivity. In this study, semi-continuous (i.e. repeated-batch at fixed harvesting frequency) and batch cultivations were compared on TAG production both at lab-scale and in outdoor cultivations. At lab-scale, the repeated-batch TAG productivity was highest for a cycle time of two days (RB1; $0.21 \text{ g L}^{-1} \text{ d}^{-1}$) and similar to the maximum obtained with the batch ($0.23 \text{ g L}^{-1} \text{ d}^{-1}$). Although TAG content was lower for RB1 (22 %) than for the batch (35 %), higher biomass productivities were obtained in RB1. Outdoors, repeated-batch cultivations were subjected to a lower degree of stress (i.e. higher amount of nitrogen present in the system relative to the given irradiance) compared to lab-scale. This yielded low and similar TAG contents (10 – 13 %) in the different repeated-batch runs that were outdone by the batch on both TAG content (15 – 25 %) and productivity (batch: $1.08 - 2.68 \text{ g m}^{-2} \text{ d}^{-1}$; repeated-batch: $0.35 - 0.85 \text{ g m}^{-2} \text{ d}^{-1}$). The lab-scale experiments showed that repeated batch strategies, besides leading to similar TAG productivities compared to the batch, could make TAG production cost-effective by valorising also non-TAG compounds. However, optimization of outdoor repeated-batch cultivations is still required. For instance, the nitrogen supply and the harvest frequency should be adjusted on the total irradiance. Additionally, future research should focus on recovery metabolism upon nitrogen resupply.

Keywords: Microalgae; TAG production; Batch; Semi-continuous; Outdoor.

4.1 Introduction

Under adverse growth conditions, microalgae can accumulate high amounts of fatty acids in the form of triglycerides (TAGs). Microalgal TAGs are increasingly discussed as sustainable feedstock for the commodity markets (i.e. food, chemical and biofuel) (Wijffels et al. 2010; Mata et al. 2010; Draaisma et al. 2013). Microalgae as TAG cell factories offer several potential advantages over agricultural crops, which are currently used to produce those commodities. Besides producing valuable co-products (Mulders et al. 2014), microalgae can be cultivated on non-arable land and they have a low freshwater and fertilizer footprint when grown on wastewaters, sea- or brackish water. Additionally, the whole microalgal biomass can be used (e.g. no branch, leaves etc.), thus allowing complete land coverage. As a consequence, higher areal TAG productivities may be obtained with microalgae compared to agricultural crops (Hu et al. 2008).

At lab-scale, under defined conditions (e.g. temperature, light), high TAG productivities have already been achieved with some microalgal species (Griffiths and Harrison 2009; Breuer et al. 2012; Benvenuti et al. 2014; Ho et al. 2014a). However, it should always be validated whether the productivities obtained at lab-scale can be translated to outdoor cultivations, in which cells are subjected to varying (e.g. light, temperature) conditions. For this reason, outdoor pilot-scale research is essential to identify technical and process bottlenecks that should be tackled before scaling up.

When producing microalgal TAGs, an important aspect to evaluate is the adopted operational strategy (i.e. batch, semi-continuous, continuous cultivations), because it strongly affects process productivity (Benvenuti et al. 2015). Presently, TAG production is widely carried out in a two-step batch process (Zemke et al. 2010; Feng et al. 2011; Münkkel et al. 2013; San Pedro et al. 2014) in which biomass is firstly produced under optimal (e.g. nitrogen replete) conditions, and subsequently subjected to nitrogen (N) starvation to trigger TAG accumulation. A batch process, besides being easy to operate, ensures high final TAG contents (>30% w/w). However, after reaching a maximum within the first days of cultivation, TAG productivity decreases, due to a declining photosynthetic activity during N-starvation (Breuer et al. 2012; Benvenuti et al. 2014). Additionally, at the start of the batch, a fraction of the facility area and time are invested in inoculum production rather than in actual TAG production. Finally, a batch process implies downtime for reactor cleaning and start-up in between runs, thus decreasing productivity and increasing labor, water and chemical demands.

These disadvantages can possibly be overcome by semi-continuous (Rodolfi et al. 2009; Bondioli et al. 2012) and continuous (Klok et al. 2013; Lucas-Salas et al. 2013; Wen et al. 2014) cultivations. Despite these operational modes are more complex to operate, they offer several advantages (Klok et al. 2014). Firstly, maximum TAG

productivities, obtained within the first hours/days of batch cultivations, can potentially be maintained for longer periods in optimized (semi)-continuous processes. Secondly, cultivation settings (e.g. cycle duration) can be adjusted to changing light conditions. Finally, biomass production and TAG accumulation occur simultaneously in the same reactor, and downtime is negligible for long-term runs. Therefore, semi-continuous or continuous processes could result in a stable and robust process with higher TAG productivity compared to the classical batch approach.

Recent advances for (semi)-continuous TAG production have been reported (Bona et al. 2014; Terigar and Theegala 2014; Wen et al. 2014; Ho et al. 2014b). However, to develop a robust alternative process, it is necessary to perform a solid comparison of (semi)-continuous and batch strategies under exactly the same cultivation conditions (e.g. reactor design, light regime, initial biomass-concentration for the TAG-accumulation phase). Additionally, it is very important to perform process comparison not only under defined lab-scale conditions, but also outdoors and assess whether the findings obtained at lab-scale can be translated to outdoor cultivations.

Aim of this study was to investigate semi-continuous (i.e. repeated-batch) cultivations both at lab-scale and outdoors and compare them to batch processes on TAG production. In the adopted strategy, the culture was partially harvested after a fixed number of days from nitrogen-depletion. The harvested volume was replaced by fresh medium containing nitrogen, and the culture was diluted to a fixed biomass concentration. Batch and repeated-batch were simultaneously tested both under defined lab-scale conditions and in outdoor reactors subjected to changing weather conditions and compared on TAG productivity.

4.2 Materials and Methods

4.2.1 Growth medium

In all pre- and cultivation steps both at lab-scale and outdoors, cells were grown on disinfected and filtered natural seawater (Oosterschelde, the Netherlands; (Benvenuti et al. 2015)) enriched with a nutrient stock consisting of (in mM): HEPES (for pre-cultivation in Erlenmeyer flasks), 20; KH_2PO_4 , 1.7; Na_2EDTA , 0.56; $\text{FeSO}_4 \cdot 7\text{H}_2\text{O}$, 0.11; $\text{MnCl}_2 \cdot 2\text{H}_2\text{O}$, 0.01; $\text{ZnSO}_4 \cdot 7\text{H}_2\text{O}$, $2.3 \cdot 10^{-3}$; $\text{Co}(\text{NO}_3)_2 \cdot 6\text{H}_2\text{O}$, $0.24 \cdot 10^{-3}$; $\text{CuSO}_4 \cdot 5\text{H}_2\text{O}$, $0.1 \cdot 10^{-3}$; $\text{Na}_2\text{MoO}_4 \cdot 2\text{H}_2\text{O}$, $1.1 \cdot 10^{-3}$; NaNO_3 , 25 (for pre-cultivation in Erlenmeyer flasks). During cultivation in reactors, nitrogen was supplied as described in section 4.2.2.

4.2.2 Experimental approach

At the start of the batch cultivations, nitrogen (N) was dosed to reach, at N-depletion, the desired starting biomass concentration for the TAG accumulation-phase. At N-depletion, a N-free nutrient stock was supplied to ensure no side effects due to other nutrients limitation. Cultures were kept for 10 days after N-depletion.

In the adopted repeated-batch strategy (Fig. 4.1), cells were inoculated in N-replete conditions (Fig. 4.1, day 0). At N-depletion (Fig. 4.1, day 1), cells started accumulating TAGs and, after a fixed number of days from N-depletion, the culture was partly harvested (Fig. 4.1, day 2) and replenished with natural seawater, enriched with N-free nutrient stock.

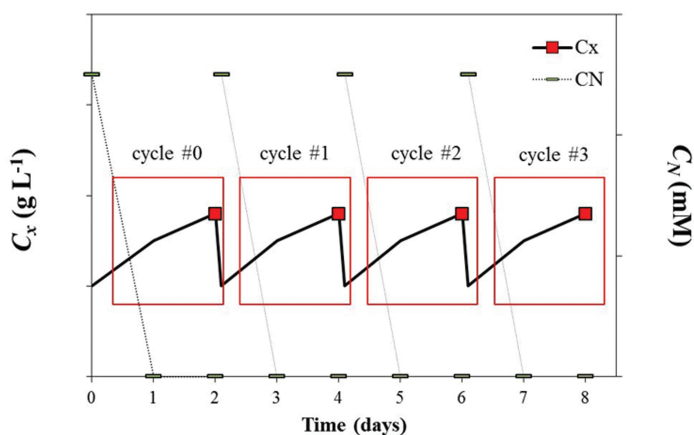


Figure 4.1 Schematic representation of a repeated-batch cultivation in which each cycle starts with addition of nitrogen to reach a set concentration, after which it is consumed within 1 day. A fixed harvest frequency of one day from nitrogen-depletion is applied. The culture is harvested to such an extent that the following cycle starts at a fixed biomass concentration. Red symbols indicate the day at which a harvest is applied. With C_x : biomass concentration and C_N : nitrogen concentration.

The harvested volume was chosen as such that the next cycle started at 1 g L^{-1} . Nitrogen was dosed in the medium as such that each cycle always started with 5 mM (lab-scale) and 2.5 mM (outdoors) of extracellular N. This ensured a re-growth phase that continued until extracellular N was depleted again. At that point, a new TAG-accumulation phase followed until a new harvest was applied.

To harvest the culture at the right frequency (i.e. the right amount of days after N-depletion), preliminary tests were conducted to identify the time at which external N-NO_3^- concentration was zero. Typically, this was at 24 hours after addition of nitrogen for both lab-scale and outdoor runs. Both at lab-scale and outdoors, three different harvest frequencies were applied: 1, 2 and 3 days from N-depletion (RB1, RB2 and RB3, respectively).

4.2.2.1 *Lab-scale cultivations*

Inoculum production and cultivation conditions

Pre-cultures of *Nannochloropsis* sp. CCAP 211/78 were maintained in 250 mL Erlenmeyer flasks, which were placed in an orbital shaker incubator (Multitron, Infors HT, The Netherlands) at 120 rpm under 2% CO₂-enriched headspace, 70% humidity. The flasks were continuously illuminated at a light intensity of 50 μmol m⁻² s⁻¹ supplied by fluorescent lamps (TL-D Reflex 36 W/840, Philips, the Netherlands). Two-week old flask cultures were centrifuged (780 g, 5 minutes) to remove remaining nutrients. Subsequently, cells were re-suspended in N-free medium and inoculated in an airlift-loop photobioreactor with a light path of 20.7 mm, 1.9 L working volume and 0.08 m² surface area (Labfors, Infors HT, 2010). Mass-flow controllers supplied 1.0 L min⁻¹ pressurized air for mixing. The pH was set at 7.5 and controlled by means of on-demand CO₂ addition. A culture temperature of 25 °C was maintained by water recirculation through water jackets that were in direct contact with the reactor cultivation chamber.

Reactors were inoculated at 0.05-0.07 g L⁻¹ biomass concentration. Each repeated-batch cultivation was stopped when three consecutive cycle repetitions were achieved (i.e. constant biomass concentration at harvest), whereas the batch culture was kept for 10 days after N-depletion.

Light supply

For the first cultivation days, the ingoing light intensity was increased daily to keep the outgoing light at about 20 μmol m⁻² s⁻¹. When the biomass concentration reached 0.7 – 0.9 g L⁻¹, simulated day/night light rhythms of a midsummer day in the Netherlands were applied. By applying sinusoidal functions (Eq. 4.1), sunrise and sunset were simulated between 6AM and 10PM. The light intensity gradually increased and reached the maximal value (1500 μmol m⁻² s⁻¹) at 2PM, after which it decreased to zero again.

$$I(t) = \sin\left(\frac{t}{P} \cdot \pi\right) \cdot I_{\max} \quad \text{Equation 4.1}$$

In which t is the amount of hours after sunrise (hours); I_{\max} is the maximum light intensity (μmol m⁻² s⁻¹), P is the duration of the light period (hours).

4.2.2.2 *Outdoor cultivations*

Repeated-batch TAG production processes were also tested under outdoor conditions and their ground areal TAG productivities were compared to those of nitrogen-run-out batch cultivations. The two cultivation strategies were tested at AlgaePARC pilot facilities in Wageningen, the Netherlands (N 51°59'45.88", 5°39'28.15") over different seasons (July-October 2014) in identical vertically stacked horizontal tubular reactors (VRs; 170 L culture volume, 4.4 m² ground area) that were simultaneously operated.

Inoculum production and cultivation conditions

Pre-cultures were maintained in 250 mL Erlenmeyer flasks, as previously described. The flask cultures were used to inoculate a 20 L panel reactor with a 4 cm light path. Mass-flow controllers (Brooks Instrument LLC 0254, Hungary) supplied 1.50 L min^{-1} pressurized air for mixing, as well as CO_2 , which ensured a culture pH of 7.5. A temperature of $25 \text{ }^\circ\text{C}$ was maintained by water recirculation through heating coils. An ingoing light intensity of $350 \mu\text{mol m}^{-2} \text{ d}^{-1}$ was supplied by fluorescence tubes placed in front of the reactor. From this flat panel reactor, a one-week old culture was used to inoculate an outdoor horizontal tubular reactor (90 L) (Benvenuti et al. 2015) operated as turbidostat at 3 g L^{-1} . The biomass produced in this horizontal tubular reactor was used to inoculate the two identical VRs at similar starting biomass concentration ($0.5 - 0.8 \text{ g L}^{-1}$) in N-free medium. One system was operated as batch and the other system as repeated-batch.

In both VRs, the residual nitrogen (N) carried along with the inoculum supported about 0.5 g L^{-1} of newly formed biomass. In such a way, the desired initial biomass concentration ($1.0 - 1.5 \text{ g L}^{-1}$) was reached. This range of biomass concentrations was chosen based on the findings of our previous study (Benvenuti et al. 2015) which identified it as most suitable to achieve high TAG productivities in outdoor tubular reactors. Nitrogen was depleted from the medium within the first 2 – 4 days of cultivation in VRs, depending on the light received in this initial period. The moment of N-depletion was considered as start of the N-starvation phase for the batch and of cycle #0 for the repeated-batch cultivation.

After a fixed number of days from N-depletion, the repeated-batch cultures were harvested and diluted to a set biomass concentration by means of harvest and supply pumps (Bosma et al. 2014). Medium was supplied into the system and, consequently, part of the culture was harvested from the system until the set turbidity value (i.e. biomass concentration) was reached. Offline dry weight determinations were used to calibrate the response curve of turbidity. In all systems, a linear relation of dry weight concentrations and turbidity was found with high accuracy ($R^2 > 0.90$).

For the repeated-batch cultivations, we aimed to harvest the culture at maximum ground areal TAG productivity. Because it was expected that more time is required when less light is available (Benvenuti et al. 2015), lower harvest frequencies were chosen when lower total irradiance was expected (Table 4.1).

The batch cultivation was kept for 10 days after N-depletion, after which the complete reactor was harvested and cleaned before repeating the process again. For the repeated-batch cultivations, the same harvest frequency was tested for about a month (Table 4.1). Exception was the repeated-batch run carried out in the second half of August (RB2). This run was stopped after 14 days because of technical problems.

Table 4.1 Operational period, corresponding time-averaged light intensity ($I_{ground}(t)$), days from N-depletion at which harvest was applied and number of harvest events are reported. RB: repeated-batch, B: batch.

<i>Run</i>	<i>Operational period (2014)</i>	$I_{ground}(t)$ (mol m ⁻² d ⁻¹)	<i># days harvest from N-depletion</i>	<i># harvest events</i>
RB1	July 16 th – August 8 th	37	1	9
B1a	July 12 th – 24 th	39	10	1
B1b	July 26 th – August 6 th	36	9	1
RB2	August 19 th – 28 th	26	2	3
B2	August 15 th – 27 th	23	10	1
RB3	September 10 th – October 6 th	20	3	5
B3a	September 3 rd – 17 th	24	10	1
B3b	September 20 th – October 4 th	18	10	1

Operational settings for the outdoor reactors

In the three outdoor tubular reactors (HR, VR1 and VR2), liquid velocity was set at 0.34 m s⁻¹. To keep the pH at 7.5, CO₂ was added to the culture on demand. Temperature was kept between 20 and 30 °C by means of valves (Proportional Integral Differential regulation) that allowed either warm water (max. 60 °C) or chilled water (8 °C) to flow through a double-walled stripper, heating up or cooling down the culture until the set point was reached. A detailed description of the outdoor systems is given by Bosma et al. (2014) and Benvenuti et al. (2015).

4.2.3 Offline-measurements

Biomass samples were taken between 9 AM and 10 AM from the outdoor cultivations and at 2:00 PM from the lab-scale ones. Biomass concentration was measured daily (optical density 750 nm and dry weight), whereas cellular TAG content was measured only when a harvest was applied. Dry weight was determined as described by Vejrazka et al. (2011) and cellular TAG content was analyzed as described by Breuer et al. (2012) and Breuer et al. (2013a). Residual N-NO₃⁻ in the medium was measured daily, until its depletion, with an AQ2 nutrient analyzer (Seal Analytical, USA) as described by Benvenuti et al. (2015).

4.2.4 Calculations and definitions

4.2.4.1 Time-averaged biomass and TAG productivity for batch and repeated-batch cultivations

Time-averaged volumetric biomass and TAG productivity ($P_{j, vol}(t)$; g L⁻¹ d⁻¹) was calculated according to Eq. 4.2;

$$P_{j, \text{vol}}(t) = \frac{\sum_{i=0}^t (H_j)}{V_R \cdot t_i} \quad \text{Equation. 4.2}$$

In which H_j (g) is the amount of biomass or TAGs present in the harvest (for batch cultivations, H_j was calculated with the total reactor harvest); V_R is the reactor volume (L); t_i is any time point during cultivation (days).

To calculate TAG productivity of the batch cultivations, besides the N-starvation period ($t_{i, \text{N-starvation}}$) also downtime (i.e. reactor cleaning and startup; t_{downtime}) and inoculum production (i.e. amount of biomass present at the moment of N-depletion; $t_{i, \text{inoculum}}$) were considered. The following assumptions were made: downtime was fixed to 1 day, and inoculum was produced in a hypothetical “growth” reactor operated in continuous-mode under optimal conditions (e.g. nitrogen replete and optimal biomass concentration). This hypothetical growth reactor supplied biomass to the batch reactor, which was subsequently subjected to N-starvation to trigger TAG accumulation. Hence, $t_{i, \text{inoculum}}$ (Table 4.2) was calculated using the average light supplied rate over the cultivation period and an average biomass yield on light of 0.59 g mol^{-1} . This biomass yield was found for the most efficient biomass production systems (i.e. flat panel PBR operated with a fixed daily dilution rate of 0.27 d^{-1} over a period of 36 days) at AlgaePARC pilot facility, the Netherlands (de Vree et al. 2015). Thus, the time considered for calculations of batch time-averaged productivities is defined as $t_{i, \text{batch}} = t_{\text{downtime}} + t_{i, \text{inoculum}} + t_{i, \text{N-starvation}}$.

Table 4.2 Time for inoculum production (t_{inoculum}), average light supply rate (I_{supply}), reactor area (A_R) and inoculum concentration ($C_{x, \text{inoculum}}$) for the lab-scale and outdoor batch runs.

	$BI_{\text{lab-scale}}$	$BII_{\text{lab-scale}}$	$B1a_{\text{out}}$	$B1b_{\text{out}}$	$B2_{\text{out}}$	$B3a_{\text{out}}$	$B3b_{\text{out}}$
t_{inoculum} (days)	1.4	1.3	1.9	2.0	3.1	2.7	3.3
I_{supply} (mol d^{-1})	4.4	4.4	172	160	102	105	78
A_R (m^2)	0.08	0.08	4.4	4.4	4.4	4.4	4.4
$C_{x, \text{inoculum}}$ (g L^{-1})	1.92	1.84	1.12	1.10	1.10	0.99	0.91

* A_R is the illuminated reactor surface area for the lab-scale systems and the reactor ground area for the outdoor systems.

For repeated-batch cultivations, both the startup procedure and the inoculum production will take place only at the beginning of the process and this time is negligible for long-term runs. Additionally, for the repeated-batch productivity, the first harvest (cycle #0) was not taken into account. As it was produced from N-replete biomass, it was not representative for a long-term operation. Thus, the start of cycle #1 was considered as start of the repeated-batch cultivations.

4.2.4.2 *Time-averaged ground areal biomass and TAG productivity*

For the outdoor runs, time-averaged ground areal biomass or TAG productivity ($P_{j, \text{ground}}(t)$; $\text{g m}^{-2} \text{d}^{-1}$) was calculated multiplying the time-averaged volumetric productivities by the reactor volume (170 L)-to- ground area (4.4 m^2) ratio.

4.2.4.3 *Biomass and TAG productivity over a repeated-batch cycle*

For the repeated-batch cultivations, biomass and TAG productivity over a repeated-batch cycle ($P_{j, \text{cycle}}$; $\text{g m}^{-2} \text{d}^{-1}$) is also discussed. $P_{j, \text{cycle}}$ was calculated by dividing the harvested biomass or TAGs (H_j ; g) at the end of the cycle by the reactor ground area (m^2) and cycle duration (days).

4.2.4.4 *Time-averaged biomass and TAG yields on light*

Time-averaged biomass ($Y_{x, \text{ph}}(t)$; g mol^{-1}) and TAG ($Y_{\text{TAG}, \text{ph}}(t)$; g mol^{-1}) yield on light were calculated by dividing the time-averaged ground areal biomass or TAG productivity by the time-averaged irradiance ($I_{\text{ground}}(t)$; $\text{mol m}^{-2} \text{d}^{-1}$) received on ground area during the considered time interval.

4.3 Results and discussions

4.3.1 Lab-scale cultivations

4.3.1.1 *Batch cultivations*

In the duplicate batch cultivations, nitrogen ran out at biomass concentrations of 1.92 and 1.84 g L^{-1} (day 4). N-depletion triggered a sharp accumulation of TAGs, which, within 24 hours, increased fourfold (Fig. 4.2).

TAG content steadily increased until stabilizing at about 0.39 g g^{-1} by the end of the cultivation. Maximum time-averaged volumetric TAG productivity ($P_{\text{TAG}, \text{vol}, \text{max}}(t)$; 0.23 $\text{g L}^{-1} \text{d}^{-1}$) and yield on light ($Y_{\text{TAG}, \text{ph}, \text{max}}(t)$; 0.10 g mol^{-1}) were observed after four days of N-depletion (day 8) (Table 4.3).

As shown by Zemke et al. (2013), higher $Y_{\text{TAG}, \text{ph}, \text{max}}(t)$ can be achieved by starting the N-starvation phase at lower biomass concentrations, thus reducing the inoculum production time.

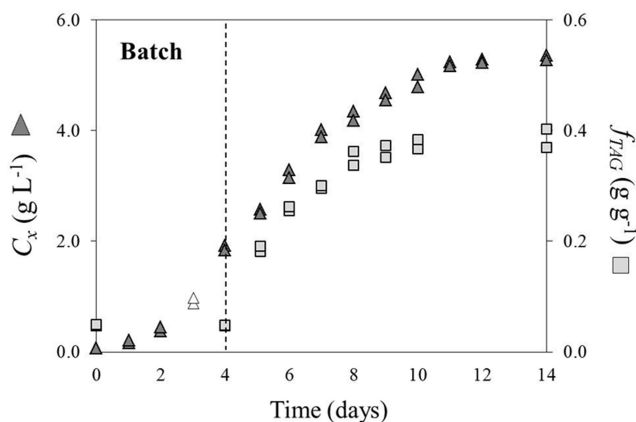


Figure 4.2 Time-evolution of biomass concentration and TAG content for the duplicate lab-scale batch cultivations. Empty symbols represent the day at which light intensity was switched to setpoint. The dotted line indicates day zero of nitrogen-starvation.

Table 4.3 Volumetric biomass productivity ($P_{x, vol}(t)$), biomass yield on light ($Y_{x, ph}(t)$), TAG content (f_{TAG}), volumetric TAG productivity ($P_{TAG, vol}(t)$) and TAG yield on light ($Y_{TAG, ph}(t)$) for the lab-scale batch and repeated-batch runs. Both values are shown for the batch duplicate cultures. RB1, RB2 and RB3 were harvested every 1, 2 and 3 days after nitrogen-depletion, respectively.

Lab-scale runs				
	Batch*	RB1	RB2	RB3
$P_{x, vol}(t)$ (g L ⁻¹ d ⁻¹)	0.68 0.66	0.94 ± 0.02	0.57 ± 0.02	0.43 ± 0.01
$Y_{x, ph}(t)$ (g mol ⁻¹)	0.29 0.28	0.40 ± 0.01	0.25 ± 0.01	0.19 ± 0.00
f_{TAG} (g g ⁻¹)	0.34 0.36	0.22 ± 0.00	0.28 ± 0.01	0.33 ± 0.01
$P_{TAG, vol}(t)$ (g L ⁻¹ d ⁻¹)	0.23 0.24	0.21 ± 0.01	0.16 ± 0.00	0.14 ± 0.00
$Y_{TAG, ph}(t)$ (g mol ⁻¹)	0.10 0.10	0.09 ± 0.00	0.07 ± 0.00	0.06 ± 0.00

* At maximum time-averaged TAG productivity

Higher $Y_{TAG, ph, max}(t)$ were found in batch cultivations under continuous light for *Scenedesmus obliquus* (Breuer et al. 2013b). Besides that the $Y_{TAG, ph, max}$ of different species differs substantially (Griffiths and Harrison 2009; Breuer et al. 2012; Benvenuti et al. 2014), the lower $Y_{TAG, ph, max}$ found in our study under day/night cycles may be explained by the very high incident light intensities experienced during the central hours of the day (up to 1500 $\mu\text{mol m}^{-2} \text{d}^{-1}$). It is indeed known that very high light intensities result in substantial yield losses, whereas lower incident light intensities are beneficial for $Y_{TAG, ph, max}(t)$ (Breuer et al. 2013b). Moreover, during the night, energy storage metabolites are likely be respired to satisfy the maintenance energy demand (Torzillo et al. 1991; Fábregas et al. 2002), thus further decreasing $Y_{TAG, ph, max}(t)$.

4.3.1.2 *Repeated-batch cultivations*

Each repeated-batch run was stopped after three consecutive cycle repetitions (Fig. 4.3A-C). Biomass concentrations (Fig. 4.3) and TAG contents (Table 4.3) at harvest were equal for the consecutive cycle repetitions, excluding the start-up cycle (#0). Furthermore, the biomass concentrations at harvest were similar for the different cycle durations tested, whereas the TAG contents increased at longer cycle durations.

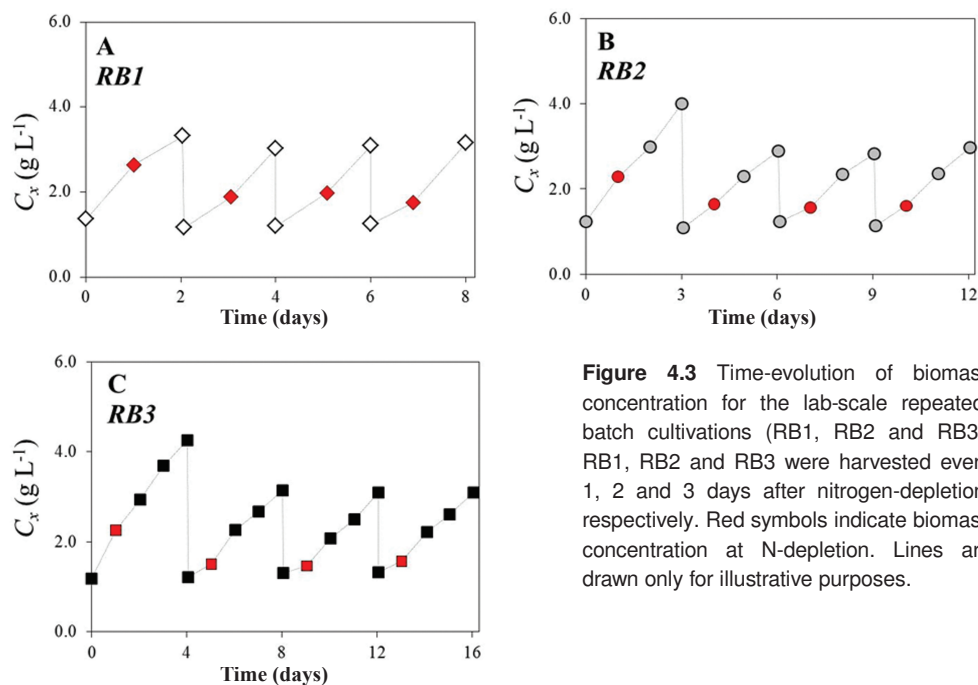


Figure 4.3 Time-evolution of biomass concentration for the lab-scale repeated-batch cultivations (RB1, RB2 and RB3). RB1, RB2 and RB3 were harvested every 1, 2 and 3 days after nitrogen-depletion, respectively. Red symbols indicate biomass concentration at N-depletion. Lines are drawn only for illustrative purposes.

Because cycles #0 (i.e. start-up cycles) started with nitrogen replete cells, higher biomass concentrations were obtained at the harvest after the first cycle compared to the consecutive cycles (# 1-3) that instead began with nitrogen depleted biomass (Fig. 3). Additionally, as also found by Han et al. (2013) for semi-continuous cultures of *Chlorella pyrenoidosa* (harvested at different time intervals and resupplied with a fixed amount of nitrate), biomass concentration at harvest was similar for the different cycle durations (3.00 ± 0.09 g L⁻¹). A possible explanation for this phenomenon is that longer cycles #0 resulted in higher biomass concentrations at harvest (Fig. 4.3) and thus in lower intracellular nitrogen contents at the start of cycles #1. Such lower intracellular nitrogen contents are typically associated with a lower photosynthetic activity (Geider et al. 1998a; Breuer et al. 2015). This likely affected the biomass productivities such that the final biomass concentrations were equal for the different cycle durations. This phenomenon then repeated itself during the following cycles.

Biomass productivity was highest for the shortest cycle duration (i.e. $0.94 \text{ g L}^{-1} \text{ d}^{-1}$ in RB1; Table 4.3). As commonly found in literature (Münkel et al. 2013; Benvenuti et al. 2014), shorter N-starvation periods (i.e. shorter repeated-batch cycles) resulted in a lower TAG content which, in our experiments, ranged from 0.22 to 0.33 g g^{-1} . However, because of the higher biomass productivity, the TAG productivity increased with decreasing cycle duration. The highest TAG productivity ($0.21 \text{ g L}^{-1} \text{ d}^{-1}$) was found for RB1 (Table 4.3).

The repeated-batch TAG productivities obtained at lab-scale are among the highest reported for semi-continuous lab-scale TAG production processes (Chiu et al. 2009; Han et al. 2013; Bona et al. 2014; Ho et al. 2014b). Nevertheless, when looking at the efficiency of light conversion into TAGs, Han et al. (2013) found a higher TAG yield on light for *Chlorella pyrenoidosa* under a much lower and continuous light intensity ($175 \mu\text{mol m}^{-2} \text{ s}^{-1}$). As previously discussed, this discrepancy in yields can likely be attributed to the different species and light regime.

4.3.1.3 Comparison of lab-scale repeated-batch and batch cultivations on TAG production

The average productivities obtained for the constant repeated-batch cycles (#1 - #3) were compared with the maximum batch TAG productivity (i.e. the productivity at the optimal harvest time for the batch). As shown in Table 4.3, the TAG productivity obtained with shortest repeated-batch cycle duration (i.e. RB1; $0.21 \text{ g L}^{-1} \text{ d}^{-1}$) was similar to the maximum TAG productivity of the batch process ($0.23 \text{ g L}^{-1} \text{ d}^{-1}$). Additionally, RB1 resulted in a lower TAG content (RB1: 0.22 g g^{-1} ; batch: 0.35 g g^{-1}) but in much higher total biomass productivities compared to the batch cultivation. About $0.43 \text{ g L}^{-1} \text{ d}^{-1}$ of non-TAG-biomass was made in the batch, whereas $0.73 \text{ g L}^{-1} \text{ d}^{-1}$ was produced in RB1. Several cellular components can contribute to the non-TAG-fraction of the biomass, such as non-acyl lipids, glyco- and phospholipids, sugars and proteins (Wang and Wang 2012; Bondioli et al. 2012). For instance, with the calculated intracellular nitrogen content (Supplementary material 4.1), it is possible to estimate the mass fraction and productivity of proteins (Breuer et al. 2012) that, besides TAGs, represent one of the major biomass constituents with a high economic value (Wijffels et al. 2010). The batch cultivations resulted in an estimated protein content of 0.21 g g^{-1} with a productivity of $0.14 \text{ g L}^{-1} \text{ d}^{-1}$. RB1 yielded similar protein contents (0.24 g g^{-1}) but higher productivities ($0.22 \text{ g L}^{-1} \text{ d}^{-1}$). Therefore, when only the TAG fraction of the biomass is valorized, the lower TAG contents obtained with RB1 will likely result in higher costs for downstream processes (harvesting, dehydration, extraction) (Molina Grima et al. 2003). However, repeated-batch TAG production may become cost-effective if a biorefinery approach is pursued (Wijffels et al. 2010). To valorize the whole biomass, mild cell disruption techniques (e.g. pulsed electric field) and separation technologies (e.g. ionic liquids), which are able to both separate hydrophobic and hydrophilic compounds, should be adopted (Vanthoor-Koopmans et al. 2013).

4.3.2 Outdoor cultivations

4.3.2.1 Batch cultivations

For the batch cultivations, N-depletion occurred at $1.04 \pm 0.09 \text{ g L}^{-1}$, after which TAG accumulation commenced. When comparing runs carried out under different irradiance, yields on light, instead of productivities, should be considered to account for the total amount of light received by the cultures. The time point chosen to compare the different batch runs was the day at which the time-averaged yield of TAG on light was maximal ($Y_{TAG, ph, max}(t)$; i.e. optimal harvest time) (Table 4.4). Under the tested conditions, the highest $Y_{TAG, ph, max}(t)$, corresponding to 0.09 g mol^{-1} , was observed for B2 and B3a (Table 4.4). These runs were performed at intermediate irradiance ($23 - 24 \text{ mol m}^{-2} \text{ d}^{-1}$). At lower irradiance, a larger proportion of the energy was likely redirected to maintenance (Vejrazka et al. 2013) and, consequently, less light was available for TAG synthesis. On the contrary, at high irradiance, light saturation occurred, thus decreasing photosynthetic efficiency.

Table 4.4 Time-averaged ground areal biomass productivity ($P_{x, ground}(t)$), time-averaged biomass yield on light ($Y_{x, ph}(t)$), TAG content (f_{TAG}), time-averaged ground areal TAG productivity ($P_{TAG, ground}(t)$) at maximum time-averaged TAG yield on light ($Y_{TAG, ph, max}(t)$) and time-averaged light intensity ($I_{ground}(t)$) for the outdoor batch runs (B1a, B1b, B2, B3a, B3b). In brackets, the day of nitrogen-starvation at which maximum time-averaged TAG yield on light was found.

Outdoor batch runs					
	B1a	B1b	B2	B3a	B3b
$P_{x, ground}(t)^*$ ($\text{g m}^{-2} \text{ d}^{-1}$)	11.85	9.23	8.99	11.45	6.33
$Y_{x, ph}(t)^*$ (g mol^{-1})	0.36	0.28	0.39	0.46	0.40
f_{TAG}^* (g g^{-1})	0.21	0.21	0.23	0.20	0.15
$P_{TAG, ground}(t)^*$ ($\text{g m}^{-2} \text{ d}^{-1}$)	2.46	1.91	2.06	2.26	0.97
$Y_{TAG, ph, max}(t)$ (g mol^{-1})	0.07 ⁽³⁾	0.06 ⁽³⁾	0.09 ⁽⁶⁾	0.09 ⁽⁵⁾	0.06 ⁽⁴⁾
$I_{ground}(t)$ ($\text{mol m}^{-2} \text{ d}^{-1}$)	39	36	23	24	18

* At maximum time-averaged TAG yield on light

Noteworthy, the lab-scale and the outdoor batch runs lead to similar $Y_{TAG, ph, max}(t)$ (Table 4.3 and Table 4.4) despite completely different culture dynamics, as is apparent from the differences in TAG content and biomass productivity between the lab-scale and outdoors experiments. Noteworthy, the $Y_{TAG, ph, max}(t)$ obtained in our outdoor batch cultivations are comparable with the ones found by Quinn et al. (2012) with the same microalgal species cultivated year-round in outdoor flat-panel photobioreactors in Colorado, USA.

4.3.2.2 Repeated-batch cultivations

In contrast with the lab-scale repeated-batch experiments, the biomass concentration at harvest greatly varied for the outdoor repeated-batch runs ($1.18 - 1.63 \text{ g L}^{-1}$, $1.30 - 1.53 \text{ g L}^{-1}$ and $1.21 - 1.52 \text{ g L}^{-1}$ for RB1, RB2 and RB3 respectively (Fig. 4.4; symbols).

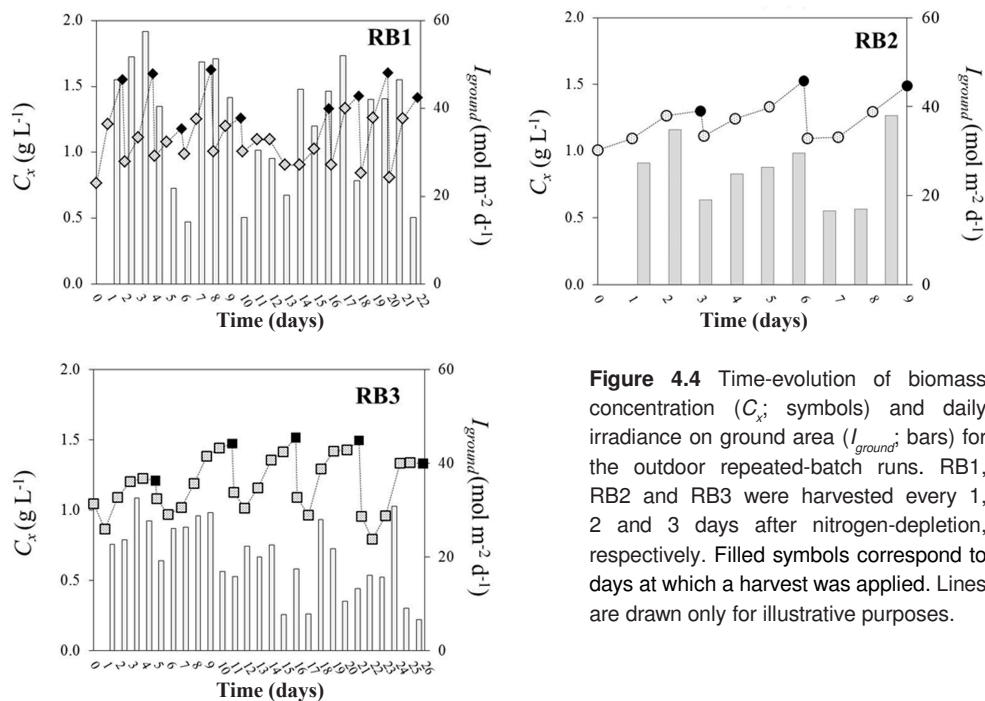


Figure 4.4 Time-evolution of biomass concentration (C_x ; symbols) and daily irradiance on ground area (I_{ground} ; bars) for the outdoor repeated-batch runs. RB1, RB2 and RB3 were harvested every 1, 2 and 3 days after nitrogen-depletion, respectively. Filled symbols correspond to days at which a harvest was applied. Lines are drawn only for illustrative purposes.

This can be attributed to the varying light conditions (Fig. 4.4; bars), and thus, constant cycle repetitions were not obtained. In RB1 and RB2, nitrogen (N) was generally consumed within 24 hours from addition. However, at lower total irradiance, i.e. RB3, N was depleted from the medium only after two or three days from addition. This resulted in longer re-growth phases, which strongly reduced the time-averaged biomass and TAG productivities and yields on light (Table 4.5). Average TAG contents at harvest were low (10 – 13 % w/w) and similar among the different repeated-batch runs (Table 4.5).

Throughout a single repeated-batch run, TAG yield on light ($Y_{TAG, ph, cycle}$) greatly differed over the cycles (Supplementary material 4.2).

Notably, the TAG content and $Y_{TAG, ph, cycle}$ of the outdoor cultures were much lower than those obtained with our lab-scale repeated-batch cultivations (Table 4.3 and Table 4.5). Likely, the outdoor cultures were subjected to a lower degree of stress compared to the lab-scale ones. In other words, outdoors, too much nitrogen was present in the system for the given irradiance and cycle durations, thus resulting in low $Y_{TAG, ph, cycle}$.

Table 4.5 Time-averaged ground areal biomass productivity ($P_{x, ground}(t)$), time-averaged biomass yield on light ($Y_{x, ph}(t)$), average TAG content at harvest (f_{TAG}), time-averaged ground areal TAG productivity ($P_{TAG, ground}(t)$), time-averaged TAG yield on light ($Y_{TAG, ph}(t)$) and time-averaged light intensity ($I_{ground}(t)$) for the outdoor repeated-batch runs. RB1, RB2 and RB3 were harvested every 1, 2 and 3 days after nitrogen-depletion, respectively.

Outdoor repeated-batch runs			
	RB1	B2	RB3
$P_{x, ground}(t)$ (g m ⁻² d ⁻¹)	8.13	4.77	2.66
$Y_{x, ph}(t)$ (g mol ⁻¹)	0.22	0.18	0.13
f_{TAG} (g g ⁻¹)	0.10 ± 0.05	0.13 ± 0.02	0.13 ± 0.01
$P_{TAG, ground}(t)$ (g m ⁻² d ⁻¹)	0.85	0.59	0.35
$Y_{TAG, ph}(t)$ (g mol ⁻¹)	0.022	0.023	0.018
$I_{ground}(t)$ (mol m ⁻² d ⁻¹)	37	26	20

Additionally, the highest $Y_{TAG, ph, cycle}$ of the outdoor repeated batch experiments (i.e. 0.04 g mol⁻¹ corresponding to a $P_{TAG, cycle}$ of 2.2 g m⁻² d⁻¹ found for RB1) was about 1.5-fold lower than the highest $Y_{TAG, ph, cycle}$ (i.e. 0.06 g mol⁻¹ corresponding to a $P_{TAG, cycle}$ of 7.7 g m⁻² d⁻¹) reported by Bondioli et al. (2012) for a semi-continuous cultivation (44% daily harvest) of *Nannochloropsis* sp.. This discrepancy mainly relies on the higher degree of stress applied to cells in the study of Bondioli et al. (2012) compared to our cultivations. Firstly, in their study, no nitrogen (N) was re-supplied after harvest. Secondly, the culture likely experienced higher light availabilities. Because of the higher total irradiance and the reactor used by Bondioli et al. (2012) (i.e. single flat panel not subjected to mutual shadowing from other panels, as was the case for the tubes used in our study), their culture received a higher amount of light. Thus, the combination of lower nitrogen in the system and higher light availabilities resulted in the higher $Y_{TAG, ph, cycle}$ reported by Bondioli et al. (2012).

4.3.3 Outlook on future research

To certainly assess whether repeated-batch TAG production represents an effective alternative to batch processes, several aspects should be further investigated.

Outdoors, focus should be put on the applied stress pressure, and both nitrogen (N) supply and harvest frequency should be adjusted based on the expected total irradiance. Accurate production models could contribute in identifying optimal “nitrogen-to-light ratios“. These models should be developed upon dedicated sets of lab-scale experiments, where the dependency of both N-supply and harvest frequency from irradiance can be investigated under well-defined light regimes.

Subsequently, the models should be validated outdoors under varying light conditions. Daily measurable parameters such as the irradiance, the biomass concentration (e.g. turbidity) and the cellular TAG content (e.g. Nile Red fluorescence (Chen et al. 2009) or FTIR spectroscopy (Miglio et al. 2013; Mayers et al. 2013)) should be used to implement the optimal operational settings in such a way that harvest is always appropriately timed for any given N-supply and any given irradiance.

Additionally, to operate an optimized repeated-batch process, a full understanding of cell recovery mechanisms upon N-replenishment is required as these may greatly affect the productivity of the entire process. Only few research papers have been published on this topic (Siaut et al. 2011; Fernandes et al. 2013; Mulders et al. 2015). In these studies, cells were replenished with an excess of nitrogen after a long N-starvation period (> 7 – 15 days). It was found that the TAGs, which were accumulated during the N-starvation period, were entirely respired within two days from N-replenishment to fuel the recovery process. However, the extent of TAG degradation and its rate depend on several factors such as species-specific photosynthetic responses to N-starvation and recovery, amount of resupplied nitrogen, harvest frequency and harvest volume. Therefore, the dependency of recovery mechanisms on these factors has to be fully understood before an optimal repeated-batch process can be designed.

Finally, as also speculated by Mulders et al. (2015), higher outdoor repeated-batch TAG productivities could possibly be achieved by resupplying the nitrogen around sunset. Culture recovery would then occur at night (Siaut et al. 2011; Přibyl et al. 2013), thereby enhancing TAG production during the light period.

4.4 Conclusions

The lab-scale experiments demonstrated that repeated batch strategies can achieve similar TAG productivities compared to a batch process. Additionally, it was shown that repeated-batch cultivations can potentially make TAG production cost-effective by valorizing also non-TAG-compounds provided that biorefinery of the whole biomass is pursued. Contrarily, further optimization of outdoor repeated-batch strategies is needed as these were always outcompeted by the batch process on both TAG content and productivities. In particular, attention should be given to the chosen repeated-batch operational settings (e.g. nitrogen supply and harvest frequency) as these, together with the total irradiance, determine the applied stress pressure and thus, the productivity of the process.

List of symbols and abbreviations

Abbreviation		Description
B		Batch
RB		Repeated-batch
TAG		Triglyceride
x		Biomass
Symbol	Unit	Description
A_{ground}	m^2	Reactor ground area
C_{N}	mM or g m^{-2}	N-NO_3^- concentration
C_x	g L^{-1}	Biomass concentration
H_j	g	Amount of biomass or TAGs present in the harvest
$I_{\text{ground}}(t)$	$\text{mol m}^{-2} \text{d}^{-1}$	Time-averaged light intensity
$P_{\text{TAG, cycle}}$	$\text{g L}^{-1} \text{d}^{-1}$ or $\text{g m}^{-2} \text{d}^{-1}$	Time-averaged TAG productivity over a repeated-batch cycle
$P_{\text{TAG, ground}}(t)$	$\text{g m}^{-2} \text{d}^{-1}$	Time-averaged ground areal TAG productivity
$P_{\text{TAG, vol}}(t)$	$\text{g L}^{-1} \text{d}^{-1}$	Time-averaged volumetric TAG productivity
$P_{\text{TAG, vol, max}}(t)$	$\text{g L}^{-1} \text{d}^{-1}$	Maximum time-averaged volumetric TAG productivity
$P_{x, \text{ground}}(t)$	$\text{g m}^{-2} \text{d}^{-1}$	Time-averaged ground areal biomass productivity
$P_{x, \text{vol}}(t)$	$\text{g L}^{-1} \text{d}^{-1}$	Time-averaged volumetric biomass productivity
V_{R}	L	Reactor volume
$Y_{\text{TAG, ph}}(t)$	g mol^{-1}	Time-averaged TAG yield on light
$Y_{\text{TAG, ph, cycle}}$	g mol^{-1}	Time-averaged TAG yield on light over a repeated-batch cycle
$Y_{\text{TAG, ph, max}}(t)$	g mol^{-1}	Maximum time-averaged TAG yield on light
$Y_{x, \text{ph}}(t)$	g mol^{-1}	Time-averaged biomass yield on light
$Y_{x, \text{ph, cycle}}$	g mol^{-1}	Time-averaged biomass yield on light over a repeated-batch cycle

Acknowledgements

The authors would like to thank the Ministry of Economic Affairs, Agriculture and Innovation and Province of Gelderland, and Biosolar Cells, BASF, BioOils, Drie Wilgen Development, DSM, Exxon Mobil, GEA Westfalia Separator, Heliae, Neste, Nijhuis, Paques, Cellulac, Proviron, Roquette, SABIC, Simris Alg, Staatsolie Suriname, Synthetic Genomics, TOTAL and Unilever for the financial support of the AlgaePARC research program.

Supplementary material

Supplementary material 4.1 Calculation example of total nitrogen concentration in the reactor ($C_{N\text{ tot}}$) and nitrogen content of the biomass at harvest ($f_{N\text{ harvest}}$) for a given initial biomass concentration ($C_{x,0}$), an assumed initial nitrogen content of nitrogen replete biomass ($f_{N,0}$), a given nitrogen supply ($C_{N\text{ supply}}$) and a measured biomass concentration at harvest ($C_{x,\text{harvest}}$).

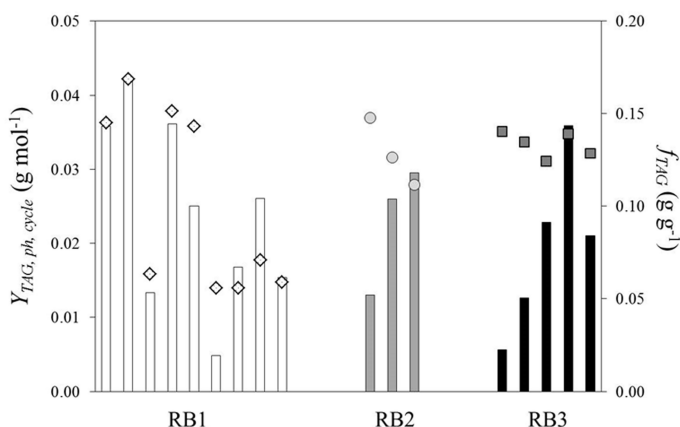
	$C_{x,0}$ (g m ⁻²)	$f_{N,0}$ (g g ⁻¹)	$C_{N,0\text{ intra}}$ (g m ²)	$C_{N\text{ supply}}$ (g m ²)	$C_{N\text{ tot}}$ (g m ²)	$C_{x\text{ harvest}}$ (g m ²)	$f_{N\text{ harvest}}$ (g g ⁻¹)
cycle #0	40	0.08	3.20	1.55	4.75	80	0.06
cycle #1	40	0.06	2.37	1.55	3.92	80	0.05
cycle #n

$$C_{N,0\text{ intra}} = C_{x,0} \cdot f_{N,0} \quad \text{Equation i}$$

where $C_{N,0\text{ intra}}$, $f_{N,0}$ and $C_{x,0}$ are intracellular nitrogen concentration, nitrogen content of nitrogen replete biomass and biomass concentration at the start of the repeated-batch cycle, respectively. A nitrogen content of 0.08 g g⁻¹ was assumed for nitrogen replete biomass as reported by Benvenuti et al. (2015).

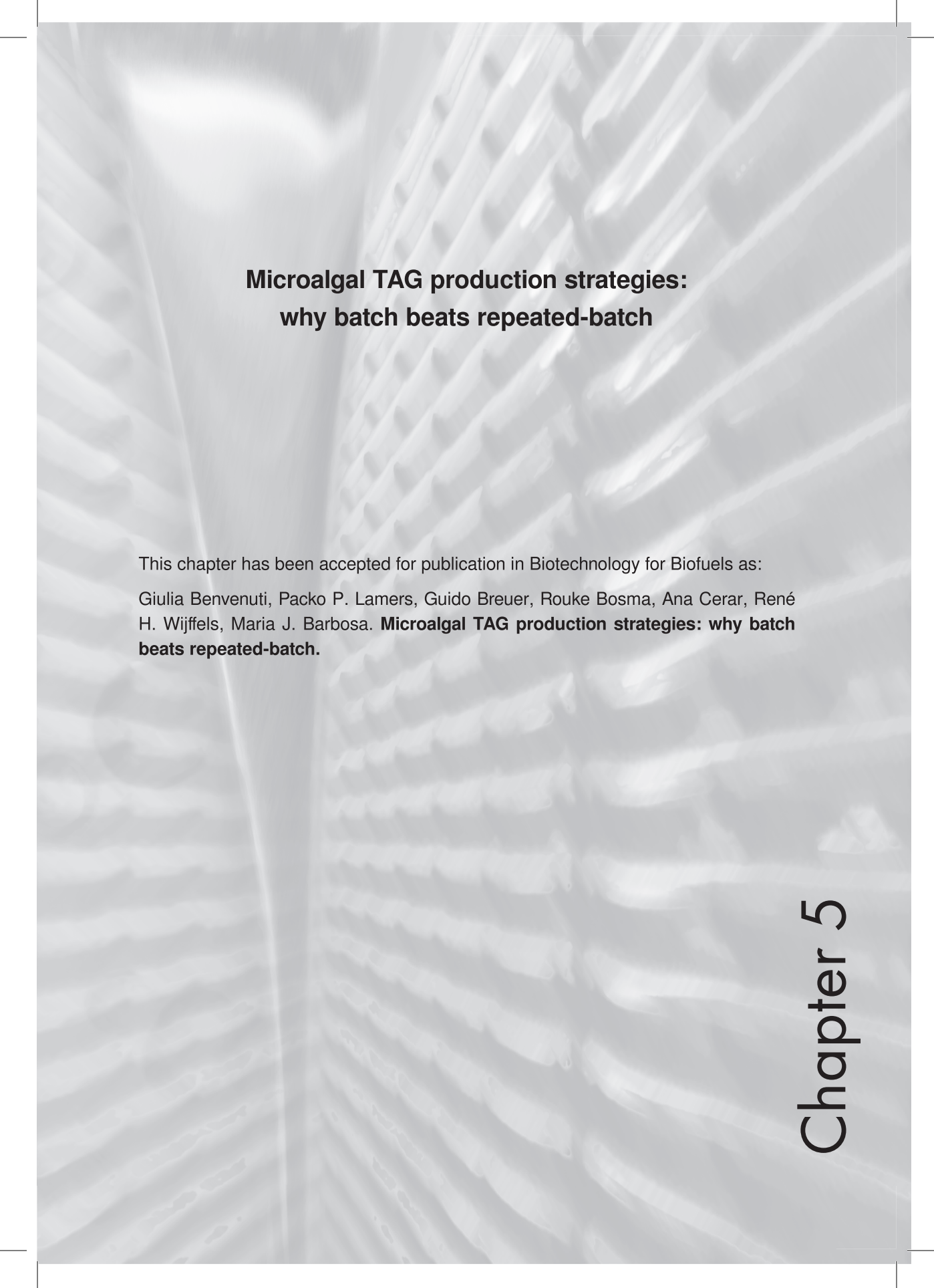
$$f_{N\text{ harvest}} = \frac{C_{N\text{ supply}} + C_{N,0\text{ intra}}}{C_{x\text{ harvest}}} = \frac{C_{N\text{ tot}}}{C_{x\text{ harvest}}} \quad \text{Equation ii}$$

where $f_{N\text{ harvest}}$ and $C_{x\text{ harvest}}$ are nitrogen content of the biomass at harvest and biomass concentration at harvest, respectively; $C_{N\text{ supply}}$ is the nitrogen concentration (in the final culture volume) supplied at the start of the repeated-batch cycle.



Supplementary material 4.2 TAG yield on light over cycle (bars) and TAG content (symbols) at harvest for each outdoor repeated-batch cultivation (RB1, RB2, RB3). RB1, RB2 and RB3 were harvested every 1, 2 and 3 days after nitrogen-depletion, respectively.



A grayscale photograph of a photobioreactor, showing a dense array of vertical tubes. The tubes are filled with a culture, and the lighting creates a strong perspective effect, drawing the eye towards the center. The overall image has a technical and scientific feel.

Microalgal TAG production strategies: why batch beats repeated-batch

This chapter has been accepted for publication in *Biotechnology for Biofuels* as:

Giulia Benvenuti, Packo P. Lamers, Guido Breuer, Rouke Bosma, Ana Cerar, René H. Wijffels, Maria J. Barbosa. **Microalgal TAG production strategies: why batch beats repeated-batch.**

Abstract

For a commercially feasible microalgal triglyceride (TAG) production, high TAG productivities are required. The operational strategy (e.g. batch, repeated-batch) affects the TAG productivity but a systematic comparison between different strategies is lacking. For this, physiological responses of *Nannochloropsis* sp. to nitrogen (N) starvation and N-replenishment were studied in lab-scale batch and repeated-batch cultivations under continuous light, and condensed into a mechanistic model that successfully described both production strategies. The effect of several model parameters (e.g. incident light intensity; maximum photosynthetic rate under nitrogen replete conditions; residual biomass fraction during N-starvation; N-resupply, cycle duration and harvest volume) was investigated. This sensitivity analysis allowed a comparison of the two processes on optimized TAG yields on light. Optimized TAG yields ranged, for batch, from 0.12 g mol⁻¹ (base case at high light) to 0.49 g mol⁻¹ (at low light and with improved strain) and, for repeated batch, from 0.07 g mol⁻¹ (base case at high light) to 0.39 g mol⁻¹ (at low light with improved strain and optimized repeated-batch settings). These base case yields are in line with the yields observed in current state-of-the-art outdoor TAG production. Based on our model simulations we conclude that for continuous light an optimized batch process will always result in higher TAG yield on light compared to an optimized repeated-batch process. This is mainly because repeated-batch cycles start with N-starved cells. Their reduced photosynthetic capacity leads to inefficient light use during the regrowth phase which results in lower overall TAG yields compared to a batch process.

Keywords: Microalgae; TAG production; batch; repeated-batch; recovery; mechanistic model.

5.1 Introduction

Triglycerides (TAGs) are a class of non-polar lipids that are regarded as a sustainable feedstock for the chemical, food and biofuel industries (Wijffels et al. 2010; Draaisma et al. 2013; Chisti 2013). In microalgae, TAGs are accumulated under unfavorable growth conditions (e.g. high light intensities and/or nitrogen limitation/starvation), leading to a reduction in TAG productivity over time (Solovchenko et al. 2007; Klok et al. 2013; Benvenuti et al. 2014). TAG production is often carried out in a two-phase process in which biomass is first produced under nitrogen (N) replete conditions in batch or continuous cultivations, and then TAGs are accumulated under N- depleted conditions in batch-operated cultivations (Benvenuti et al. 2015). In our previous study (Chapter 4), lab-scale repeated-batch cultivations (during which part of the culture is periodically harvested and fresh medium is re-supplied) were investigated leading to similar TAG productivities compared to batch cultivations. Nevertheless, a full optimization of repeated-batch TAG production is still lacking whereas a systematic process comparison is needed. For this, understanding of cell recovery mechanisms upon nitrogen re-addition is necessary as such recovery may greatly affect the productivity of the entire process. In previous studies (Siaut et al. 2011; Přebyl et al. 2013; Mulders et al. 2015) it was found that, once the cells were re-supplied with nitrogen (N) after a long N-starvation period, the TAGs, which were accumulated during N-starvation, were rapidly degraded, thus drastically reducing the TAG productivity of the entire process. Cell recovery depends both on the microalgal species and operational conditions, such as amount of re-supplied nitrogen, harvest frequency and harvest volume.

The aim of this study was to thoroughly assess whether repeated-batch TAG production represents an effective alternative to the classical batch mode for achieving higher TAG productivities. For this, the physiological response of *Nannochloropsis* sp. to nitrogen N-starvation and N-replenishment was investigated in lab-scale batch and repeated-batch cultivations and condensed into a mechanistic model that describes photosynthesis and carbon-partitioning under N-starvation (Breuer et al. 2015) and during recovery after N-replenishment. The model was used to identify potential improvements for both batch and repeated-batch processes and to compare the two processes on optimized TAG yields on light.

5.2 Materials and methods

5.2.1 Growth medium

In all pre- and cultivation steps, cells were grown on disinfected and filtered natural seawater (Oosterschelde, the Netherlands; Benvenuti et al. (2015)) enriched with a nutrient stock consisting of (in mM final concentration): HEPES (for pre-cultivation in Erlenmeyer flasks only), 20; KH_2PO_4 , 1.7; Na_2EDTA , 0.56; $\text{FeSO}_4 \cdot 7\text{H}_2\text{O}$, 0.11; $\text{MnCl}_2 \cdot 2\text{H}_2\text{O}$, 0.01; $\text{ZnSO}_4 \cdot 7\text{H}_2\text{O}$, $2.3 \cdot 10^{-3}$; $\text{Co}(\text{NO}_3)_2 \cdot 6\text{H}_2\text{O}$, $0.24 \cdot 10^{-3}$; $\text{CuSO}_4 \cdot 5\text{H}_2\text{O}$, $0.1 \cdot 10^{-3}$; $\text{Na}_2\text{MoO}_4 \cdot 2\text{H}_2\text{O}$, $1.1 \cdot 10^{-3}$. For pre-cultivation in Erlenmeyer flasks 25 mM of NaNO_3 was added. In the actual experiments, nitrogen was supplied as described in section 5.2.2.

5.2.2 Batch nitrogen run-out and repeated-batch cultivations

Pre-cultures of *Nannochloropsis* sp. CCAP 211/78 were maintained in 250 mL Erlenmeyer flasks, which were placed in an orbital shaker incubator (Multitron, Infors HT, The Netherlands) at 120 rpm under 2% CO_2 -enriched headspace, 70% humidity. The flasks were continuously illuminated at a light intensity of $50 \mu\text{mol m}^{-2} \text{s}^{-1}$ supplied by fluorescent lamps (TL-D Reflex 36 W/840, Philips, the Netherlands). Two-week-old flask cultures were centrifuged (780 g, 5 minutes) to remove remaining nutrients. Subsequently, cells were re-suspended in N-rich medium such that the biomass concentration in the reactor was 0.4 - 0.6 g L^{-1} . Cultivations were performed in a flat panel photobioreactor with a light path of 0.02 m, 1.9 L working volume and 0.08 m^2 surface area (Labfors, Infors HT, 2010). Mass-flow controllers supplied 1.0 L min^{-1} pressurized air for mixing. The pH was set at 7.5 and controlled by means of on-demand CO_2 addition. A culture temperature of 25 °C was maintained by water recirculation through water jackets in direct contact with the reactor cultivation chamber. Initially the ingoing light intensity was kept at $150 \mu\text{mol m}^{-2} \text{d}^{-1}$. When the biomass concentration reached 0.9 - 1.1 g L^{-1} , the light intensity was set at $636 \mu\text{mol m}^{-2} \text{d}^{-1}$. Experiments were carried out under continuous light to isolate the effects of nitrogen replenishment on cell recovery from those due to night respiration.

At N-depletion, the batch cultures were supplied with the N-free stock, to prevent side effects due to limitation of other nutrients than nitrogen, and subsequently cultured for 17 days. In case of repeated batch cultures, every 72 hours 50% of the culture volume was harvested, after which fresh N-rich medium was added to fill the reactor. The nitrogen source was dosed such that the final N-NO_3^- concentration in the reactor at the start of each cycle was either 70 mg L^{-1} (low N supply, LM) or 140 mg L^{-1} (high N supply, HN).

5.2.3 Batch nitrogen replenished cultivation

To study the dynamics of cell recovery after a prolonged nitrogen (N) starvation period, N-rich medium, containing an excess of nitrogen (i.e. 590 mg L⁻¹ final N-NO₃⁻ concentration in the reactor), was re-supplied to the batch culture. 700 mL of N-rich medium were added to 1200 mL of culture broth such that the initial biomass concentration after nutrient replenishment was 2.81 g L⁻¹. The moment of medium addition was considered as the start of the N-replenished batch cultivation. The culture was monitored until the external N-resupply was depleted again (i.e. 120 hours after N-addition).

5.2.4 Offline measurements

Biomass dry weight was determined as described by Vejrazka et al. (2011). The biomass content and profile of both triacylglycerols and polar lipids were analyzed as described by Breuer et al. (2012) and Breuer et al. (2013a). The total carbohydrates were quantified using the method described by Dubois et al. (1956). Cellular nitrogen content of the N-replete biomass at the start of the cultivation was measured with a Flash EA 2000 elemental analyser (ThermoFisher Scientific, USA) at Twente University, the Netherlands. Protein content was estimated by a presumed nitrogen content in proteins of 0.16 g g⁻¹ and by assuming that all nitrogen was present in proteins (Breuer et al. 2012). Residual N-NO₃⁻ in the medium was measured with an AQ2 nutrient analyzer (Seal Analytical, USA) as described by Benvenuti et al. (2015). Cellular nitrogen content throughout the cultivation period was calculated by the increase in biomass concentration, the amount of N-NO₃⁻ consumed during the considered time period and the measured cellular nitrogen at the start of cultivation. Absorption cross-section was measured as described by Vejrazka et al. (2011).

In general, the sum of TAG, polar lipids, carbohydrates and estimated protein mass fractions was always about 0.9 g g⁻¹. Photosystem II maximum efficiency (F_v/F_m) was measured in a portable pulse-amplitude modulated fluorimeter (AquaPen-C AP-C 100, Photon Systems Instruments, Czech Republic; emission peak: 620 nm, saturating light pulse: 2100 μmol m⁻² s⁻¹), as described by Benvenuti et al. (2014).

5.2.5 Modeling batch and repeated-batch TAG production

5.2.5.1 Model structure

The model of Breuer et al. (2015) for batch TAG production with *Scenedesmus obliquus* in flat panel photobioreactors was adapted to describe photosynthesis and carbon partitioning in batch and repeated-batch cultivations of *Nannochloropsis* sp. and to calculate TAG yield on light as a function of the operational strategy. The model

consists of a photosynthesis, a metabolic network and a carbon partitioning module. The photosynthesis module uses the light intensity, reactor geometry and biomass concentration to calculate the biomass-specific photosynthetic rate (Appendix A.1.1). The carbon partitioning module (Fig. 5.1) describes the partitioning of the available photosynthetic capacity, as calculated by the photosynthesis module, into the different biomass constituents (i.e. reproducing biomass, TAG and residual biomass). For this, the photosynthetic and conversion yields are calculated with flux balance analysis in the metabolic network module. Finally, material balances are used to calculate with ordinary differential equations (ODEs, Eq. 5.A.12 – 5.A.15) the biomass concentration and composition during the cultivation using the rates derived from the carbon partitioning module. The cellular nitrogen content is used as proxy for the extent of N-starvation and regulates both the photosynthesis and the carbon partitioning modules. The availability of extracellular nitrogen is used as a switch between metabolic processes occurring at nitrogen replete or nitrogen depleted conditions.

The photosynthesis module, as proposed by Breuer et al. (2015), was adopted without any modification to its mechanisms. The carbon-partitioning mechanism used by Breuer et al. (2015) for the starchless *Scenedesmus* mutant was used because, as it could be deduced from the changes in biomass composition observed during our cultivations, no starch or other storage metabolites are accumulated by *Nannochloropsis* sp. in response to N-starvation. Furthermore, a mechanism for TAG degradation upon N-resupply was devised and implemented into the carbon partitioning module (Fig. 5.1). For this, we included an on/off switch for such TAG degradation that was dependent on the cellular nitrogen concentration, and the enzymatic reactions involved in TAG catabolism (e.g. beta-oxidation) were added to the metabolic network module. Based on our observations, zero-order kinetics for TAG degradation were used. A detailed description of the model equations and the changes compared to the original model of Breuer et al. (2015) are reported in Appendix 5.A.1.

5.2.5.2 Model calibration and validation

The batch model of Breuer et al. (2015) was calibrated using the parameter inputs derived from the nitrogen run-out batch cultivations (Fig. 5.2, Appendix 5.A.2). Next, the physiological insights into cell dynamics upon nitrogen re-addition and recovery metabolism (e.g. TAG degradation), gathered from the repeated-batch and nitrogen replenished batch cultivations (Fig. 5.3 – 5.5), were incorporated into the calibrated model to describe repeated-batch TAG production. As described in detail in Appendices 5.A.1.3 and 5.A.3, the conversion of TAGs into reproducing biomass was modeled using the critical cellular nitrogen content (0.025 g g^{-1}) at which TAG degradation commences, and the TAG degradation rate ($0.011 \text{ g g}^{-1} \text{ h}^{-1}$) as estimated from the N-replenished batch cultivation.

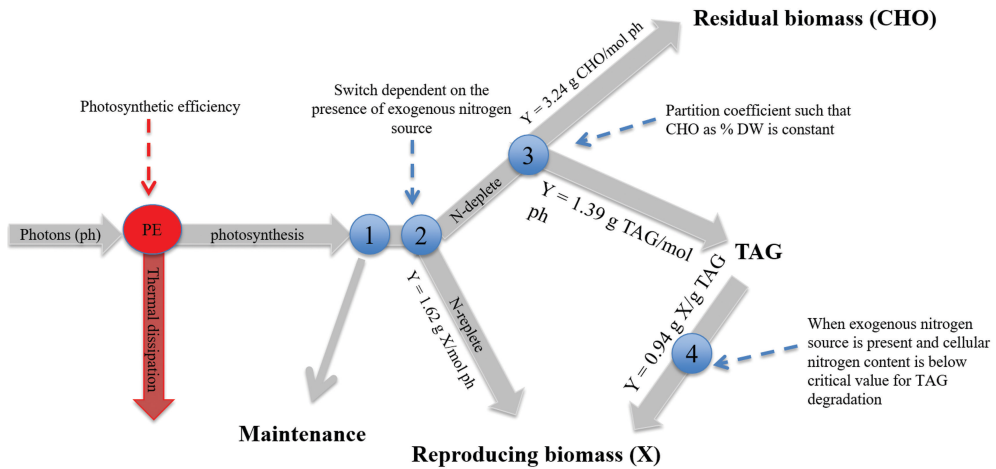


Figure 5.1 Schematic overview of the carbon partitioning module of Breuer et al. (2015) that was supplemented with a mechanism describing TAG degradation upon nitrogen resupply. The photosynthesis module provides the energy available for metabolism at a certain photosynthetic rate (node PE). This photosynthetic capacity is first used to fulfill maintenance (node 1). The latter is assumed to be proportional only to the fraction of reproducing biomass in the total biomass, and thus not to be dependent on the amount of accumulated storage metabolites. In case an extracellular nitrogen source is present, the remaining photosynthetic capacity is used to produce reproducing biomass (node 2), which is constituted of a constant ratio of proteins, carbohydrates, TAGs and other lipids (Appendix 5.A.1.2). Under N-starvation, it is assumed that no reproducing biomass is made, but that a fraction of the remaining photosynthetic capacity is first used for the synthesis of residual biomass (CHO), made of structural carbohydrates, such that the CHO content in the total biomass remains constant (node 3), as also observed during our cultivations. Finally, the remaining photosynthetic capacity is channeled into TAG synthesis. Then, a mechanism for TAG degradation upon N-resupply is devised and implemented in the model. The underlying hypothesis is that, once nitrogen is resupplied in repeated-batch cultivations, TAG degradation occurs only when the photosynthetic capacity of the cells is too low to initiate recovery and reproductive processes. In the model, the intracellular nitrogen content is used as a proxy for the photosynthetic capacity. Thus, when nitrogen is re-supplied following a N-starvation period such that the cellular nitrogen content is above a critical level (i.e. 0.025 g g^{-1} , Appendices 5.A.1.3 and 5.A.3), no TAG degradation will occur. Differently, when nitrogen is re-supplied after a prolonged N-starvation period, during which the cellular nitrogen content has decreased below the critical level, TAGs are converted into reproducing biomass (node 4) at a fixed rate. The illustrated photosynthetic and inter-conversion yields were calculated using flux balance analysis, as shown in Appendix 5.A.1.2.

Figure adapted from Breuer et al. (2015).

5.2.5.3 *Optimization of TAG yield on light*

The impact of several biological and process model parameters on the TAG yield on light was investigated and potential improvements for TAG yield on light was identified. This was done performing Monte-Carlo-sampled combinations of either 1) light intensity, biomass concentration at onset of N-starvation and reactor light path; 2) light intensity, maximum photosynthetic rate under N-replete conditions and residual biomass fraction made during N-starvation; or 3) light intensity, cycle duration, harvest volume and N-supply (Table 5.1). These model parameters were randomly varied within the ranges shown in Table 5.1, after which the model was run to calculate the TAG yield on light obtained for this set of input values. As reference, these simulations were also performed using the value of the parameter under study as estimated from the experimental data (Table 5.A.1 and Table 5.A.2).

The TAG yield on light was chosen as optimization target as this is directly related to areal TAG productivity and represents the best parameter to compare different process strategies and light intensities (Mulders et al. 2014; Breuer et al. 2015). The obtained TAG yield on light of each batch simulation corresponded to the maximum time-averaged yield found during the batch period, corrected for the inoculum production phase. For repeated batch, the simulated yield corresponded to the yield obtained during one constant cycle repetition (Appendix 5.A.1.4, Eq. 5.A.20 – 21).

For the batch, the ODEs, as presented in Appendix 5.A.1.3 (Eq. 5.A.12 – 15), were integrated for a time interval between 0 and 1300 hours, as this was confirmed to be sufficiently large to ensure that maximum TAG yield was always achieved within that interval. For repeated-batch, 20 constant cycle repetitions were simulated. For each combination of tested parameters, 1000 iterations were performed to generate 1000 combinations of parameter values and the corresponding maximum TAG yield on light.

Finally, the optimized TAG yields on light were used to compare batch and repeated-batch on TAG production (Table 5.3).

Table 5.1 Ranges in which parameters were varied for the Monte-Carlo-sampled simulations for batch TAG production. With I_0 : incident light intensity; z : reactor light path; $C_{x, N=0}$: biomass concentration at onset of nitrogen (N) starvation, $q_{ph, max, replete}$: maximum photosynthetic rate of nitrogen replete cells, X_{cho} : residual biomass fraction made during N-starvation; N : amount of nitrogen resupplied after each harvest; f : remaining fraction in the reactor after harvest; Δ : cycle duration.

Monte-Carlo-sampled simulations	I_0 ($\mu\text{mol m}^{-2} \text{s}^{-1}$)	z (m)	$C_{x, N=0}$ (g m^{-3})	$q_{ph, max, replete}$ ($\text{mol g}^{-1} \text{h}^{-1}$)	X_{cho} (g g^{-1})	N (mg L^{-1})	f	Δ (hours)
Batch								
Reference case	200 - 1500	0.02	2451	0.026	0.31	-	-	-
Variable $I_0, C_{x, N=0}, z$	200 - 1500	0.01 - 0.04	1226 - 4903	0.026	0.31	-	-	-
Variable $I_0, q_{ph, max, replete}, X_{cho}$	200 - 1500	0.02	2451	0.013 - 0.039	0.10 - 0.40	-	-	-
Repeated-batch								
Reference case	200 - 1500	0.02	-	0.026	0.17	70	0.5	72
Variable I_0, N, f, Δ	200 - 1500	0.02	-	0.026	0.17	14 - 204	0.1 - 0.9	24 - 192
Variable $I_0, q_{ph, max, replete}, X_{cho}$	200 - 1500	0.02	-	0.013 - 0.039	0.10 - 0.40	70	0.5	72
Variable $I_0, N, f, \Delta, q_{ph, max, replete}, X_{cho}$	200 - 1500	0.02	-	0.013 - 0.039	0.10 - 0.40	14 - 204	0.1 - 0.9	24 - 192

5.3 Results and discussion

5.3.1 Nitrogen run-out batch cultivation

In the batch cultivations, nitrogen (N) was depleted at a biomass concentration of about 2.45 g L^{-1} (Fig. 5.2A). At the end of the cultivation, a 3.5 fold-increase in biomass concentration was observed. Although the biomass specific absorption cross-section (a_x) showed a sudden decrease after the onset of N-starvation (Fig. 5.1B), the volumetric absorption cross-section ($a_{x, vol}$) increased for about 75 hours from the onset of N-starvation, suggesting that, during that period, pigment synthesis continued before declining during N-starvation.

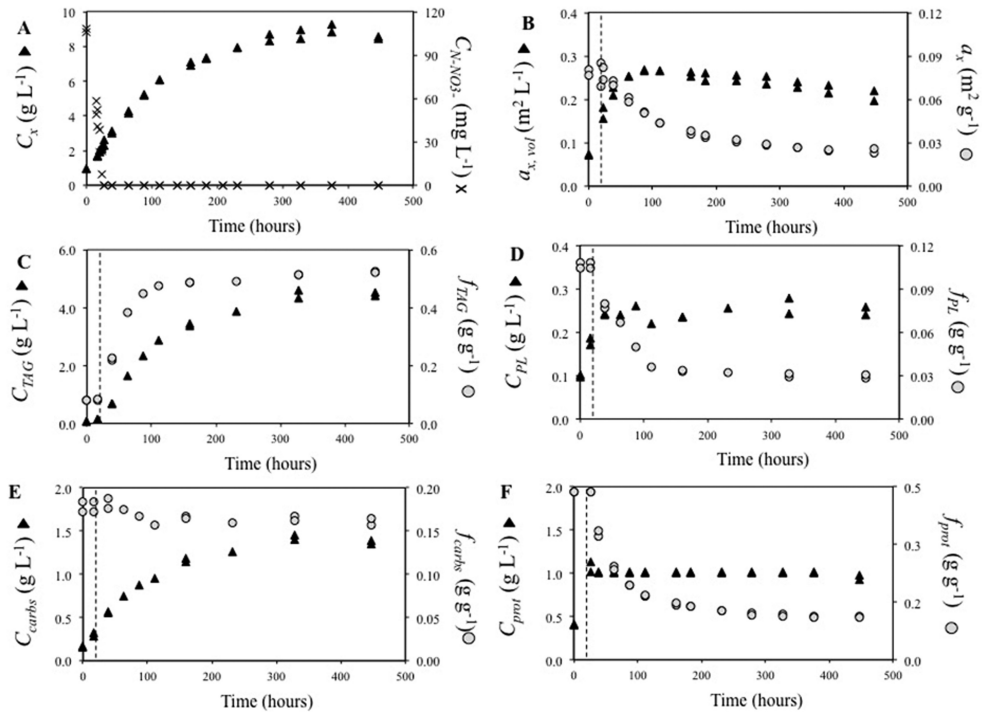


Figure 5.2 Batch nitrogen run-out cultivations. Time-evolution of (A) biomass (C_x) and N-NO_3^- ($C_{\text{N-NO}_3^-}$) concentrations, (B) volumetric ($a_{x, vol}$) and biomass-specific (a_x) absorption cross-section, (C) TAG concentration (C_{TAG}) and content (f_{TAG}), (D) polar lipid concentration (C_{PL}) and content (f_{PL}), (E) carbohydrate concentration (C_{carbs}) and content (f_{carbs}), (F) estimated protein concentration (C_{prot}) and content (f_{prot}). The dotted line indicates the time point at which extracellular N-NO_3^- concentration was zero. Data points for each of the duplicate cultivations are reported, indicating a very high degree of reproducibility.

TAG concentration increased linearly during the first 120 hours of N-starvation (Fig. 5.2C) and, within the first 75 hours of N-starvation, TAGs already represented 45% of cellular dry weight. This resulted in a maximum (time-averaged) TAG yield on light of 0.21 g mol^{-1} (calculated as described in Appendix 5.A.1.4).

Contrarily to TAGs, estimated protein concentration did not increase from the onset of N-starvation, whereas polar lipid production ceased after 75 hours. However, no net polar lipid and protein degradation occurred, as their concentration remained more or less constant until the end of the cultivation, while their content progressively decreased from 0.10 to 0.03 g g^{-1} and from 0.44 to 0.12 g g^{-1} , respectively (Fig. 5.2D and Fig. 5.2F). From the onset of N-starvation, carbohydrate concentration increased more or less proportionally to the increase in TAGs. Hence, carbohydrate content showed only a minor decrease over time (Fig. 5.2E).

5.3.2 Batch nitrogen replenished cultivation

To study the dynamics of cell recovery after a prolonged nitrogen (N)-starvation period, 700 mL of nutrient-enriched natural seawater was resupplied to 1200 mL of the N-starved culture leading to a final N-NO_3^- concentration of 590 mg L^{-1} and to a biomass concentration of 2.81 g L^{-1} . No N-NO_3^- uptake was observed for the first 24 hours after replenishment (Fig. 5.3A). During that period, biomass and TAG concentrations decreased from 2.81 to 2.55 g L^{-1} and from 1.47 to 1.17 g L^{-1} , respectively, with TAG content declining from 0.52 to 0.46 g g^{-1} . Subsequently, within the next 96 hours, N-NO_3^- was completely consumed concurrently with an increase in biomass concentration (Fig. 5.3A), absorption cross-section (Fig. 5.3B), as well as polar lipid (Fig. 5.3D), carbohydrate (Fig. 5.3E) and estimated protein (Fig. 5.3F) concentrations. Inversely, TAG concentration continued decreasing until 72 hours from nutrient-replenishment and TAG content returned to basal-levels (0.08 g g^{-1}) (Fig. 5.3C).

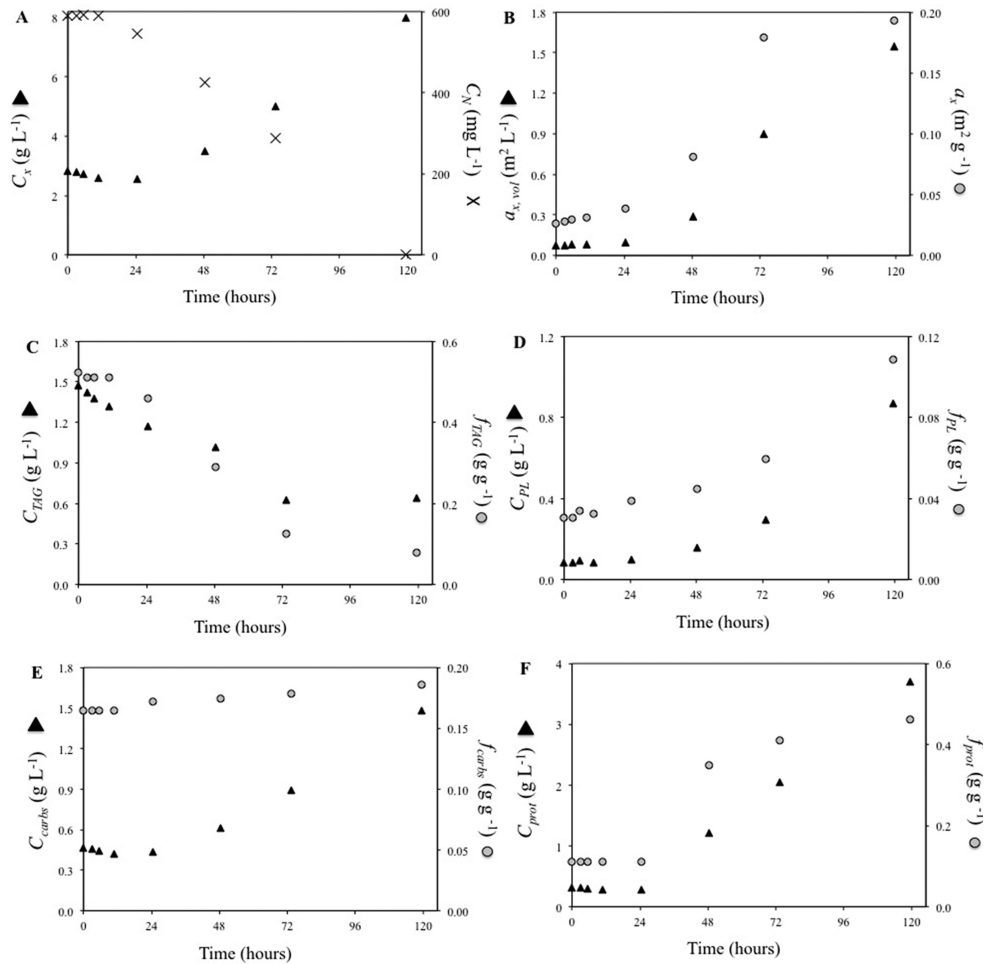


Figure 5.3 Nitrogen-replenished batch cultivation. Time-evolution of (A) biomass (C_x) and N- NO_3^- ($C_{x,\text{vol}}$) concentrations, (B) volumetric ($a_{x,\text{vol}}$) and biomass-specific (a_x) absorption cross-section, (C) TAG concentration (C_{TAG}) and content (f_{TAG}), (D) polar lipid concentration (C_{PL}) and content (f_{PL}), (E) carbohydrate concentration (C_{carbs}) and content (f_{carbs}), (F) estimated protein concentration (C_{prot}) and content (f_{prot}).

5.3.3 Repeated-batch cultivations

The repeated-batch cultivations were stopped when three consecutive and constant cycle repetitions (i.e. steady-state cycles) were achieved (cycles #2 – 4 for the low nitrogen resupply [LN], and cycles #6 – 8 for the high nitrogen resupply [HN]) (Fig. 5.4, Fig. 5.5 and Supplementary material 5.1). At the harvest of the constant cycle repetitions, biomass, TAG, estimated protein and carbohydrate concentrations, pigmentation as well as biomass specific TAG production rates and nitrogen

consumption rates were equal for the consecutive steady-state cycles (standard deviation within 5% of average). The following sections and discussion will primarily focus on the constant cycle repetitions.

Overall, biomass concentration was higher for HN than for LN. In the constant cycle repetitions, biomass concentration increased from $2.88 \pm 0.10 \text{ g L}^{-1}$ to $5.52 \pm 0.05 \text{ g L}^{-1}$ for LN (Fig. 5.4A) and from $3.78 \pm 0.07 \text{ g L}^{-1}$ to $7.30 \pm 0.01 \text{ g L}^{-1}$ for HN (Fig. 5.5A). The volumetric absorption cross section ($a_{x, vol}$) increased until the end of the cycle for HN, and only for the first 34 hours of the cycle for LN, suggesting net pigment production during those periods. Contrarily, a sudden decrease in biomass specific absorption cross-section (a_x) was observed immediately after culture harvest and dilution for both cultivations (Fig. 5.4B and Fig. 5.5B). Then, a_x increased before declining again with the progression of N-starvation.

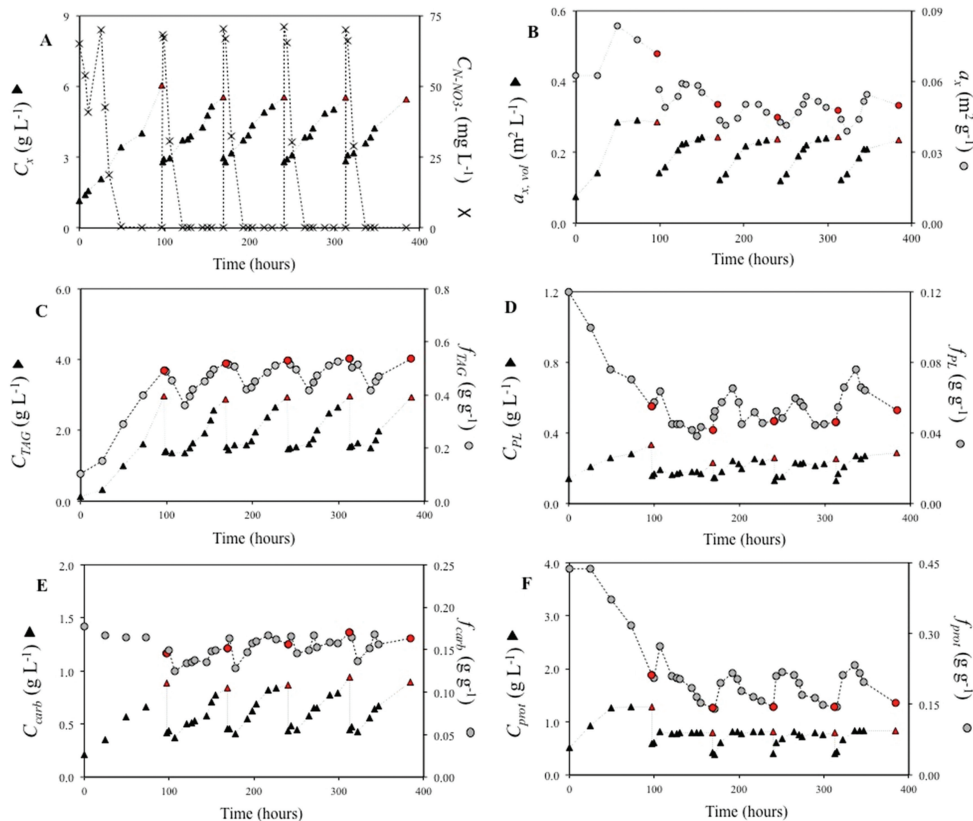


Figure 5.4 Low nitrogen (LN) resupply repeated-batch cultivation. Time-evolution of (A) biomass (C_x) and N-NO_3^- ($C_{\text{N-NO}_3^-}$) concentrations, (B) volumetric ($a_{x, vol}$) and biomass-specific (a_x) absorption cross-section, (C) TAG concentration (C_{TAG}) and content (f_{TAG}), (D) polar lipid concentration (C_{PL}) and content (f_{PL}), (E) carbohydrate concentration (C_{carbs}) and content (f_{carbs}), (F) estimated protein concentration (C_{prot}) and content (f_{prot}). Red symbols indicate the moment at which a harvest was applied. Lines are drawn only for illustrative purposes.

At the harvest of the constant cycle repetitions, TAG concentration was similar ($2.95 \pm 0.02 \text{ g L}^{-1}$ for LN and $3.07 \pm 0.04 \text{ g L}^{-1}$ for HN) for the two cultivations, thus resulting in similar TAG yields on light ($0.13 \pm 0.01 \text{ g mol}^{-1}$ for LN and $0.12 \pm 0.01 \text{ g mol}^{-1}$ for HN) (Supplementary material 5.1), whereas TAG content was $0.54 \pm 0.01 \text{ g g}^{-1}$ for LN and $0.42 \pm 0.01 \text{ g g}^{-1}$ for HN. In both LN and HN cultures, only negligible amounts of TAGs were degraded upon N-resupply (Fig. 5.4C and Fig. 5.5C). During the first 24 - 30 hours of the constant cycle repetitions, TAG concentration remained rather constant while the cellular TAG content decreased from 0.54 ± 0.01 to $0.42 \pm 0.01 \text{ g g}^{-1}$ (LN) and from 0.42 ± 0.01 to $0.27 \pm 0.03 \text{ g g}^{-1}$ (HN). Remarkably, in both cultures, the decrease in TAG content proceeded for about 10 hours after nitrogen was depleted from the medium (Fig. 5.4C and Fig. 5.5C).

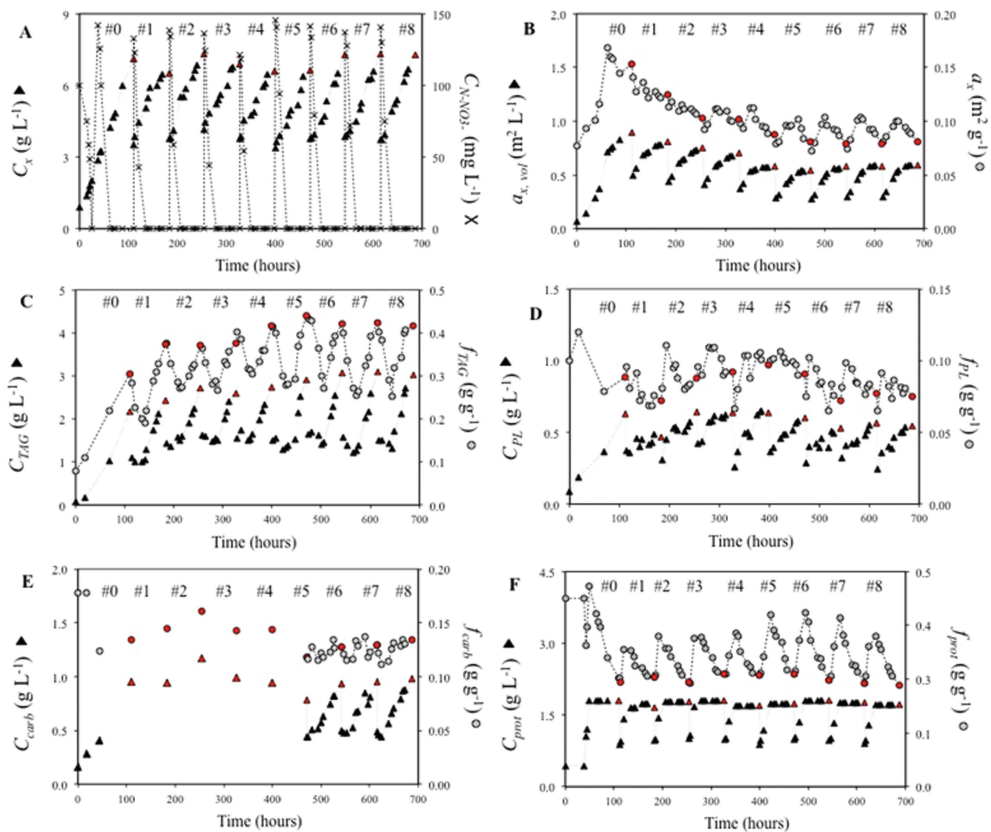


Figure 5.5 High nitrogen (HN) resupply repeated-batch cultivation. Time-evolution of (A) biomass (C_x) and N-NO_3^- ($C_{\text{N-NO}_3^-}$) concentrations, (B) volumetric ($a_{x, \text{vol}}$) and biomass-specific (a_x) absorption cross section, (C) TAG concentration (C_{TAG}) and content (f_{TAG}), (D) polar lipid concentration (C_{PL}) and content (f_{PL}), (E) carbohydrate concentration (C_{carb}) and content (f_{carb}), (F) estimated protein concentration (C_{prot}) and content (f_{prot}). Red symbols indicate the day at which a harvest was applied. Lines are drawn only for illustrative purposes.

Polar lipid concentration increased until harvest in both cultivations, indicating a net production of polar lipids during the cycle, whereas polar lipid content remained rather constant ($0.07 - 0.04 \text{ g g}^{-1}$ for LN and $0.11 - 0.07 \text{ g g}^{-1}$ for HN) (Fig. 5.4D and Fig. 5.5D). Carbohydrate concentration steadily increased over the cycle, indicating a net production of carbohydrates in both cultures, whereas carbohydrate content showed only minor fluctuations upon N-depletion (Fig. 5.4E and Fig. 5.5E).

Cellular nitrogen content fluctuated between $0.026 \pm 0.000 \text{ g g}^{-1}$ and $0.038 \pm 0.001 \text{ g g}^{-1}$ (LN) and between 0.041 ± 0.001 and $0.065 \pm 0.005 \text{ g g}^{-1}$ (HN), peaking, in both cases, at 24 hours of the cycle. In both cultivations, estimated protein concentration increased during the first 10 - 24 hours after nitrogen (N)-supply (Fig. 5.4F and Fig. 5.5F). Upon N-depletion, estimated protein concentration remained constant in both cultures.

5.3.4 Physiological responses to nitrogen starvation and replenishment

5.3.4.1 *Carbon partitioning during N-starvation*

As it is reflected by the high TAG contents of early N-starvation, TAGs were produced at high rates in both nitrogen run-out batch and repeated-batch cultivations (Fig. 5.2C, Fig. 5.4C and Fig. 5.5C), and no other storage compound was accumulated in response to N-starvation (Fig. 2E, Fig. 5.4E and Fig. 5.5E). Differently, Li et al. (2014) reported for *Nannochloropsis oceanica* IMET1 during early N-starvation, a sequential expression of genes involved first in β -(1,3)-glucans (e.g. chrysolaminarin and laminarin) synthesis and then in their degradation. The authors concluded that these sugars were inter-converted into TAGs. However, as it could be deduced from the changes in biomass composition during all our experiments (Figures 5.2 - 5.5), this was not the case for our strain. In fact, in our cultivations, carbohydrate concentration increased proportionally to all other biomass components (i.e. polar lipids, TAGs and estimated proteins) such that their content showed only minor fluctuations. Furthermore, the increase in carbohydrate concentration was observed immediately after N-resupply, thus indicating that the carbohydrates produced during N-starvation were not degraded. Hence, it can be concluded that carbohydrates have a structural role rather than a storage function in *Nannochloropsis* sp.. In addition, as no net degradation of polar lipids was observed during our cultivations (Fig. 5.2D, Fig. 5.4D and Fig. 5.5D), a net conversion of polar lipids into TAGs could be excluded for *Nannochloropsis* sp., which is in contrast from what is reported for *Nannochloropsis gaditana* (Simionato et al. 2013) and *Nannochloropsis oceanica* IMET1 (Li et al. 2014).

5.3.4.2 *Nitrogen uptake upon N-resupply*

In both repeated-batch cultivations, N-uptake started immediately after N-resupply and so did the synthesis of polar lipids, proteins and carbohydrates (i.e. reproducing biomass). Differently, in the N-replenished batch cultivation no net nitrogen uptake, and thus no synthesis of reproducing biomass, was observed during the first 24 hours after N-resupply (Fig. 5.3). This is in contrast with similar N-replenishment batch studies on *Chlorella zofingiensis* (Mulders et al. 2015) and *Dunaliella tertiolecta* (Young and Beardall 2003), for which an almost immediate N-uptake was observed. Besides species-specific differences, the delayed N-uptake can likely be attributed to an energy shortage to fuel N-uptake, which could be due to a low remaining photosynthetic activity caused by the much higher stress pressure to which our N-replenished batch culture was subjected. Indeed, the combination of higher light intensity (636 vs. 150, Young and Beardall (2003) or 500 $\mu\text{mol m}^{-2} \text{s}^{-1}$, Mulders et al. (2015)) and longer N-starvation resulted in a severe impairment of the photosynthetic machinery as indicated by the low maximum PSII efficiency (F_v/F_m) at the moment of N-resupply (Supplementary material 5.2). Moreover, F_v/F_m at the moment of N-resupply was substantially lower in our N-replenished batch culture (0.20) than in our repeated-batch cultivations (0.40 – 0.50) for which N-uptake did commence immediately after N-resupply.

5.3.4.3 *TAG degradation upon N-resupply*

Net TAG degradation was observed for the N-replenished batch cultivation (Fig. 5.3C), whereas it was negligible in both repeated-batch cultures (Fig. 5.4C and Fig. 5.5C). In the N-replenished batch culture, TAG degradation commenced immediately after N-replenishment, likely to generate energy and building blocks to initiate N-uptake and the recovery process. TAGs were degraded at a constant rate to baseline-levels promoting full cell recovery after 72 – 120 hours from N-addition. The observed TAG respiration is in line with the hypothesis that TAGs are accumulated as energy reserve to fuel nitrogen and carbon metabolism once favorable growth conditions are restored but photosynthesis alone cannot initiate recovery and reproductive processes (Turpin 1991; Siaux et al. 2011; Přibyl et al. 2013). For the repeated-batch cultivations, substantial TAG degradation was not observed, because, although the cells were repeatedly subjected to N-starvation cycles, they were exposed to shorter N-starvation periods. The hypothesis that TAG degradation after N-replenishment occurs only when the photosynthetic capacity is heavily impaired, is further supported by the lower F_v/F_m value of the N-replenished batch cultivation compared to the F_v/F_m of the repeated-batch cultures at the moment of N-resupply (Supplementary material 5.2). Thus, in repeated-batch cultivations, TAG degradation is expected only for very high stress pressures (i.e. combinations of long cycle durations, low amounts of re-supplied nitrogen and low harvest volumes).

5.3.5 Comparison with literature

Table 5.2 compares the TAG yields on light obtained in this study with the yields reported in literature for similar batch and repeated-batch cultivations in flat panel PBRs. Note that for batch, only the nitrogen starvation period is considered. In such a way, the effect of the different N-replete growth phases, which were performed under different and, possibly, suboptimal conditions, is neglected.

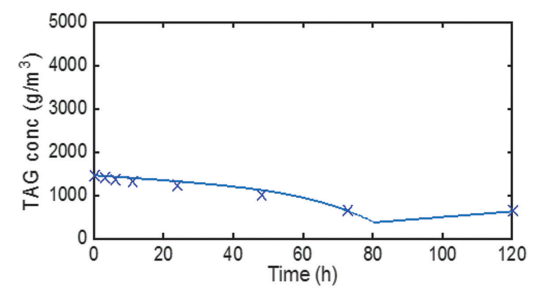
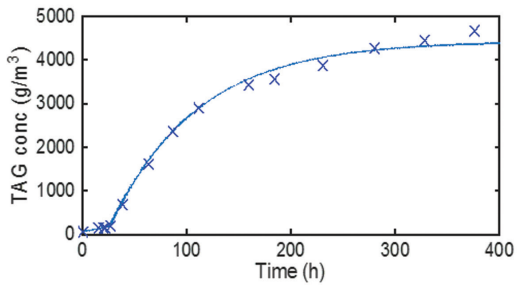
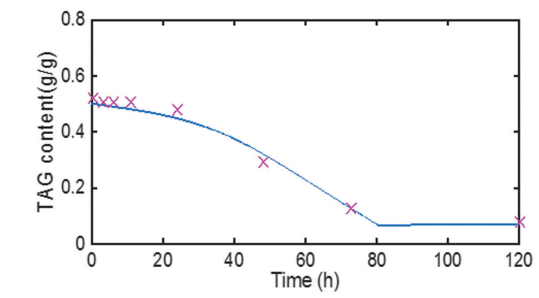
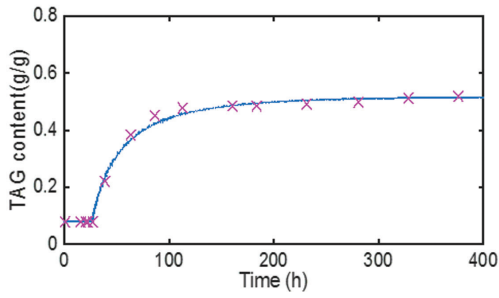
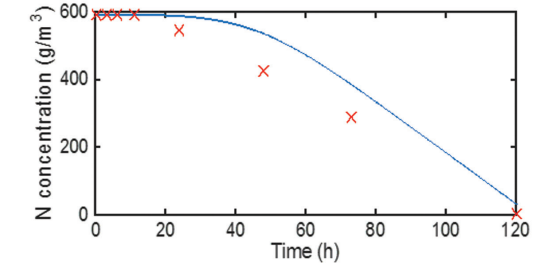
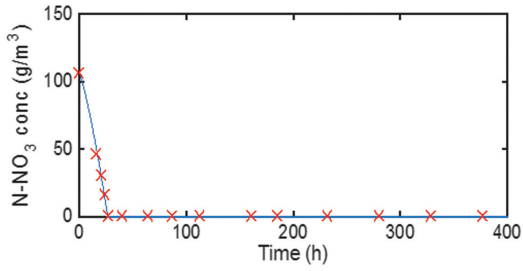
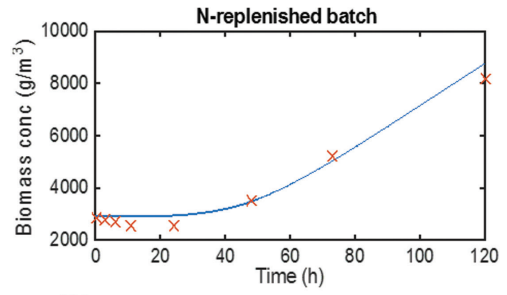
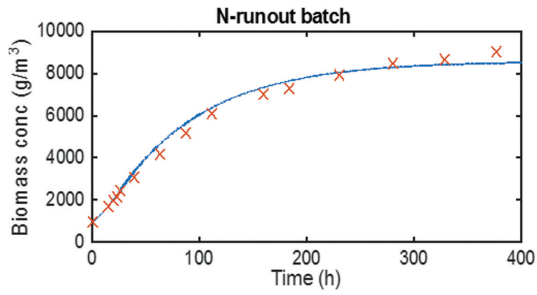
Table 5.2 Comparison of TAG yield on light obtained with various species for both lab-scale batch and repeated-batch cultivations in flat panel PBRs. The nitrogen starvation phase and the constant cycle repetitions are considered for batch and repeated-batch, respectively.

Batch (nitrogen starvation phase)			
Species	TAG yield (g mol ⁻¹)	Light intensity ($\mu\text{mol m}^{-2} \text{s}^{-1}$)	Reference
<i>C. zofingiensis</i>	0.19	500	Mulders et al. (2014)
<i>C. vulgaris</i>	0.05	270	Pruvost et al. (2011)
<i>N. oculata</i>	0.17	250	Van Vooren et al. (2012)
<i>Nannochloropsis</i> sp.	0.14	636 ¹⁾	Chapter 4
<i>Nannochloropsis</i> sp.	0.34	636	This study
<i>N. oleoabundans</i>	0.17	218	Santos et al. (2014)
<i>N. oleoabundans</i>	0.03	270	Pruvost et al. (2009)
<i>S. obliquus</i>	0.22	500	Breuer et al. (2014)
Starchless <i>S. obliquus</i>	0.37	500	Breuer et al. (2014)
Repeated-batch (constant cycle repetitions)			
Species	TAG yield (g mol ⁻¹)	Light intensity ($\mu\text{mol m}^{-2} \text{s}^{-1}$)	Reference
<i>C. pyrenoidosa</i>	0.12	175	Han et al. (2013)
<i>Nannochloropsis</i> sp.	0.07	636 ¹⁾	Chapter 4
<i>Nannochloropsis</i> sp.	0.13	636	This study (LN)
<i>Nannochloropsis</i> sp.	0.12	636	This study (HN)

¹⁾ Average daily light intensity supplied as a day/night cycle.

Despite that in the studies of Pruvost et al. (2009); Pruvost et al. (2011); Van Vooren et al. (2012); Han et al. (2013); Breuer et al. (2014); Santos et al. (2014); Mulders et al. (2014) with different species, a lower incident light intensity was applied, which is a condition known to be beneficial for TAG yield on light (Breuer et al. 2013b), comparable or higher batch and repeated-batch TAG yields were obtained with *Nannochloropsis* sp. in the present study. This confirms that this species is a highly productive microalga (Benvenuti et al. 2014).

The lower yields reported in chapter 4 for lab-scale batch and repeated-batch cultivations of the same microalga subjected to day/night cycles can likely be attributed to losses due to photo-saturation at the very high light intensities experienced during the central hours of the day.



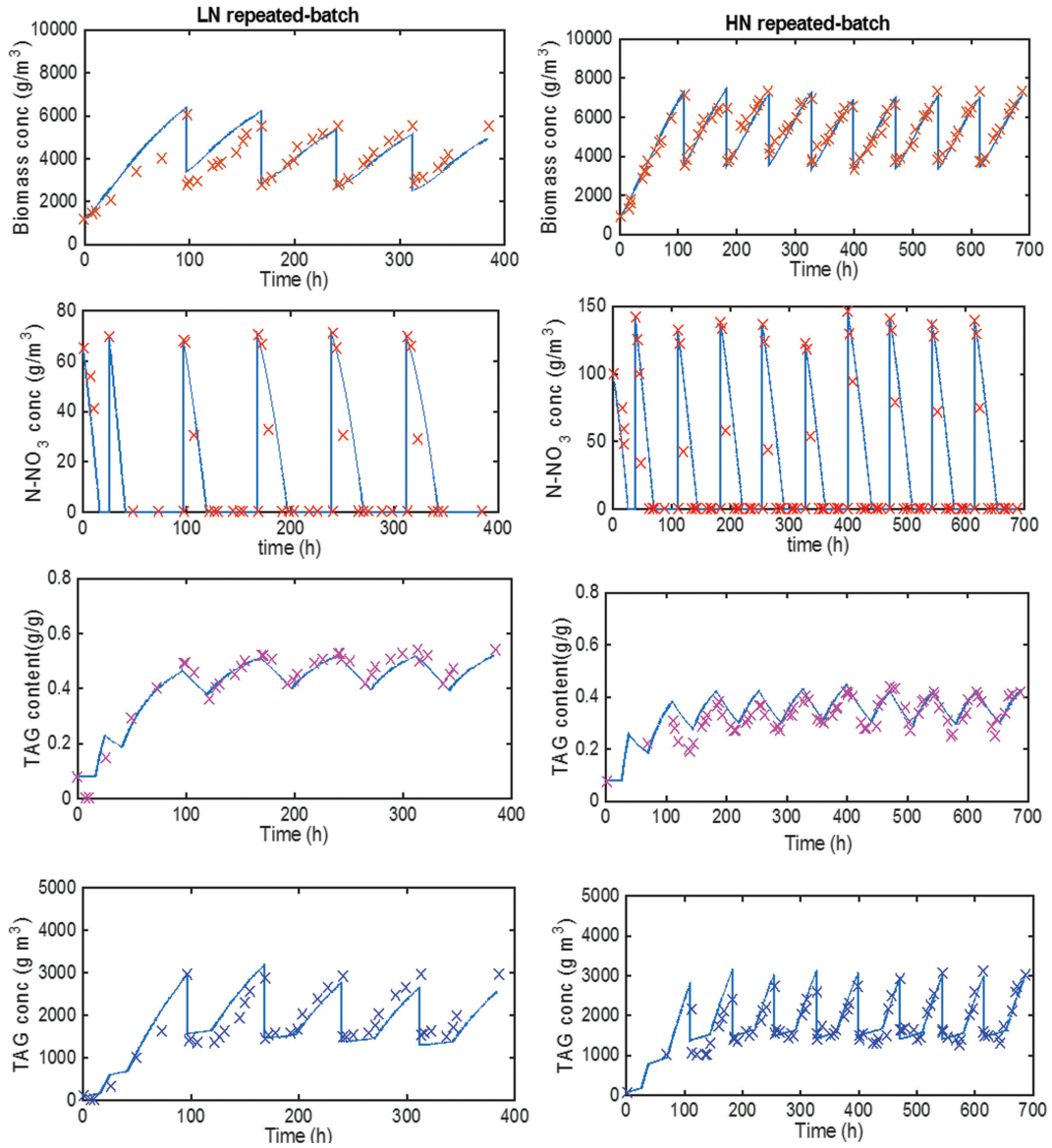


Figure 5.6 Model simulations (lines) and experimental data (symbols) of biomass, external N-NO_3^- and TAG concentrations as well as TAG content for the N-run-out batch, N-replenished batch, low nitrogen supply ($70 \text{ mg N-NO}_3^- \text{ L}^{-1}$) repeated-batch and high nitrogen supply ($140 \text{ mg N-NO}_3^- \text{ L}^{-1}$) repeated-batch cultivations performed in this study.

5.3.6 Model simulations

When model simulations are performed using the calibrated parameters reported in Tables 5.A.1-5.A.2, it can be seen that the model closely follows the experimental data (Fig. 5.6). Furthermore, the predicted TAG yields (0.22, 0.14 and 0.15 g mol⁻¹, for N-run-out batch, low N-resupply repeated-batch and high N-resupply repeated-batch, respectively) are in close agreement with the measured TAG yields (0.21, 0.13 and 0.12 g mol⁻¹, for N-run-out batch, low N-resupply repeated-batch and high N-resupply repeated-batch, respectively).

5.3.7 Optimized TAG yield on light for batch and repeated-batch process

The model was used to identify potential for improvement of TAG yield on light for both batch and repeated-batch processes by performing Monte-Carlo sampled combinations of model parameters as reported in Table 5.1.

5.3.7.1 *Effect of incident light intensity and enhanced photosynthetic machinery*

In our model simulations, the incident light intensity and the maximum photosynthetic rate of nitrogen replete cells ($q_{ph}^{max, replete}$) were varied in order to assess the effect of these two model parameters on the photosynthetic efficiency and thus on the TAG yield on light.

For both batch and repeated-batch, decreasing the incident light intensity had the largest positive impact on the TAG yield (Fig. 5.7A, D, G). For instance, in the reference case (red dots in Fig. 5.7), the TAG yield increased up to fourfold when the light intensity was decreased from 1500 to 200 $\mu\text{mol m}^{-2} \text{s}^{-1}$ (from 0.12 to 0.41 g mol⁻¹ and from 0.07 to 0.29 g mol⁻¹ for batch and repeated-batch, respectively). By reducing the incident light intensity, the extent of photosaturation decreased (Breuer et al. 2013b; Breuer et al. 2015). In practice, a reduction of light intensity can be partly achieved by applying the principle of light dilution using vertically oriented PBRs (Posten 2009).

The maximum photosynthetic rate decreases during N-starvation (Geider et al. 1998b) and consequently, the photosystem becomes saturated at lower light intensities (Eq. 5.A.1). Another approach to diminish photosaturation under N-starvation is to enhance the photosynthetic machinery by increasing the maximum photosynthetic rate under nitrogen (N) replete conditions ($q_{ph}^{max, replete}$) (Eq. 5.A.3). In our model simulations, increasing $q_{ph}^{max, replete}$ resulted in higher TAG yields on light (Fig. 5.7B and 5.7E). The largest relative improvement (32 - 34%) was observed at high light intensity, where photosaturation mostly occurs, rather than at low light intensity, for which an 11- 13% relative improvement was nonetheless found.

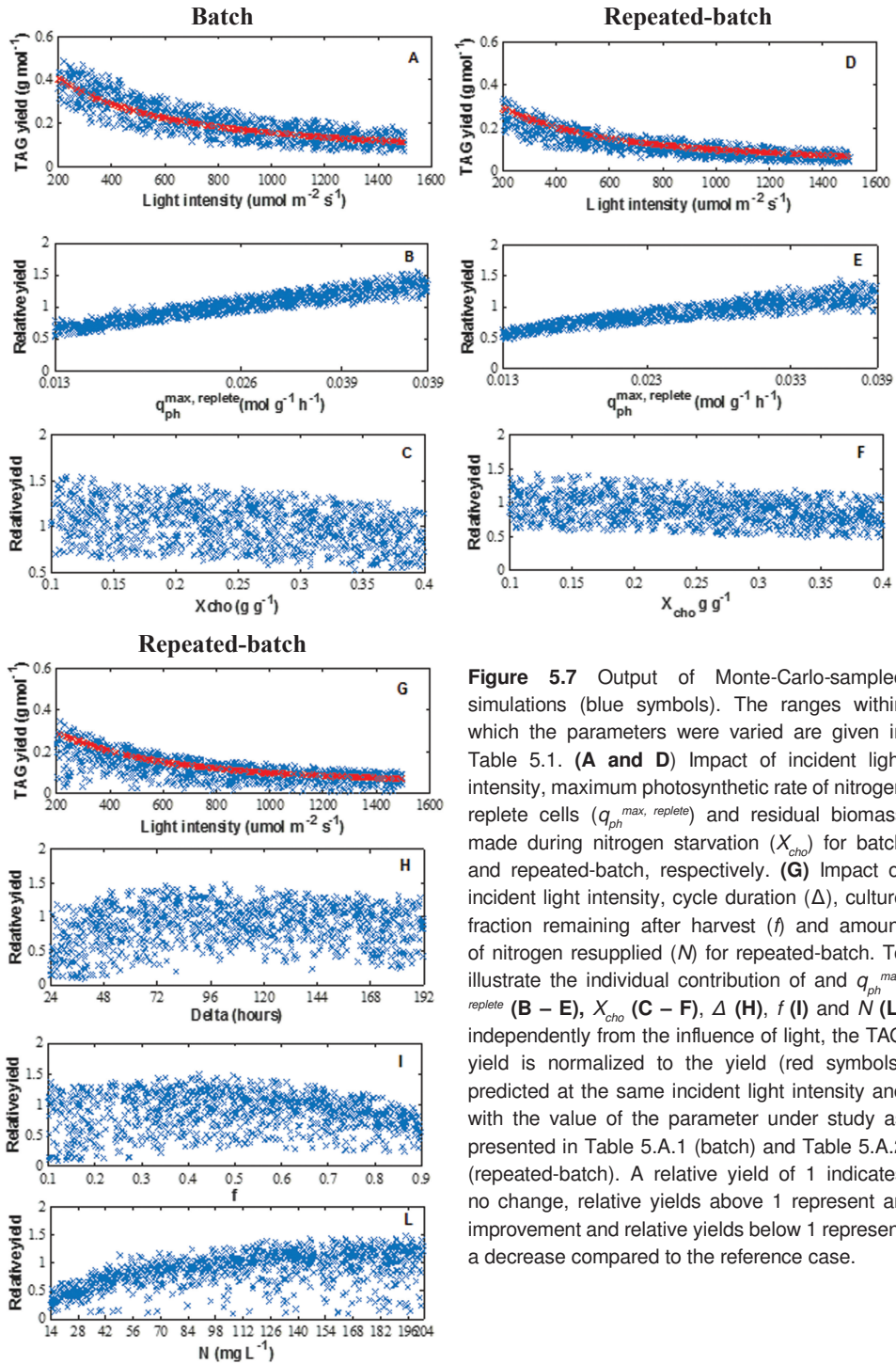


Figure 5.7 Output of Monte-Carlo-sampled simulations (blue symbols). The ranges within which the parameters were varied are given in Table 5.1. **(A and D)** Impact of incident light intensity, maximum photosynthetic rate of nitrogen replete cells ($q_{ph}^{max, replete}$) and residual biomass made during nitrogen starvation (X_{cho}) for batch and repeated-batch, respectively. **(G)** Impact of incident light intensity, cycle duration (Δ), culture fraction remaining after harvest (f) and amount of nitrogen resupplied (N) for repeated-batch. To illustrate the individual contribution of $q_{ph}^{max, replete}$ **(B – E)**, X_{cho} **(C – F)**, Δ **(H)**, f **(I)** and N **(L)** independently from the influence of light, the TAG yield is normalized to the yield (red symbols) predicted at the same incident light intensity and with the value of the parameter under study as presented in Table 5.A.1 (batch) and Table 5.A.2 (repeated-batch). A relative yield of 1 indicates no change, relative yields above 1 represent an improvement and relative yields below 1 represent a decrease compared to the reference case.

5.3.7.2 Higher TAG yield on light by improved carbon partitioning

As *Nannochloropsis* sp. does not accumulate other storage compounds besides TAGs during N-starvation (Figures 5.2 – 5.5 and section 5.3.4.1), this alga already has a much more favorable carbon partitioning mechanism compared to other species (Breuer et al. 2013b; Breuer et al. 2014; Mulders et al. 2014). However, a further improvement of the carbon partitioning could be achieved by decreasing the residual biomass fraction of N-starved biomass (X_{cho}). Regardless of the incident light intensity, a lower X_{cho} can result in a 10 – 16% relative improvement for the batch (Fig. 5.7C), whereas a negligible improvement was observed for the repeated-batch (Fig. 5.7F), which was already characterized by a relatively low X_{cho} compared to the batch experiment.

5.3.7.3 Higher TAG yield on light by optimized operational settings

The operational settings have a strong influence on the TAG yield on light for both batch and repeated-batch TAG production processes. The influence of biomass concentrations at the onset of nitrogen (N) starvation ($C_{x, N=0}$) and reactor light path (z) has been already highlighted by several authors (Zijffers et al. 2010; Zemke et al. 2013; Ho et al. 2014b; Takache et al. 2015; Benvenuti et al. 2015). However, in our model simulations, almost no improvement in yield was observed compared to the reference case (Supplementary material 5.3). This can be attributed to the low maintenance coefficient (m_s) that was used as model input. The low m_s limited the negative effect of the high maintenance requirements that are usually associated to long z and high $C_{x, N=0}$ (Bosma et al. 2007; Breuer et al. 2015).

For repeated-batch, the effect of the amount of resupplied nitrogen (M), cycle duration (Δ) and remaining culture fraction after harvest (f) was assessed. Trends for individual settings could be identified. For instance, regardless of the light intensity, short Δ (< 48 hours) result in a lower yield compared to the reference case (Fig. 5.7H), whereas longer Δ led to a 1.5-fold maximum relative improvement. Higher yields compared to the reference case could be identified when lowering f (Fig. 5.7I), whereas the opposite was found for N (Fig. 5.7L). For the latter case, the high yields at high N-resupply are attributed mostly to an enhanced biomass production rather than to high TAG contents.

In general, the combination of low N-supply, long cycle and large harvest volume resulted in a high TAG content but severely reduced biomass production, thus causing low TAG yields on light. The same result was observed when a low stress pressure (e.g. combinations of high N-supply, short cycle and small harvest volume) was applied. Highest yields were found for optimal combinations of the abovementioned settings. For instance, at low (LL: 200 – 300 $\mu\text{mol m}^{-2} \text{s}^{-1}$), intermediate (IL: 550 - 650 $\mu\text{mol m}^{-2} \text{s}^{-1}$) and high light (HL: 1400 – 1500 $\mu\text{mol m}^{-2} \text{s}^{-1}$) intensities, the highest TAG yields (0.31, 0.18 and 0.10 g mol^{-1} on average, for LL, IL and HL, respectively) were achieved with combinations of: 138 Δ , 0.34 f , 149 N (LL); 128 Δ , 0.37 f , 154 N (IL); 115 Δ , 0.37 f , 154 N (HL).

5.3.7.4 *Effect of operational settings on TAG degradation*

According to our hypothesis and experimental data, TAG degradation occurs only when high stress pressures are applied (Fig. 5.1), namely only for combinations of long cycle durations ($\Delta > 72$ hours), low amounts of re-supplied nitrogen ($N < 70$ mg L⁻¹) and low harvest volumes ($f > 0.5$). Under such operational settings, TAG yields on light are generally much lower (0.02 – 0.13 g mol⁻¹) compared to those obtained under optimized operational settings where no TAG degradation occurs (0.10 – 0.31 g mol⁻¹). Nevertheless, in our model, TAG degradation has a beneficial effect on the TAG yield on light. For example, when the longest cycle ($\Delta = 192$ hours), the lowest N-supply ($N = 14$ mg L⁻¹) and the lowest harvest volume ($f = 0.9$) are simulated for an incident light intensity of 636 $\mu\text{mol m}^{-2} \text{s}^{-1}$, approximately 5% of the TAGs made during the previous cycle are degraded. However, TAG yield is about 1.3-fold higher compared to the case in which operational settings and light intensity are the same but TAG degradation is switched off. This can be explained by the fact that, as a result of TAG degradation, a faster restoration of the photosynthetic capacity was obtained. This translates in a higher photosynthetic rate, faster uptake of nitrogen, larger biomass production and slightly lower TAG content.

The quality of the model predictions in the range of those settings for which TAG degradation is modeled to occur depends on the validity of our hypothesis on the TAG degradation mechanism. Although the experimental data (Fig. 5.3 -5.5 and Supplementary material 5.2) do not contradict our hypothesis and the model is able to well describe TAG degradation in N-replenished batch cultivations (Fig. 5.6), the dataset is not complete enough, and the TAG degradation mechanism should still be validated for repeated-batch operations.

5.3.8 **Process comparison**

In this section, batch and repeated-batch TAG production processes are compared on the optimized TAG yields (Table 5.3), as identified with the Monte-Carlo sampled simulations of model parameters (Table 5.1).

Optimized TAG yields on light were always higher for the batch than for repeated-batch. For the batch, optimized TAG yields ranged from 0.12 g mol⁻¹ (scenario 1B) to 0.49 g mol⁻¹ (scenario 6B) and, at harvest, a TAG content of 0.42 - 0.53 g g⁻¹ was obtained. For the repeated-batch, optimized TAG yields ranged from 0.07 g mol⁻¹ (scenario 1RB) to 0.39 g mol⁻¹ (scenario 12RB). At harvest, TAG contents of 0.35 – 0.60 g g⁻¹ were predicted. Furthermore, as it can be deduced from Table 5.3, during TAG production also the non-TAG-biomass yield on light was generally higher for the batch than for the repeated-batch. Several cellular compounds contribute to the non-TAG- biomass yield on light, such as proteins, sugars, non-acyl lipids, glyco- and phospholipids (Wang and Wang

2012; Bondioli et al. 2012). Therefore, provided that biorefinery of the complete biomass is pursued (Vanthoor-Koopmans et al. 2013), the potential for biomass valorization for both TAGs and non-TAG compounds is better for batch than for repeated-batch.

Table 5.3 Optimized TAG yields on light and TAG contents. **B**: batch; **RB**: repeated-batch. High, intermediate and low light intensities correspond to incident light intensities of 1500, 600 and 200 $\mu\text{mol m}^{-2} \text{s}^{-1}$, respectively. TAG degradation did not occur for any of the reported RB cases. The model parameter values at which the TAG yields on light and TAG contents were achieved, are reported in Supplementary material 5.4.

Scenario			TAG yield on light (g mol ⁻¹)	TAG content (g g ⁻¹)	
Batch	1B	High light intensity (Base case)	0.12	0.42	
	2B	Intermediate light intensity	0.23	0.42	
	3B	Low light intensity	0.41	0.43	
	Increased maximum photosynthetic rate and decreased residual biomass fraction				
	4B	• High light intensity	0.18	0.52	
	5B	• Intermediate light intensity	0.31	0.52	
6B	• Low light intensity	0.49	0.53		
Scenario			TAG yield on light (g mol ⁻¹)	TAG content (g g ⁻¹)	
Repeated-batch	1RB	High light intensity (Base case)	0.07	0.54	
	2RB	Intermediate light intensity	0.15	0.52	
	3RB	Low light intensity	0.29	0.44	
	Optimal N-resupply, cycle duration and harvest volume				
	4RB	• High light intensity	0.09	0.50	
	5RB	• Intermediate light intensity	0.18	0.51	
	6RB	• Low light intensity	0.33	0.48	
	Increased maximum photosynthetic rate and decreased residual biomass fraction				
	7RB	• High light intensity	0.10	0.60	
	8RB	• Intermediate light intensity	0.19	0.54	
	9RB	• Low light intensity	0.34	0.49	
	Optimal N-resupply, cycle duration and harvest volume & Increased maximum photosynthetic rate and decreased residual biomass fraction				
10RB	• High light intensity	0.11	0.35		
11RB	• Intermediate light intensity	0.22	0.47		
12RB	• Low light intensity	0.39	0.48		

The advantage of the batch relies on starting with a N-replete inoculum, thus with cells that have an intact photosynthetic capacity (Supplementary material 5.2). Differently, repeated-batch cycles start with N-starved cells. Likely, the reduced photosynthetic capacity of these cells leads to an inefficient use of light during the regrowth phase, thus resulting in lower TAG yields on light compared to batch processes.

Nonetheless, it should be underlined that the physiological responses to N-resupply in repeated-batch processes might differ when cells are subjected to day/night cycles. By supplying the nitrogen at night, cell recovery may take place in the dark (Přibyl et al. 2013) such that the daylight period can be efficiently used for TAG production. Besides that also batch cultures are likely to benefit from the nightly recovery, further research under day/night cycles is necessary to assess whether nightly recovery could represent an advantage of repeated-batch over batch.

Finally, attention should be paid when using the model, which was developed based on lab-scale cultivations under continuous light, to predict outdoor yields/productivities. Outdoor cultivations are subjected to varying light profiles. Hence, at equal daily light supply rates, lower yields (Benvenuti et al. 2015) are obtained compared to continuously illuminated cultivations. However, when correcting the TAG yields obtained at high light intensity (scenarios 1B and 1RB of Table 5.3) for an assumed average loss of 15% due to night respiration (Tredici 2010; Breuer et al. 2015), comparable yields with those reported for outdoor batch (Quinn et al. (2012); Guccione et al. (2014); Benvenuti et al. (2015); chapter 4) and repeated-batch (Rodolfi et al. (2009); Bondioli et al. (2012); chapter 4) cultivations are found.

5.4 Conclusion

Batch and repeated-batch TAG production processes were successfully described using a mechanistic model which further allowed process comparison based on optimized TAG yields on light. According to our model simulations for continuous light, we can conclude that an optimized batch process will result in higher TAG productivities compared to an optimized repeated-batch process. This is mainly because, in repeated-batch mode, each cycle starts with nitrogen starved cells. The reduced photosynthetic capacity of these cells leads to inefficient light-use during the regrowth phase, consequently resulting in lower overall TAG yields on light compared to batch processes.

Appendix

The model developed by Breuer et al. (2015) for batch TAG production with *Scenedesmus obliquus* in flat panel photobioreactors was further developed to describe the effect of nitrogen (N)-starvation and N-replenishment on photosynthesis and carbon partitioning in batch and repeated-batch cultivations of *Nannochloropsis* sp.. In particular, a TAG degradation mechanism was devised for repeated-batch cultivations and implemented in the model. The following sections describe in detail the modifications made compared to the original model of (Breuer et al. 2015).

5.A.1 Model equations

5.A.1.1 Photosynthesis module

The equations used by Breuer et al. (2015) for the photosynthesis module were adopted without any modification to its mechanism. These equations are listed below. For discussion of underlying assumptions, we refer to Breuer et al. (2015).

The biomass specific photosynthetic rate (q_{ph}) at a given incident light intensity I was calculated using the hyperbolic tangent equation of Jassby and Platt (1976) (Eq. 5.A.1).

$$q_{ph} = q_{ph}^{\max} \tanh\left(\frac{a\psi_N I}{q_{ph}^{\max}}\right) \quad \text{Equation 5.A.1}$$

Where ψ_N is the photosynthetic quantum yield, a is the absorption cross-section and q_{ph}^{\max} is the maximum photosynthetic rate. The three parameters are affected by nitrogen (N) starvation and thus, they vary during a N-starved cultivation (Eq. 5.A.2 – 5.A.4).

A linear relation between the absorption cross-section and the cellular nitrogen content (Q) was found also for *Nannochloropsis* sp. (Fig. 5.A.1). Therefore, Eq. 5.A.2, as proposed by Breuer et al. (2015) could be adopted.

$$a = a_{\text{replete}} \frac{Q}{Q_{\max}} \quad \text{Equation 5.A.2}$$

Where a_{replete} and Q_{\max} are the biomass-specific absorption cross-section and the cellular nitrogen content of N-replete biomass, respectively.

The maximum photosynthetic rate decreases linearly with decreasing nitrogen content reaching zero at the minimum nitrogen content (Q_{\min}). To describe this phenomenon, the equation proposed by Geider et al. (1998b) was adopted (Eq. 5.A.3).

$$q_{ph}^{\max} = q_{ph}^{\max, \text{replete}} \left(\frac{Q - Q_{\min}}{Q_{\max} - Q_{\min}} \right) \quad \text{Equation 5.A.3}$$

Where $q_{ph}^{max, replete}$ is the maximum photosynthetic rate under nitrogen replete conditions.

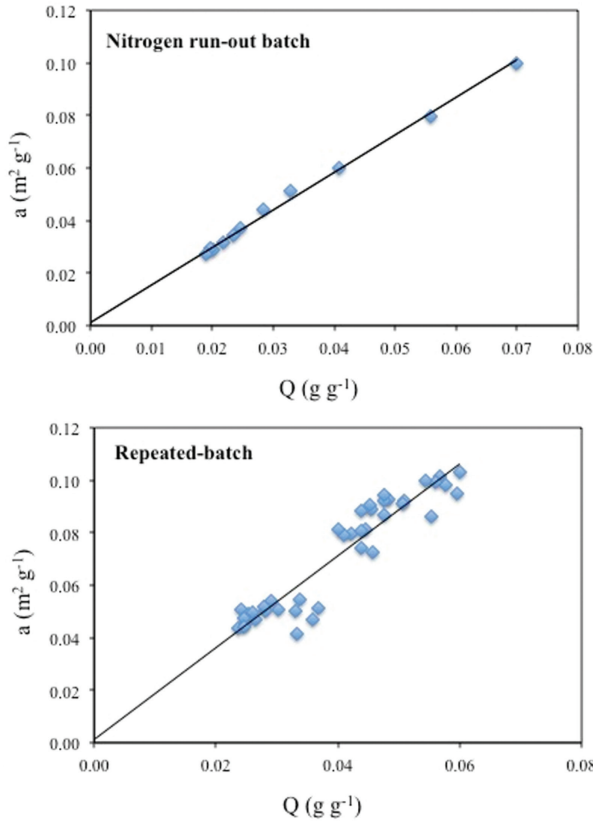


Figure 5.A.1 Linear relation between absorption cross-section (a) and cellular nitrogen content (Q) for the nitrogen run-out batch and repeated-batch cultivations.

Furthermore, N-starvation results in a reduction of the photosynthetic quantum yield (Benvenuti et al. 2014). The physiological changes that determine a reduced photosynthetic quantum yield are lumped together in Ψ_N , assuming that Ψ_N decreases with decreasing cellular nitrogen content following a modified Droop equation (Droop 2009) (Eq. 5.A.4).

$$\Psi_N = \left(1 - \frac{Q_{min}}{Q}\right) \left(1 - \frac{Q_{min}}{Q_{max}}\right)^{-1} \quad \text{Equation 5.A.4}$$

A light gradient is present in photobioreactors, thus cells are exposed to different (high and low) local light intensities due to culture mixing. When assumed that the characteristic times of photosynthesis (1 – 10 ms, Sukenik et al. 1987) are much smaller than mixing times (order of seconds), the photosynthetic rate depends on the local light intensities throughout the photobioreactor. Therefore, the average

photosynthetic rate ($\overline{q_{ph}}$) for a flat panel photobioreactor is described by Eq. 5.A.5, which neglects the effect of light scattering. Furthermore, it is assumed that the light is parallel (not diffuse) and enters the photobioreactor perpendicularly to its surface.

$$\overline{q_{ph}} = \frac{1}{Z} \int_0^Z q_{ph}^{\max} \tanh\left(\frac{a\psi_N I_0 e^{(-aC_x z)}}{q_{ph}^{\max}}\right) dz \quad \text{Equation 5.A.5}$$

Where z is the reactor light path, I_0 is the incident light intensity and C_x is the biomass concentration.

5.A.1.2 Calculation of photosynthetic and inter-conversion yields using flux balance analysis

The theoretical maximum photosynthetic and conversion yields, as depicted in Fig. 5.1, were calculated using flux balance analysis (MATLAB: *linprog*) (Eq. 5.A.6). For this, the metabolic network as described by Breuer et al. (2015) for the *Scenedesmus* starchless mutant was adopted with some modifications, which are listed below.

- 1) Based on our observations, reproducing biomass consists, on average, of 45% protein, 0.2% DNA, 6% RNA, 8% TAG (containing three palmitic acid molecules), 20% carbohydrates, 13.8% membrane lipids (considered as monogalactosyl-diacylglycerol molecules) and 7% ash.
- 2) It is assumed that all fatty acids in TAGs are palmitic acid (C16:0) molecules instead of C18:1 as presumed by Breuer et al. (2015) for *Scenedesmus*. C16:0 is indeed the most abundant fatty acid in *Nannochloropsis* sp. (Benvenuti et al. 2014). Due to chemical differences between these fatty acids, a slightly higher theoretical TAG yield on light is obtained for *Nannochloropsis* sp. (1.39 g mol⁻¹) compared to *Scenedesmus obliquus* (1.33 g mol⁻¹).
- 3) In our repeated-batch model, the conversion of TAGs into reproducing biomass was included. Therefore, the metabolic reactions of TAG activation, hydrolysis and oxidation were added to the metabolic network. The oxidation of C16:0 produces 8 AcCoA, 7 NADH and 7 FADH₂. In our modified network, FADH₂ was converted into NADH at the expenses of ATP (1 ATP per NADH). The AcCoA produced by the beta-oxidation can either be oxidized in the citric acid cycle to produce ATP and NADH, or it can be used in the glyoxylate cycle to produce malate. Both pathways were already present in the network model so no extra reactions were added to the metabolic network.

Flux balance analysis was used to determine the flux distribution that results in the highest yield on photons for each of the biomass compounds (MATLAB: *linprog*) (Eq. 5.A.6).

Objective: Maximize V_M

Constrained with

Equation 5.A.6

$S \cdot v = 0$ (stoichiometric constraints)

$v_{\text{photon}} = 1$ (all rates are normalized to the photosynthetic rate)

$v_{\text{min}} \leq v \leq v_{\text{max}}$ (flux constraints used to describe reversibility of reactions)

Where S is the stoichiometric matrix and v is the vector containing the flux rates. The boundaries of the flux rates were set according to reversibility of reactions as described by Kliphuis et al. (2012). To calculate the yield of reproducing biomass (X) on TAG, v_{TAG} is set to -1, v_{photon} is set to 0, v_x is maximized and the conversion yield is calculated as $v_x / -v_{\text{TAG}}$.

This procedure results in theoretical maximum yields of 1.62 g X /mol photon ($Y_{x, ph}$) (for growth on nitrate), 3.24 g CHO/mol photon ($Y_{CHO, ph}$), 1.39 g TAG/mol photon ($Y_{TAG, ph}$) and 0.94 g X /g TAG ($Y_{x, TAG}$).

5.A.1.3 Carbon-partitioning module

It is assumed that when the extracellular nitrogen concentration (N) is above 0, the remaining photosynthetic capacity that is not used to fulfill maintenance requirements (m_g) is used for the synthesis of reproducing biomass (X). When N is zero, the synthesis of X is completely impaired (Eq. 5.A.7) and the remaining photosynthetic capacity is first used for the synthesis of CHO, such that CHO content in the biomass remains constant (Eq. 5.A.9), as also observed in our cultivations (Fig. 5.2, 5.4 and 5.5, section 5.3.4.1). Finally, the remainder is channeled towards TAG synthesis (Eq. 5.A.10).

A mechanism describing TAG degradation upon nitrogen resupply is also considered. It is assumed that, when extracellular nitrogen is resupplied after a N-starvation period such that the cellular nitrogen content is above a critical level (i.e. $Q_{deg} = 0.025 \text{ g g}^{-1}$), no TAG degradation will occur. Differently, when nitrogen is re-supplied after a prolonged N-starvation period, during which the cellular nitrogen content has decreased below Q_{deg} , TAGs are converted into reproducing biomass (X) and TAG degradation follows 0th order kinetics at the rate ($r_{TAG, x}^{max}$) observed in our nitrogen replenished batch cultivation (Eq. 5.A.7).

$$r_{TAG, x} = \begin{cases} r_{TAG, x}^{max} & \text{if } Q \leq Q_{deg} \text{ and } N > 0 \text{ and } TAG > 0 \\ 0 & \text{if } Q > Q_{deg} \text{ or } N \leq 0 \text{ or } TAG \leq 0 \end{cases} \quad \text{Equation 5.A.7}$$

To also describe conversion of TAGs into X , the biomass-specific production rates of reproducing biomass (q_x) and TAGs (q_{TAG}) were redefined as shown in Eq. 5.A.8 and 5.A.10, respectively.

$$q_x = \left\{ \begin{array}{ll} Y_{x, \text{ph}} \left(\overline{q_{\text{ph}}} - m_s \frac{Q}{Q_{\text{max}}} \right) + \overbrace{r_{\text{TAG}, x} \cdot Y_{x, \text{TAG}}}^{\text{Conversion of TAG to biomass}} & \text{if } N > 0 \\ 0 & \text{if } N \leq 0 \end{array} \right\} \quad \text{Equation 5.A.8}$$

$$q_{\text{CHO}} = \left\{ \begin{array}{ll} 0 & \text{if } \frac{\text{CHO}}{c_x} > X_{\text{CHO}} \text{ or } N > 0 \\ \overbrace{\left(\overline{q_{\text{ph}}} - m_s \frac{Q}{Q_{\text{max}}} \right)}^{\text{Available photons}} \cdot \overbrace{Y_{\text{CHO}, \text{ph}}}^{\text{De novo CHO production}} & \text{if } \frac{\text{CHO}}{c_x} \leq X_{\text{CHO}} \text{ and } N \leq 0 \end{array} \right\} \quad \text{Equation 5.A.9}$$

$$q_{\text{TAG}} = \left\{ \begin{array}{ll} 0 & \text{if } N > 0 \\ \left(\overbrace{\overline{q_{\text{ph}}} - m_s \frac{Q}{Q_{\text{max}}}}^{\text{Available photons}} - \overbrace{\frac{q_{\text{CHO}}}{Y_{\text{CHO}, \text{ph}}}}^{\text{Photons remaining after CHO production}} \right) \cdot \overbrace{Y_{\text{TAG}, \text{ph}}}^{\text{De novo TAG production}} - \overbrace{r_{\text{TAG}, x}}^{\text{TAG degradation}} & \text{if } N \leq 0 \end{array} \right\} \quad \text{Equation 5.A.10}$$

As nitrogen is present only in reproducing biomass (X), the biomass-specific nitrogen uptake rate (q_N) depends on the production rate of X and its nitrogen content (Q_{max}), resulting in Eq. 5.A.11.

$$q_N = -q_x Q_{\text{max}} \quad \text{Equation 5.A.11}$$

Ordinary differential equations (ODEs) were adopted to describe change in reproducing biomass (X), CHO , TAG and extracellular nitrogen concentration (N) (Eq. 5.A.12 – 5.A.15). ODEs were integrated as functions of time using the 4th/5th order Runge-Kutta algorithm by means of the MATLAB *ode45* function.

$$\frac{dX}{dt} = q_x C_x \quad \text{Equation 5.A.12}$$

$$\frac{dTAG}{dt} = q_{\text{TAG}} C_x \quad \text{Equation 5.A.13}$$

$$\frac{dCHO}{dt} = q_{\text{CHO}} C_x \quad \text{Equation 5.A.14}$$

$$\frac{dN}{dt} = q_N C_x \quad \text{Equation 5.A.15}$$

The total biomass concentration (C_x) is calculated as shown in Eq. 5.A.16.

$$C_x = X + CHO + TAG \quad \text{Equation 5.A.16}$$

The cellular nitrogen content of total biomass is calculated according to Eq. 5.A.17.

$$Q = \frac{Q_{\max} \cdot X}{C_x} \quad \text{Equation 5.A.17}$$

As *Nannochloropsis* sp. does not accumulate other metabolites besides TAGs during N-starvation (Fig. 5.2 Fig. 5.4 – 5.5 and section 5.3.4.1), the carbon partitioning mechanism used by Breuer et al. (2015) for the starchless *Scenedesmus* mutant was adopted, therefore no conversion of starch (or any other compound) into TAGs was considered.

Moreover, because *Nannochloropsis* sp., in contrast to *Scenedesmus obliquus*, contains considerable amounts of TAG (0.08 g g⁻¹) in the N-replete reproducing biomass, the TAG content during N-starvation was corrected for the TAGs present in the reproducing biomass ($X_{TAG, x}$), according to Eq. 5.A.18.

$$\text{TAG content} = \frac{X_{TAG, x} \cdot X + \text{TAG}}{C_x} \quad \text{Equation 5.A.18}$$

CHO content was instead calculated as proposed by Breuer et al. (2015), resulting in Eq. 5.A.19.

$$\text{CHO content} = \frac{X_{CHO, x} \cdot X + \text{CHO}}{C_x} \quad \text{Equation 5.A.19}$$

Where $X_{CHO, x}$ is the CHO fraction in reproducing biomass and assumed to be 0.31 g g⁻¹ for batch (Table 5.A.1) and 0.17 g g⁻¹ for repeated-batch (Table 5.A.2).

5.A.1.4 Calculation of projected TAG yield on light for batch and repeated-batch

Eq. 5.A.20 was used to calculate projected TAG yields on light ($Y_{TAG, ph}$). For the batch, the TAG yield is the maximum time-averaged yield, whereas for the repeated-batch, it is the yield at the harvest of the constant cycle repetitions.

To perform a fair comparison between batch and repeated-batch strategies, $Y_{TAG, ph}$ of the batch was corrected the inoculum production. Therefore, the factor $C_x, N=0 / Y_{inoc, ph}$ was included in Eq. 5.A.20 assuming that for the batch the inoculum, which is defined as the biomass present at the onset of nitrogen starvation ($C_x, N=0$), was produced at a certain biomass yield on light ($Y_{inoc, ph}$) in a continuous-operated PBR at a biomass concentration equal to $C_x, N=0$. Differently, for (long-term) repeated-batch cultivations, it can be assumed that inoculum production would be required only at the start of the cultivation and thus it can be neglected. Hence, $C_x, N=0 / Y_{inoc, ph}$ was set to zero for repeated-batch.

$$\text{TAG yield on light} = \frac{\text{TAG (t)}}{I_0 t + \frac{C_x, N=0}{Y_{inoc, ph}}} \quad \text{Equation 5.A.2.20}$$

Differently from the original model of Breuer et al. (2015), in which the inoculum of the batch cultivation was always produced at a $Y_{inoc, ph}$ of 1 g mol⁻¹, in our modified model,

$Y_{inoc, ph}$ was calculated as a function of incident light intensity, biomass concentration and reactor light path (Eq. 5.A.21), as the dynamics of cell recovery and thus the re-growth phase in repeated-batch cycles are also dependent on these parameters.

$$Y_{inoc, ph} = \frac{Y_{x, ph} \cdot \overline{q_{ph}} - m_s}{\frac{I_0}{Z \cdot C_{x, N=0}}} \quad \text{Equation 5.A.21}$$

5.A.2 Model calibration for nitrogen run-out batch cultivations of *Nannochloropsis* sp.

Upon the adaptations made as described in Appendix 5.A.1, the model of Breuer et al. (2015) was calibrated using the results of our nitrogen (N) run-out batch experiment. The results of the duplicate cultivations were combined and treated, by averaging, as a single dataset. The first experimental point, immediately after setting the light at $636 \mu\text{mol m}^{-2} \text{s}^{-1}$, was used as initial condition for integration and was considered as $t = 0$. The following data points, until biomass decay was observed, were used for parameter estimation (MATLAB: Monte-Carlo algorithm and *fminsearch*) as described by Breuer et al. (2015), yielding the calibrated values as presented in Table 5.A.1. The experimental settings for incident light intensity and reactor light path, and the experimentally observed absorption cross-section and cellular nitrogen content of N-replete cells were used as model constants.

5.A.3 Model validation for N-replenished batch and repeated-batch cultivations

The model was validated on the repeated-batch cultivations using the calibrated values of the batch experiments, with the exception of X_{cho} . The two repeated-batch cultivations led to similar residual biomass fractions (X_{cho}). However, these were much lower compared to X_{cho} during the batch (Table 5.A.1). Consequently, the parameter estimation procedure was performed on X_{cho} only, while the maximum photosynthetic rate of nitrogen-replete cells ($q_{ph}^{max, replete}$), the minimum cellular nitrogen content (Q_{min}) and the maintenance coefficient (m_s) were fixed to the estimated values from the batch model. Regardless of the repeated-batch dataset used, an estimated value of 0.17 g g^{-1} was obtained for X_{cho} .

A TAG degradation mechanism was devised (Fig. 5.1) and then implemented in the model (Eq. 5.A.7 -8 and 5.A.10). Although net TAG degradation was not observed with the tested repeated-batch cultivations (Fig. 5.4C and Fig. 5.5C), this did occur in the N-replenished batch cultivation (Fig. 5.3C). Thus, the values for the critical cellular nitrogen content at which TAG degradation commences (Q_{deg}) and the TAG degradation rate ($r_{TAG, x}$) were estimated from the N-replenished batch cultivation.

For each of the two repeated-batch cultivations, the first experimental point, immediately after setting the light at $636 \mu\text{mol m}^{-2} \text{s}^{-1}$, was used as initial condition for integration and was considered as $t = 0$.

Table 5.A.1 Estimated parameters, constants and boundary conditions used for solving the material balances presented by Breuer et al. (2015) for batch TAG production.

<i>Nitrogen run out batch calibration experiment</i>		
Estimated parameters	Unit	Value
$q_{ph}^{max, \text{replete}}$	$\text{mol g}^{-1} \text{h}^{-1}$	0.026
Q_{min}	g g^{-1}	0.020
m_s	$\text{mmol g}^{-1} \text{h}^{-1}$	0.093
X_{cho}	g g^{-1}	0.310
Constants	Unit	Value
Q_{max}	g g^{-1}	0.070
$a_{replete}$	$\text{m}^2 \text{g}^{-1}$	0.080
z	m	0.020
I_0	$\mu\text{mol m}^{-2} \text{s}^{-1}$	636
$X_{CHO, x}$	g g^{-1}	0.180
$X_{TAG, x}$	g g^{-1}	0.080
Initial values	Unit	Value
C_x	g m^{-3}	928
TAG and CHO	g m^{-3}	0
N-NO_3	g m^{-3}	107

Table 5.A.2 Estimated parameter, constants and boundary conditions used for solving the material balances for repeated-batch TAG production.

<i>Repeated-batch calibration experiment</i>		
Estimated parameter	Unit	Value
X_{cho}	g g^{-1}	0.170
Constants	Unit	Value
$q_{ph}^{max, \text{replete}}$	$\text{mol g}^{-1} \text{h}^{-1}$	0.026
Q_{min}	g g^{-1}	0.020
m_s	$\text{mmol g}^{-1} \text{h}^{-1}$	0.093
Q_{max}	g g^{-1}	0.070
$a_{replete}$	$\text{m}^2 \text{g}^{-1}$	0.080
z	m	0.020
I_0	$\mu\text{mol m}^{-2} \text{s}^{-1}$	636
$X_{CHO, x}$	g g^{-1}	0.180
$X_{TAG, x}$	g g^{-1}	0.080
$r_{TAG, x}$	$\text{g g}^{-1} \text{h}^{-1}$	0.011
Q_{deg}	g g^{-1}	0.025
Initial values	Unit	Value
C_x	g m^{-3}	1173 (LN); 900 (HN)
TAG and CHO	g m^{-3}	0
N-NO_3	g m^{-3}	65 (LN); 100 (HN)

List of symbols

Symbol	Unit	Description
a	$\text{m}^2 \text{g}^{-1}$	Absorption cross-section
a_{replete}	$\text{m}^2 \text{g}^{-1}$	Absorption cross-section of nitrogen replete biomass
CHO	g m^{-3}	Concentration of residual biomass made during N-starvation
C_x	g m^{-3}	Biomass concentration
$C_{x, N=0}$	g m^{-3}	Biomass concentration at onset of nitrogen starvation
f	% (v/v)	Remaining fraction in the reactor after harvest
I_0	$\text{mol m}^{-2} \text{s}^{-1}$	Incident light intensity
m_s	$\text{mmol g}^{-1} \text{h}^{-1}$	Maintenance coefficient
N	g m^{-3}	Amount of nitrogen resupplied after each harvest
N-NO_3^-	g m^{-3}	Extracellular nitrate concentration
Q	g g^{-1}	Cellular nitrogen content
Q_{deg}	g g^{-1}	Cellular nitrogen content below which TAG degradation begins
Q_{max}	g g^{-1}	Maximum cellular nitrogen content of N-replete biomass
Q_{min}	g g^{-1}	Minimum cellular nitrogen content
$\overline{q_{\text{ph}}}$	$\text{mol g}^{-1} \text{h}^{-1}$	Biomass-specific photosynthetic rate averaged throughout the reactor
$q_{\text{ph}}^{\text{max, replete}}$	$\text{mol g}^{-1} \text{h}^{-1}$	Maximum photosynthetic rate of N-replete cells
q_i	$\text{g g}^{-1} \text{h}^{-1}$	Biomass specific production rate of component i
$r_{\text{TAG}, x}$	$\text{g g}^{-1} \text{h}^{-1}$	Conversion rate of TAG into reproducing biomass
t	h	Time
TAG	g m^{-3}	TAG concentration
$X_{\text{cho}, x}$	g g^{-1}	CHO content in reproducing biomass
X_{cho}	g g^{-1}	CHO content in newly formed biomass during N-starvation, excluding reproducing biomass
$X_{\text{TAG}, x}$	g g^{-1}	TAG content in reproducing biomass
$Y_{i,j}$	g mol^{-1} or g g^{-1}	Yield of component i on component j (subscript ph refers to photons)
z	m	Reactor light path
Δ	h	Repeated-batch cycle duration

Acknowledgements

The authors would like to thank the Ministry of Economic Affairs, Agriculture and Innovation and Province of Gelderland, and Biosolar Cells, BASF, BioOils, Drie Wilgen Development, DSM, Exxon Mobil, GEA Westfalia Separator, Heliae, Neste, Nijhuis, Paques, Cellulac, Proviron, Roquette, SABIC, Simris Alg, Staatsolie Suriname, Synthetic Genomics, TOTAL and Unilever for the financial support of the AlgaePARC research program.

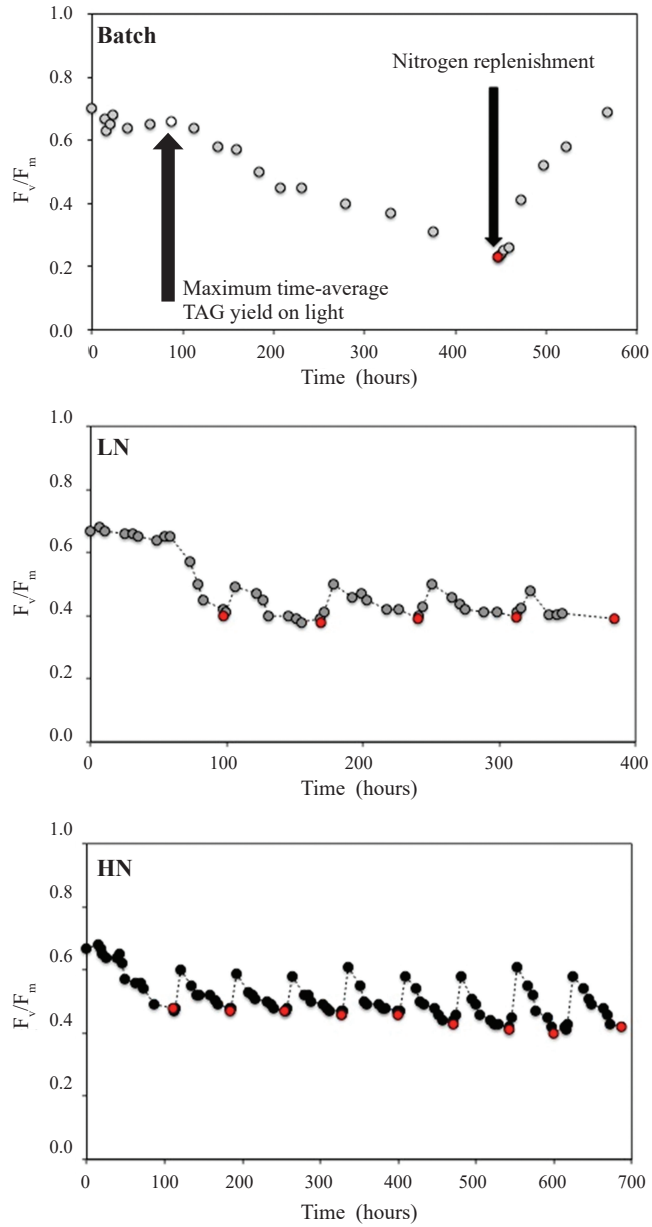
Supplementary material

Supplementary material 5.1 Time of nitrogen-depletion ($t_{N=0}$), biomass-specific nitrogen uptake ($-q_N$) and TAG production (q_{TAG}) rates, time-averaged biomass ($Y_{x, ph, HARV, CYCLE}(t)$) and TAG ($Y_{TAG, ph, HARV, CYCLE}(t)$) yields on light at the harvest of each cycle for the low and high nitrogen supply repeated-batch cultivations. Biomass specific rates were calculated by normalizing the volumetric rates to the average biomass concentration during the considered time interval. Volumetric rates were calculated with linear regression of concentrations vs. time. R^2 of linear regressions were always > 0.90 . Productivities are corrected for the amount of biomass and TAGs present at the start of each cycle (i.e. $t = 0$). Constant cycle repetitions are highlighted in bold.

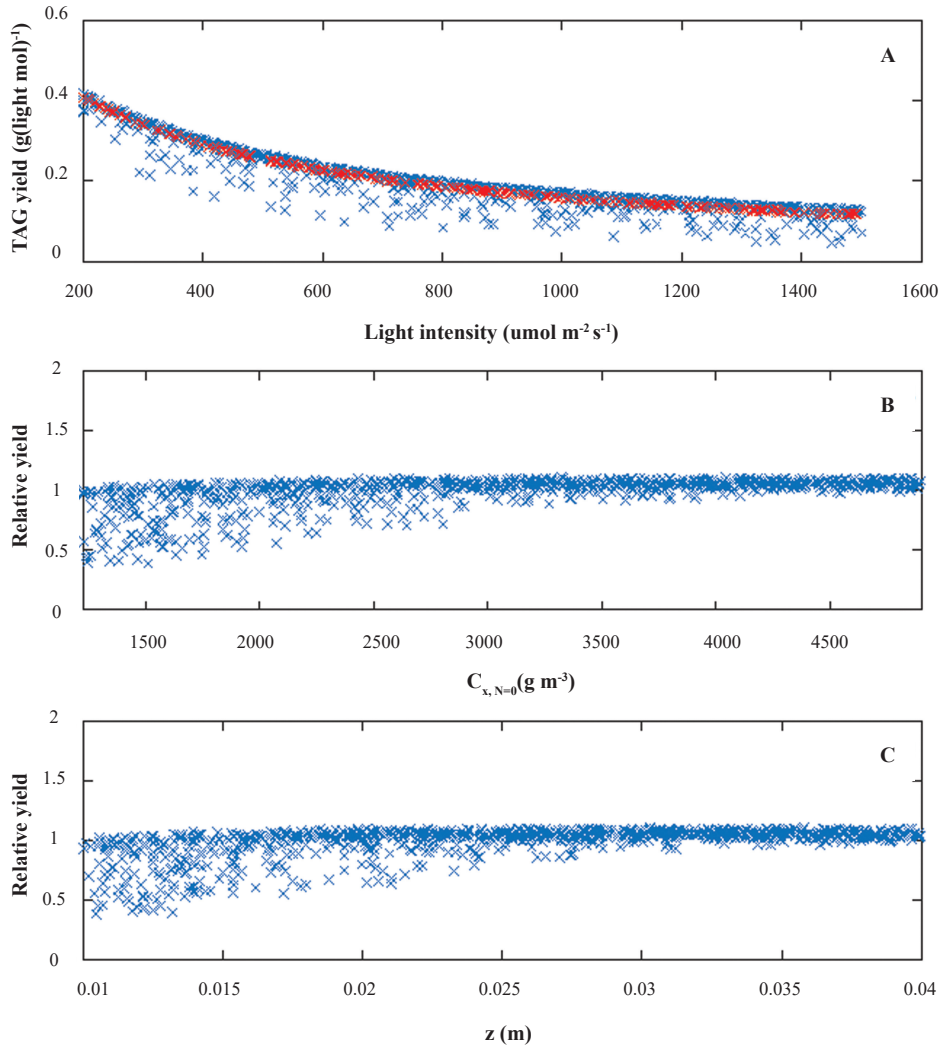
<i>Low nitrogen supply repeated-batch cultivation</i>					
	$t_{N=0}$ (h)	$-q_N$ (mg g ⁻¹ h ⁻¹)	q_{TAG} (mg g ⁻¹ h ⁻¹)	$Y_{x, ph, HARV, CYCLE}(t)$ (g mol ⁻¹)	$Y_{TAG, ph, HARV, CYCLE}(t)$ (g mol ⁻¹)
cycle #0	13	2.7	9.6	0.29	0.14
cycle #1	18	1.4	7.9 [*]	0.25	0.12
cycle #2	18	1.3	6.5[*]	0.25	0.13
cycle #3	17	1.5	6.5[*]	0.25	0.13
cycle #4	17	1.4	6.8[*]	0.25	0.13
<i>High nitrogen supply repeated-batch cultivation</i>					
	$t_{N=0}$ (h)	$-q_N$ (mg g ⁻¹ h ⁻¹)	q_{TAG} (mg g ⁻¹ h ⁻¹)	$Y_{x, ph, HARV, CYCLE}(t)$ (g mol ⁻¹)	$Y_{TAG, ph, HARV, CYCLE}(t)$ (g mol ⁻¹)
cycle #0	14	3.0	5.9	0.32	0.10
cycle #1	14	2.5	5.3 ^{**}	0.28	0.10
cycle #2	16	2.3	4.5 ^{**}	0.31	0.11
cycle #3	16	2.0	4.5 ^{**}	0.28	0.10
cycle #4	18	1.7	4.8 ^{**}	0.27	0.11
cycle #5	19	2.0	7.2 ^{**}	0.28	0.12
cycle #6	22	1.7	6.8^{**}	0.30	0.12
cycle #7	21	1.7	6.8^{**}	0.30	0.12
cycle #8	21	1.8	6.6^{**}	0.30	0.12

(^{*}) Calculated excluding the first 24 hours of the cycle

(^{**}) Calculated excluding the first 30 hours of the cycle



Supplementary material 5.2 Time-evolution of maximum photosystem II efficiency (F_v/F_m) for the batch and the low (LN) and high (HN) nitrogen supply repeated-batch cultivations. Red symbols indicate the value of maximum photosystem II efficiency at nitrogen-resupply.

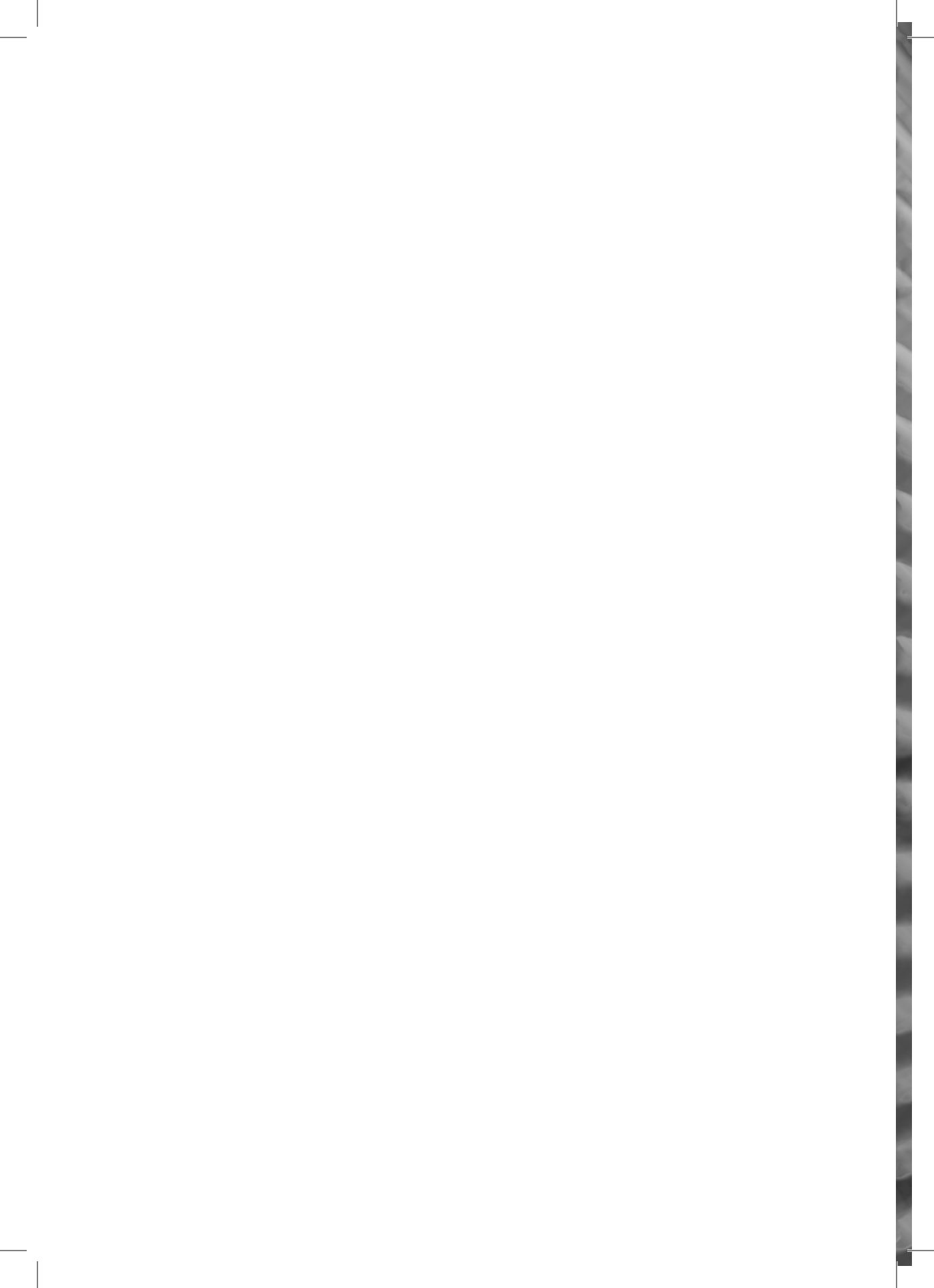


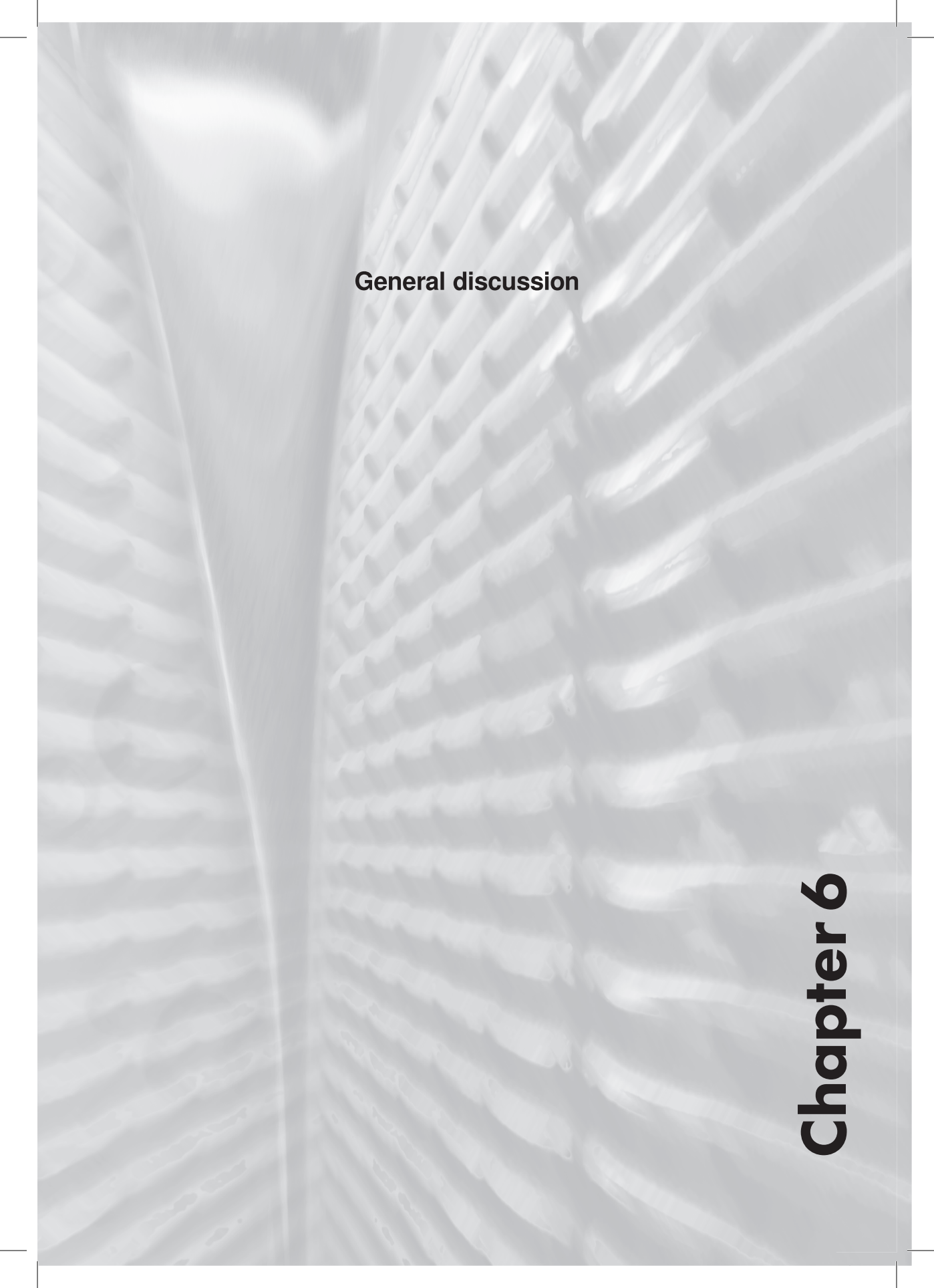
Supplementary material 5.3 Batch process. Output of Monte-Carlo-sampled simulations on maximum TAG yield on light (blue symbols). The ranges within which the parameters were varied are given in Table 5.1. **A)** Impact of incident light intensity, biomass concentration at onset of nitrogen starvation ($C_{x,N=0}$) and reactor light path (z). **(B- C)** To illustrate the contribution of $C_{x,N=0}$ and z independently from the influence of light, the TAG yield was normalized to the yield predicted at the same incident light intensity and with the value of the parameter under study as presented in Table 5.A.1 (red symbols). A relative yield of 1 indicates no change, relative yields above 1 represent an improvement and relative yields below 1 represent a decrease compared to the reference case.

Supplementary material 5.4 Optimized TAG yields on light and TAG contents and corresponding model parameter values at which these were achieved. **B**: batch; **RB**: repeated-batch. High, intermediate and low light intensities correspond to incident light intensities of 1500, 600 and 200 $\mu\text{mol m}^{-2} \text{s}^{-1}$, respectively.

Scenario	TAG yield on light (g mol^{-1})	TAG content (g g^{-1})	z (m)	$C_{x, N=0}$ (g m^{-3})	X_{cho} (g g^{-1})	$q_{\text{ph}}^{\text{max, repetitive}}$ ($\text{mol g}^{-1} \text{h}^{-1}$)
1B	High light intensity (Base case)	0.12	0.42			
2B	Intermediate light intensity	0.23	0.42		0.31	0.026
3B	Low light intensity	0.41	0.43			
4B	Increased maximum photosynthetic rate and decreased residual biomass fraction (High light intensity)	0.18	0.52		0.12	0.037
5B	Increased maximum photosynthetic rate and decreased residual biomass fraction (Intermediate light intensity)	0.31	0.52	0.02	2451	
6B	Increased maximum photosynthetic rate and decreased residual biomass fraction (Low light intensity)	0.49	0.53		0.11	0.030
Scenario	TAG yield on light (g mol^{-1})	TAG content (g g^{-1})	N (g m^{-3})	f (%)	Δ (hours)	$q_{\text{ph}}^{\text{max, repetitive}}$ ($\text{mol g}^{-1} \text{h}^{-1}$)
1RB	High light intensity (Base case)	0.07	0.54			
2RB	Intermediate light intensity	0.15	0.52	70	72	0.026
3RB	Low light intensity	0.29	0.44			

4RB	Optimal N-resupply, cycle duration and harvest volume (High light intensity)	0.09	0.50	134	0.29	85	
5RB	Optimal N-resupply, cycle duration and harvest volume (Intermediate light intensity)	0.18	0.51	171	0.46	134	0.026
6RB	Optimal N-resupply, cycle duration and harvest volume (Low light intensity)	0.33	0.48	142	0.38	155	
7RB	Increased maximum photosynthetic rate and decreased residual biomass fraction (High light intensity)	0.10	0.60				0.038
8RB	Increased maximum photosynthetic rate and decreased residual biomass fraction (Intermediate light intensity)	0.19	0.54	70	0.50	72	0.037
9RB	Increased maximum photosynthetic rate and decreased residual biomass fraction (Low light intensity)	0.34	0.49				0.038
10RB	Optimal N-resupply, cycle duration and harvest volume & Increased maximum photosynthetic rate and decreased residual biomass fraction (High light intensity)	0.11	0.35	167	0.21	47	0.038
11RB	Optimal N-resupply, cycle duration and harvest volume & Increased maximum photosynthetic rate and decreased residual biomass fraction (Intermediate light intensity)	0.22	0.47	161	0.14	87	0.037
12RB	Optimal N-resupply, cycle duration and harvest volume & Increased maximum photosynthetic rate and decreased residual biomass fraction (Low light intensity)	0.39	0.48	177	0.29	133	0.038





General discussion

Chapter 6

Abstract

Microalgal triglycerides (TAGs) hold great promise as sustainable feedstocks for the commodity industries. The biological improvement and process optimization strategies that are needed to maximize TAG productivity and reduce production costs are discussed. Furthermore, we present a techno-economic assessment of a two-step TAG production process, where growth reactors are operated in continuous mode such that multiple batch-operated stress reactors are inoculated and harvested sequentially. The analysis is conducted for a hypothetical 100-ha plant in southern Spain using vertically stacked tubular photobioreactors (PBRs). The base-case is based on outdoor pilot-scale data from AlgaePARC and current process strategy and PBR technology, resulting in a cost of 7.4 € per kg of biomass containing 24% TAG (w/w). By optimizing both the biological performance and the process technology, the production cost can be decreased to 3.0 € per kg of biomass containing 60% TAG (w/w). We believe to be on the right track to achieve an economically feasible TAG production platform provided that photosynthetic efficiency is further improved, the whole biomass is valorized and cheaper PBRs are designed.

6.1 Introduction

Currently, microalgal products are mainly sold in niche markets. Commercially relevant microalgal products are basically biomass or extracts rich in PUFAs (EPA, DHA), essential and antioxidants (carotenoids, tocopherols and phenols) as supplements for human health and cosmetics (Spolaore et al. 2006; Paul et al. 2012). However, in the last ten years, industry has been looking at alternative and sustainable feedstocks for commodities in the food, feed, chemical and biofuel sectors. This is mainly due to the social and political awareness for sustainability, the instability of fossil fuel prices, the pressure on agriculture crops for non-food applications, the growth in population and limited availability of arable land. In this context, microalgal triglycerides (TAGs) are regarded as an attractive source to supplement or substitute oils derived from fossil resources and/or agricultural crops (Chisti 2007; Draaisma et al. 2013). Microalgae can grow on non-arable lands and they have a low freshwater and fertilizer footprint when grown on wastewater, sea- or brackish water (Draaisma et al. 2013). In addition to TAGs, also the remaining biomass has value and therefore the whole biomass can be used (Vanthoor-Koopmans et al. 2013). A commercial microalgal bulk industry would represent an enormous incentive for national economies. Malik et al. (2015) calculated that the production of 1 Mton of bio-crude oil from microalgae could generate 13,000 new jobs in Australia and turnover of 2.6 billion €. Despite the high potential of microalgae as sustainable TAG cell factories, microalgal TAGs are not listed among the most valuable components for the commodity industries (Ruiz et al., manuscript submitted).

This thesis focused on increasing microalgal TAG productivity by selecting a highly productive strain and assessing the impact of a batch and a repeated-batch nitrogen starvation process on the productivity, both at lab-scale and outdoor pilot cultivations. We showed that maintaining a high photosynthetic efficiency, while accumulating TAGs, is key for achieving high TAG productivities. Additionally, we demonstrated that in a batch process the highest TAG productivity is obtained.

This chapter first gives an outlook on the research needed to further improve TAG productivity. Then, a two-step-100 ha-scale TAG production process is designed in which, in the first step, biomass is grown under nitrogen replete conditions in continuously operated photobioreactors (PBRs) and, in the second step, multiple batch-operated stress PBRs are inoculated and sequentially harvested, thus ensuring a daily harvest of TAG-enriched biomass. Finally photosynthetic efficiencies based on outdoor pilot data are used as model input to conduct a techno-economic analysis. The production costs of TAG-enriched biomass are presented based on current process technology. A sensitivity analysis is performed and a scenario with reduced production cost is evaluated.

6.2 How to increase TAG productivity

Several approaches for increasing TAG productivity have been proposed (Table 6.1). These are essentially related to the selection and/or development of the production strain as well as to the optimization of process conditions. In the following sections, the most relevant approaches are discussed and guidelines for improving TAG productivities are presented.

Table 6.1 Possible strategies to increase TAG productivity.

	Target	Approach	Example for realization of approach
BIOLOGY	Favorable carbon partitioning towards TAG production	1. Strain selection 2. Metabolic engineering 3. Laboratory evolution	1. High throughput screening 2. Targeted overexpression/knockdown of key genes 3. Mutagenesis & selective pressure & FACS
	High photosynthetic efficiency	4. Reactor design and configuration	4. Vertical PBRs, High S/V PBRs
PROCESS	Optimal process strategy	5. Batch 6. Repeated-batch 7. Continuous	5 - 6. Tune harvest frequency 6 - 7. Nutrient dosing based on irradiance 5 - 7. Optimal IBS-light availability

ALE: Adaptive Laboratory Evolution

FACS: Fluorescence Assisted Cell Sorting

S/V: Surface/Volume ratio

IBS: Initial-biomass-specific

6.2.1 Biological approach

6.2.1.1 *Exploring genetic diversity of microalgae*

Several screening studies have been performed (Rodolfi et al. 2009; Doan et al. 2011; Griffiths et al. 2011; Breuer et al. 2012; San Pedro et al. 2013; Benvenuti et al. 2014; Guccione et al. 2014; Taleb et al. 2015). In practice, only few microalgal species (e.g. *Nannochloropsis*, *Chlorella*, *Scenedesmus*, *Neochloris*) have been tested. However, the high genetic diversity of microalgae should be fully explored to select a robust production strain. To reduce risks of contamination and decrease costs during cultivation (e.g. cooling, pH control) microalgae should be isolated from highly selective and extreme environments such as deserts, hot and alkaline-saline waters.

Additionally, high-throughput screening protocols (e.g. 96-well plates) (Doan et al. 2011) for which the target product (e.g. TAG) can be quantified (Cabanelas et al. 2015) should be used. The predictability of such high-throughput screenings should be validated at lab-scale with the selected strains and processes should be developed under simulated outdoor production conditions (Taleb et al. 2015). Finally, the selected

strains should be tested outdoors in pilot PBRs under relevant climate conditions (Guccione et al. 2014; Bosma et al. 2014; Fon-Sing and Borowitzka 2015).

6.2.1.2 Strain development

Besides the natural diversity of microalgae, strain development can further enhance TAG productivity. Improving carbon partitioning towards TAG production and photosynthetic efficiency are the two main targets (Stephenson et al. 2011; De Bhowmick et al. 2015). Recently, successful attempts in increasing TAG productivity and/or content have been achieved either by targeted knockdown of a key gene involved in TAG catabolism (Trentacoste et al. 2013), or by disabling competitive carbon pathways with starchless mutants (Li et al. 2010; Breuer et al. 2014; de Jaeger et al. 2014). Similar results could also be achieved by decreasing the fraction of residual biomass made during N-starvation (e.g. reducing the carbon flow towards polysaccharide and glycoprotein matrix of the cell wall). Besides metabolic engineering, also Adaptive laboratory evolution (ALE) to a selective pressure combined with Fluorescence Assisted Cell Sorting (FACS) can lead to increased TAG productivities (Yu et al. 2013; Cabanelas et al. 2015).

Higher photosynthetic efficiencies could be achieved by increasing the electron flow through the electron transport chain (Chida et al. 2007), the activity and specificity of limiting enzymes, e.g. RuBisCo, involved in anabolic pathways (Atsumi et al. 2009; Lin et al. 2014) and also with reduced antenna size mutants (Kirst et al. 2014).

6.2.2 Process approach

6.2.2.1 Effect of reactor design on photosynthetic efficiency

As extensively reviewed by Zittelli et al. (2013), much research on developing or improving PBR design is ongoing (e.g. optimal distance between panels/loops, culture depth, mixing times, light distribution in the reactor). The ideal PBR should intercept all available sunlight while ensuring high photosynthetic efficiencies (Posten 2009). This can possibly be achieved with flat panel PBR designs that allow tilting the reactor to the incoming light (e.g. GWP-III flat panel, F&M Srl, www.femolnine.it).

In general, for high TAG productivities, PBRs with a high surface-to-volume ratio (e.g. Solix Biofuels® and Proviron Holding NV flat panels and thin-layer cascades ponds) should be preferred as, if properly mixed, they ensure high photosynthetic efficiencies and high volumetric TAG concentrations (Masojídek et al. 2011; Quinn et al. 2012; Jerez et al. 2014). Finally, the selection of optimal designs should be guided by techno-economic analyses considering both the biological productivities and production costs associated to each design.

6.2.2.2 *Operational strategy: Batch vs. (semi-) continuous operations*

In the effort of identifying optimal strategies for TAG production, much focus has been addressed on the batch vs. (semi-) continuous debate (**chapter 4**; Klok et al. 2013; Bona et al. 2014; Wen et al. 2014; Ho et al. 2014; San Pedro et al. 2014; Fuentes-Grünewald et al. 2015).

In **chapter 5** we showed that the batch process is the most effective strategy for TAG production. This is because batch cultures start with N-replete cells to which a sudden and large energy imbalance is applied (i.e. N-starvation). These cells have a high residual photosynthetic capacity for both biomass and TAG production. Likely in both semi-continuous and continuous cultures, cell recovery occurs at low photosynthetic efficiencies thus reducing the overall TAG productivity.

6.3 Two-step TAG production in southern Spain: a techno-economic analysis

In the following section a techno-economic analysis of a two-step TAG production is presented.

To ensure a continuous supply of inoculum for the TAG accumulation phase, nitrogen (N) replete biomass is produced in continuous (chemostat)-operated PBRs (“growth PBRs”) such that multiple batch-operated “stress PBRs” are sequentially inoculated and harvested ensuring a daily harvest of TAG-enriched biomass (Fig. 6.1). Projections were made for a 100 ha-scale plant using vertically stacked tubular PBRs in southern Spain (37°15' N 6° 56' W). The techno-economic model originally developed by Ruiz et al. (manuscript submitted) for nitrogen replete biomass production was extended with the TAG production phase. Our evaluation includes the cultivation phase and the biomass concentration step to obtain 15% w/w algal slurry as final product. The production costs of TAG-enriched biomass are presented.

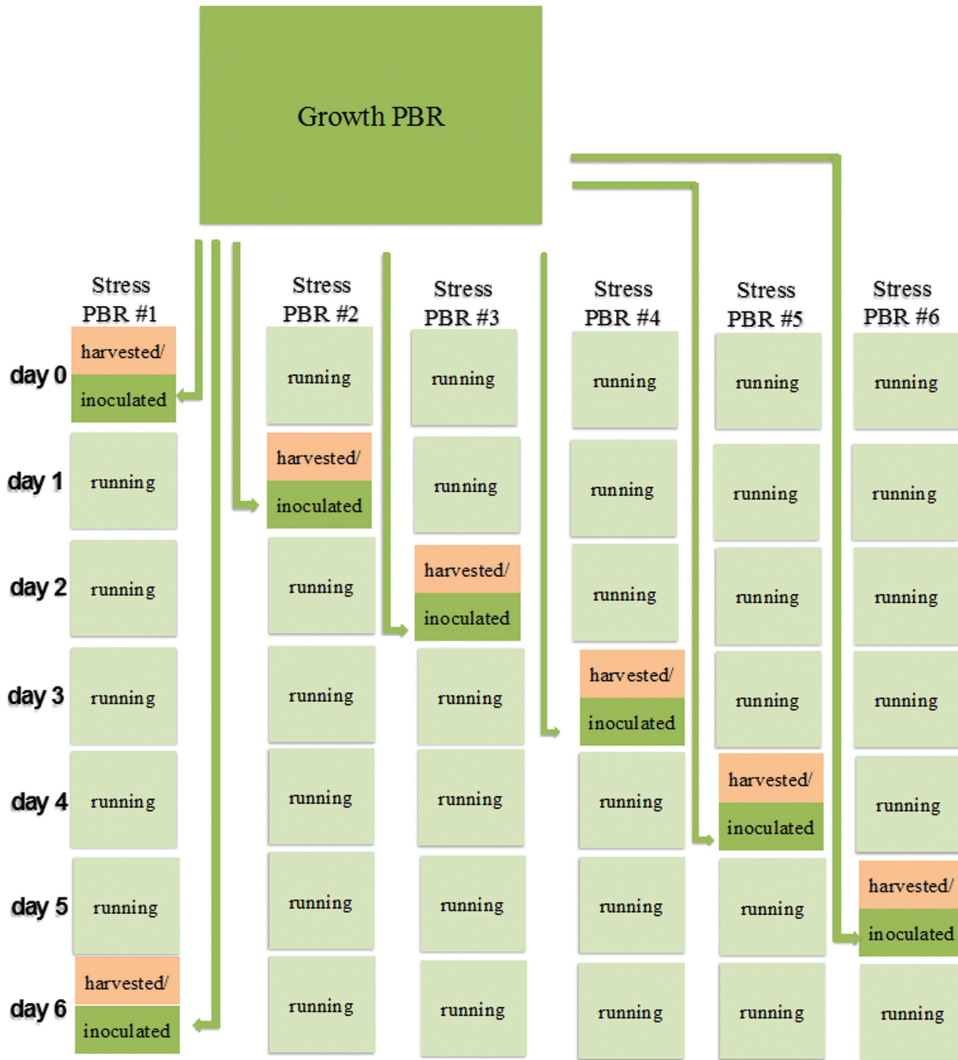


Figure 6.1 Schematic view of a two-step TAG production process. For simplicity, only one growth PBR and six stress PBRs are depicted. The growth PBR is operated in chemostat-mode. The outflow of the growth PBR is free of nitrogen and, every day, it fills one stress PBR. In each stress PBR, the TAG-accumulation phase starts immediately after inoculation (time to fill one unit is negligible) and runs in batch-mode for six days. The sequential inoculation and harvesting of all stress PBRs over a period of six days ensures a constant daily harvest of TAG-enriched biomass from the entire stress area.

6.3.2.1 *Process description*

The production area (100 ha) is divided in two stages: the growth phase, where biomass is produced in chemostat-operated PBRs, and the stress phase, producing TAG-enriched biomass in batch-operated PBRs (Figure 6.2). The process starts by filtering natural seawater, which is then mixed with nutrients in an automatized mixing unit and pumped into the growth PBRs. The seawater-based medium enters the growth PBRs only during daylight hours, and, concurrently, the same culture volume leaves the reactors. This outflow sequentially fills different stress PBRs to which no nutrients are added to promote TAG accumulation. In each stress PBR unit, the TAG-accumulation phase starts immediately after inoculation. For this, it is assumed that the culture leaving the growth PBRs is free of an extracellular nitrogen source (i.e. in the growth PBR, nitrogen is dosed based on productivity) and the time for filling a stress PBR unit is negligible. In the stress phase, independent PBR units are harvested sequentially, resulting in a batch strategy with a certain retention time. Thus, from the entire stress area there is a constant daily harvest of TAG-enriched biomass. When the stress PBRs are harvested, the TAG-enriched biomass is pumped to the centrifuge where 15% algal slurry is obtained. In both growth and stress PBRs, the culture is mixed by a recirculation pump and supplied with CO₂. Degassers ensure that oxygen partial pressure never exceeds 300%. Culture temperature is controlled between 20 and 30 °C with heat exchangers that recirculate cooling water available from an external water reservoir at a constant temperature of 25 °C. Wastewater treatment is not performed because the effluent of the stress PBRs is considered free of nutrients and organic matter. As also in Ruiz et al. (manuscript submitted), the plant is operational for 300 days per year, three cleanings per year are performed and one manager, three supervisors and 28 operators are required to run the plant.

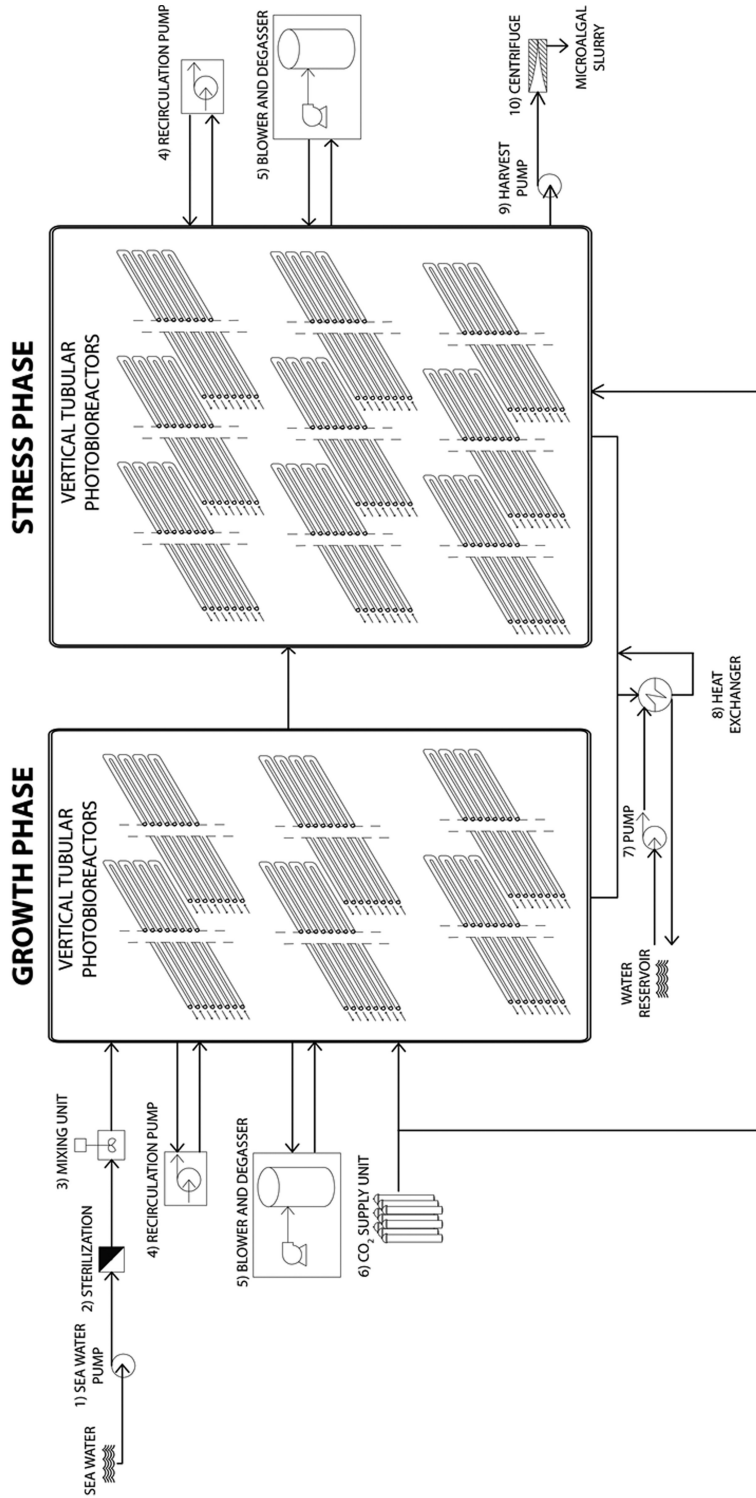


Figure 6.2 Plant schematic view.

6.3.2.2 *Empirical data and area allocation*

The yearly biomass and TAG productivities were calculated from the photosynthetic efficiencies obtained outdoors at AlgaePARC in the Netherlands (de Vree et al. (2015), for biomass production and **chapter 3** for TAG production) and the total irradiance in southern Spain. For the growth phase, an average photosynthetic efficiency of 2.23% for biomass production (containing 4% TAG w/w) and a daily culture dilution rate of 27% were used. For the stress phase, an average photosynthetic efficiency of 1.48% for biomass production (containing 24% TAG w/w) was used (Supplementary material 6.1). Under low light conditions in the Netherlands ($14 \text{ mol m}^{-2} \text{ d}^{-1}$), total TAG productivity is maximal after nine days in the stress reactor, whereas at high light conditions ($36 \text{ mol m}^{-2} \text{ d}^{-1}$), the productivity is maximal after six days. Because southern Spain has longer periods of high light compared to the Netherlands, we chose to always harvest the TAG-enriched biomass after six days in the stress PBRs. This retention time of six days can thus be regarded as a 17% daily dilution of the PBRs in the stress area.

The total production area (100 ha) was allocated between growth and stress phase using mass balances based on total area and the aforementioned dilution rates. It resulted in areas of 38.2 and 61.8 ha for the growth and stress phase, respectively; with 10% of the growth area being allocated to inoculum production to fill the growth PBRs after a routine cleaning or culture crash. The area for inoculum production is considered identical to the growth area in terms of operational and capital costs (OPEX and CAPEX). However, since this biomass is only incidentally transferred to the growth PBRs, the inoculum production area is assumed as non-productive. The area occupied by side-equipment and piping is considered as 10% of the production area, thus resulting in a total facility area of 110 ha.

As described by Ruiz et al. (manuscript submitted), the model uses location-specific parameters such as climatic conditions, energy costs, labor costs and employer's contribution to labor costs as well as workweek hours. For model specifications, we refer to the work of Ruiz et al. (manuscript submitted). In Supplementary material 6.2, the changes in major equipment (numbers 1 – 10 in Fig. 6.2) capacity and power requirement are reported. These modifications were made due to the different process strategy adopted in this study (i.e. different area, flows and volumes) compared to Ruiz et al. (manuscript submitted).

6.3.2.3 *Production cost of TAG-enriched biomass: base-case based on pilot plant data*

The photosynthetic efficiencies and TAG contents obtained at pilot-scale using current process technology and design were used as model base-case (Table 6.2). A TAG-enriched biomass production cost of 7.4 €·kg⁻¹ was obtained and the Net Energy Ratio (NER) was 1.1, indicating that the amount of energy (i.e. chemical energy) generated by the process was slightly higher than the energy required for operating the plant.

A cost breakdown analysis was conducted (Fig. 6.3). Our analysis shows that, in both phases, the largest contribution to total costs (38% for growth and 31% for stress) is given by construction and other fixed costs (e.g. land, property tax, insurance, contractor's fee). The main contributing factors to major equipment costs are recirculation pumps (45% for growth and 37% for stress) and temperature control (22% for growth and 30% for stress) (Fig. 6.3C-D).

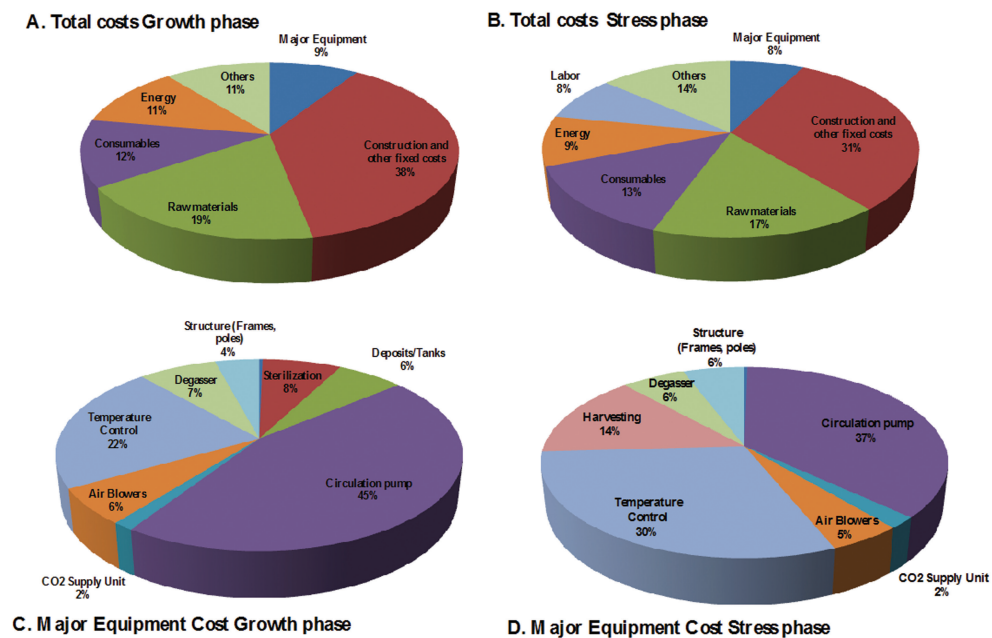


Figure 6.3 Cost breakdown for growth (A and C) and stress (B and D) phases for a two-step-continuous TAG production process in vertically stacked tubular PBRs. Labor costs are included only in the stress phase for the total plant area (100 ha).

Table 6.2 Results of the techno-economic analysis.

	Base case	Optimized case
	Growth phase: 2.17% PE, 4% TAG w/w Stress phase: 1.48% PE, 24% TAG w/w 30 °C culture temperature for cooling Current process technology	Growth phase: 6% PE, 4% TAG w/w Stress phase: 4.10% PE, 60% TAG w/w 40 °C culture temperature for cooling Optimized process technology ¹⁾
Total costs (M€·yr ⁻¹)	28.4	30.9
Biomass production (Kton·yr ⁻¹)	3.8	10.2
TAG production (Kton·yr ⁻¹)	0.5	3.0
Biomass cost (€·kg ⁻¹)	7.4	3.0
CAPEX (M€·yr ⁻¹)	12.0	15.8
OPEX (M€·yr ⁻¹)	16.4	15.1
Initial investment (M€)	174.9	230.8
Produced energy (GWh·yr ⁻¹)	26.0	76.3
Consumed energy (GWh·yr ⁻¹)	23.5	43.5
NER	1.1	1.8

¹⁾ Flow velocity is reduced from 0.45 to 0.3 m s⁻¹ during the day and to 0.23 m s⁻¹ during the night. Concentration of the biomass is performed by microfiltration and subsequent centrifugation; flue gas is used as CO₂ source; 310 operational days per year instead of 300; reduced number of employees (one manager, one supervisor, eight operators); cleaning reduced from three times to one per year; the fraction of the facility used to prepare inoculum is reduced from 10 to 5% of the growth area.

6.3.2.4 *Production cost of TAG-enriched biomass: optimized scenario*

For a substantial cost reduction, both the biological performance of the production strain and the process technology should be optimized. For this, a sensitivity analysis was performed. The PE during the growth phase was increased to 6% (Cuaresma et al. 2011; Ruiz et al. manuscript submitted). The PE of stress phase was increased proportionally to 4.1%, while the TAG content was augmented to 60% w/w (Breuer et al. 2014). Furthermore, the culture temperature required for cooling was increased from 30 to 40 °C (Guccione et al. 2014). The process technology was optimized by reducing the flow velocity from 0.45 to 0.3 m s⁻¹ during the day (Norsker et al. 2011) and to 0.23 m s⁻¹ during the night (Gómez-Pérez et al. 2015); TAG-enriched biomass was pre-concentrated by microfiltration and subsequently centrifuged; flue gas instead of commercial CO₂ was used; the plant was operational for 310 days per year instead of 300; the number of employees was reduced to one manager, one supervisor and eight operators; reactors were cleaned once per year instead of three; the fraction of the facility used to prepare inoculum was reduced from 10 to 5% of the growth area (Ruiz et al., manuscript submitted).

The TAG-enriched biomass production cost were substantially reduced, decreasing from 7.4 to 3.0 €·kg⁻¹ (Table 6.2).

Nevertheless, to enter the commodity markets, production costs should decrease further. As shown by Ruiz et al. (manuscript submitted), cost reduction can be achieved using plastic film flat panels that, compared to tubular systems, require lower installation and operational costs (e.g. no recirculation pumps). Furthermore, to ensure the economic viability of microalgal TAGs at the current commodity market values (0.5 – 2.5 €·kg⁻¹, Ruiz et al., manuscript submitted), the whole biomass components should be valorized and/or the selling price of microalgal TAGs should be increased (e.g. enriching the TAG composition in specific fatty acids).

6.4 Conclusions

Guidelines for optimization of TAG productivity are given. A great potential relies both on strains with enhanced photosynthetic machinery and carbon partitioning towards TAGs and on PBRs able to intercept all the sunlight while ensuring high photosynthetic efficiencies. With a techno-economic analysis of a two-step TAG production process in vertically stacked tubular PBRs, we showed that the production costs of TAG-enriched biomass can be substantially decreased by optimizing both the process technology and the biological performance. However, high TAG productivities and contents alone do not directly guarantee the economic feasibility of the process, when comparing to the present market value of TAGs. Cost-competiveness strictly relies on the valorization of the whole biomass components and on development of cheaper PBR designs (e.g. plastic film flat panels).

Concluding, with this work we laid down a solid basis for assessing the economic potential of microalgae and we identified the crucial bottlenecks that should be overcome to enable profitable and sustainable microalgal TAG production for the commodity markets.

Supplementary material

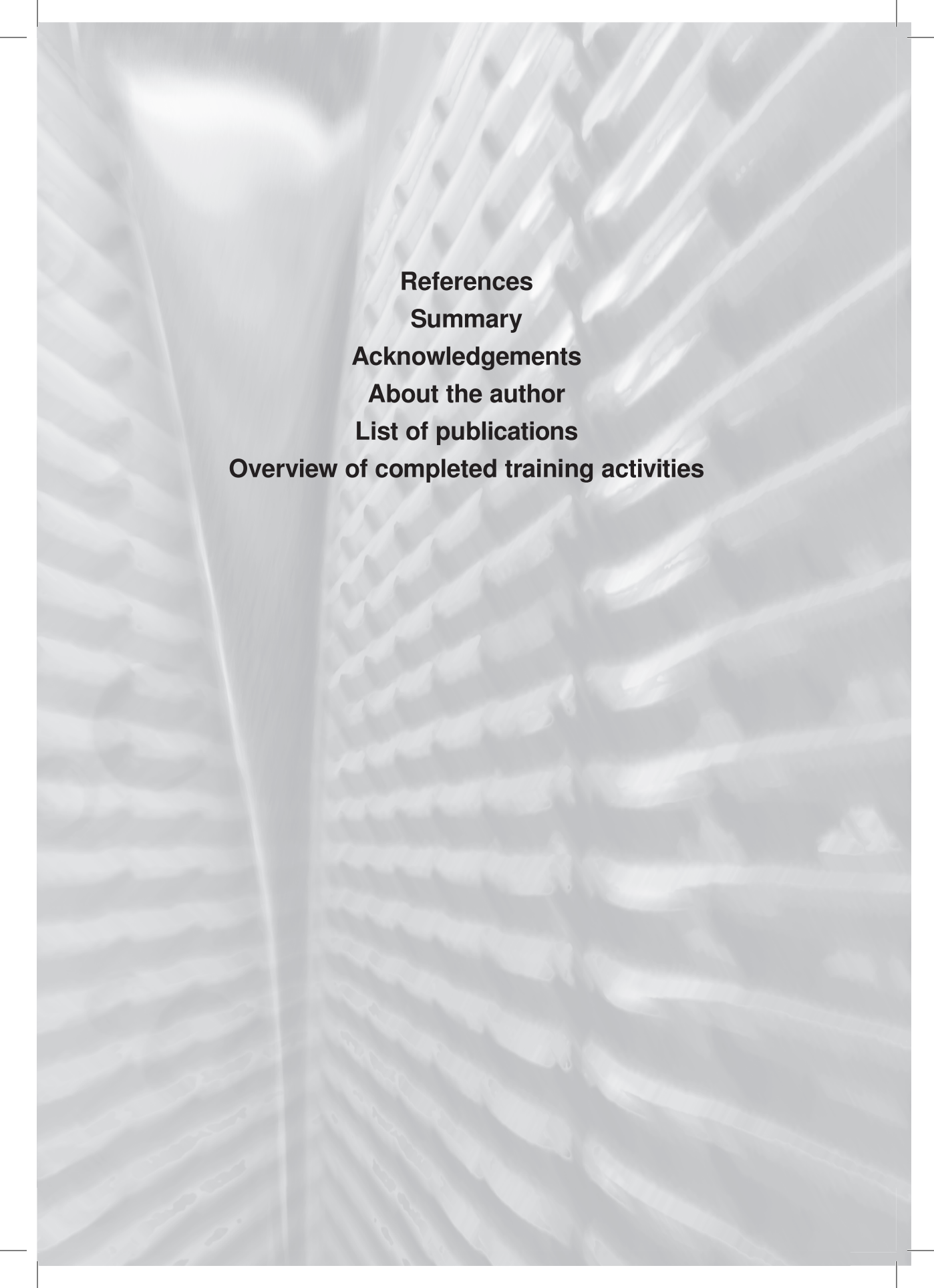
Supplementary material 6.1 Biological inputs regarding nitrogen (N) replete and TAG-enriched biomass obtained in outdoor pilot cultivations at AlgaePARC, the Netherlands. To calculate the N- replete and TAG-enriched biomass productivities as well as biomass concentration and TAG content at the two light intensities, mathematical fit of experimental data vs. PFD is used ($R^2 > 0.95$).

Growth phase (chemostat-operation; 31 m ² reactor ground area)				
Light intensity (mol m ⁻² d ⁻¹)	N-replete biomass productivity (g m ⁻² d ⁻¹)	N-replete biomass yield on light (g mol ⁻¹)	Cellular TAG content (%)	PE (%)
14	6.8	0.49	4	2.12
36	18.4	0.51	4	2.22
Stress phase* (batch-operation; 4.4 m ² reactor ground area)				
Average light intensity (mol m ⁻² d ⁻¹)	TAG-enriched biomass productivity* (g m ⁻² d ⁻¹)	TAG-enriched biomass yield on light (g mol ⁻¹)	Cellular TAG content (%)	PE (%)
14	4.97	0.36	19	1.75
36	8.38	0.23	29	1.20

* At day 6 of cultivation.

Supplementary material 6.2 Modified major equipment compared to the original model.

#	Scheme	Equipment	Stage	Capacity	Units	Cost (€)	Power (kW)
1 and 9	Seawater pump	Growth	200	m ³ h ⁻¹	13,544	5.9	
2	Sterilization	Growth	59.9	m ³ h ⁻¹	117,979	-	
3	Mixing unit	Growth	1	m ³	199000	0.5	
4	Recirculation pump	Growth and stress	700	m ³ h ⁻¹	28,105	See "Power requirement for liquid circulation" in Ruiz et al.	
5	Blower	Growth and stress	200	m ³ h ⁻¹	3,027	0.99	
5	Degasser	Growth and stress	0.66	m ³	1,214	-	
6	CO ₂ Supply unit	Growth and stress	1	Ha	4,717	Insignificant	
7	Pump (cooling)	Growth and stress	28000	m ³ h ⁻¹	595,600	See "temperature control" in Ruiz et al.	
8	Heat exchanger	Growth and stress	See "temperature control" in Ruiz et al.				
10	Centrifuge	Stress	65	m ³ h ⁻¹	300,000	55	
-	Steel structures (poles)	Growth and stress	3.8	kg m ⁻¹	621 € ton ⁻¹	-	



References
Summary
Acknowledgements
About the author
List of publications
Overview of completed training activities

References

- Ación FG, Fernández JM, Magán JJ, Molina E (2012) Production cost of a real microalgae production plant and strategies to reduce it. *Biotechnol Adv* 30:1344–53. doi: 10.1016/j.biotechadv.2012.02.005
- Atsumi S, Higashide W, Liao JC (2009) Direct photosynthetic recycling of carbon dioxide to isobutyraldehyde. *Nat Biotechnol* 27:1177–80. doi: 10.1038/nbt.1586
- Bayliss C, Zanain M, Pooley C, et al (2015) Evaluation of batch and semi-continuous culture of *Porphyridium purpureum* in a photobioreactor in high latitudes using Fourier Transform Infrared spectroscopy for monitoring biomass composition and metabolites production. *Bioresour Technol* 189:357–63. doi: 10.1016/j.biortech.2015.04.042
- Benvenuti G, Bosma R, Cuaresma M (2014) Selecting microalgae with high lipid productivity and photosynthetic activity under nitrogen starvation. *J Appl Phycol* 27:1425 – 1431. doi: 10.1007/s10811-014-0470-8
- Benvenuti G, Bosma R, Klok AJ, et al (2015) Microalgal triacylglycerides production in outdoor batch-operated tubular PBRs. *Biotechnol Biofuels* 8:100. doi: 10.1186/s13068-015-0283-2
- Berges JA, Charlebois DO, Mauzerall DC, Falkowski PG (1996) Differential Effects of Nitrogen Limitation on Photosynthetic Efficiency of Photosystems I and II in Microalgae. *Plant Physiol* 110:689–696. doi: 10.1104/pp.110.2.689
- Berges JA, Falkowski PG (1998) Physiological stress and cell death in marine phytoplankton: Induction of proteases in response to nitrogen or light limitation. *Limnol Oceanogr* 43:129–135. doi: 10.4319/lo.1998.43.1.0129
- Bona F, Capuzzo A, Franchino M, Maffei ME (2014) Semicontinuous nitrogen limitation as convenient operation strategy to maximize fatty acid production in *Neochloris oleoabundans*. *Algal Res* 5:1–6. doi: 10.1016/j.algal.2014.03.007
- Bondioli P, Della Bella L, Rivolta G, et al (2012) Oil production by the marine microalgae *Nannochloropsis* sp. F&M-M24 and *Tetraselmis suecica* F&M-M33. *Bioresour Technol* 114:567–72. doi: 10.1016/j.biortech.2012.02.123
- Bosma R, de Vree JH, Slegers PM, et al (2014) Design and construction of the microalgal pilot facility AlgaePARC. *Algal Res* 6 PartB:160 – 169. doi: 10.1016/j.algal.2014.10.006
- Bosma R, van Zessen E, Reith JH, et al (2007) Prediction of volumetric productivity of an outdoor photobioreactor. *Biotechnol Bioeng* 97:1108–20. doi: 10.1002/bit.21319
- Breuer G, de Jaeger L, Artus VPG, et al (2014) Superior triacylglycerol (TAG) accumulation in starchless mutants of *Scenedesmus obliquus*: (II) evaluation of TAG yield and productivity in controlled photobioreactors. *Biotechnol Biofuels* 7:70. doi: 10.1186/1754-6834-7-70
- Breuer G, Evers WAC, de Vree JH, et al (2013a) Analysis of Fatty Acid Content and Composition in Microalgae. *J Vis Exp* 80:e50628. doi: doi:10.3791/50628
- Breuer G, Lamers PP, Janssen M, et al (2015) Opportunities to improve the areal oil productivity of microalgae. *Bioresour Technol* 186:294–302. doi: 10.1016/j.biortech.2015.03.085
- Breuer G, Lamers PP, Martens DE, et al (2012) The impact of nitrogen starvation on the dynamics of triacylglycerol accumulation in nine microalgae strains. *Bioresour Technol* 124:217–26. doi: 10.1016/j.biortech.2012.08.003
- Breuer G, Lamers PP, Martens DE, et al (2013b) Effect of light intensity, pH, and temperature on triacylglycerol (TAG) accumulation induced by nitrogen starvation in *Scenedesmus obliquus*. *Bioresour Technol* 143:1–9. doi: 10.1016/j.biortech.2013.05.105
- Cabanelas ITD, Zwart M van der, Kleinegris DMM, et al (2015) Rapid method to screen and sort lipid accumulating microalgae. *Bioresour Technol* 184:47–52. doi: 10.1016/j.biortech.2014.10.057
- Chen W, Zhang C, Song L, et al (2009) A high throughput Nile red method for quantitative measurement of neutral lipids in microalgae. *J Microbiol Methods* 77:41–7. doi: 10.1016/j.mimet.2009.01.001
- Chida H, Nakazawa A, Akazaki H, et al (2007) Expression of the algal cytochrome c6 gene in *Arabidopsis* enhances photosynthesis and growth. *Plant Cell Physiol* 48:948–57. doi: 10.1093/pcp/pcm064

References

- Chisti Y (2007) Biodiesel from microalgae. *Biotechnol Adv* 25:294–306. doi: 10.1016/j.biotechadv.2007.02.001
- Chisti Y (2013) Constraints to commercialization of algal fuels. *J Biotechnol* 167:201–14. doi: 10.1016/j.jbiotec.2013.07.020
- Chiu S-Y, Kao C-Y, Tsai M-T, et al (2009) Lipid accumulation and CO₂ utilization of *Nannochloropsis oculata* in response to CO₂ aeration. *Bioresour Technol* 100:833–8. doi: 10.1016/j.biortech.2008.06.061
- Cuaresma M, Janssen M, Vilchez C, Wijffels RH (2011) Horizontal or vertical photobioreactors? How to improve microalgae photosynthetic efficiency. *Bioresour Technol* 102:5129–37. doi: 10.1016/j.biortech.2011.01.078
- De Bhowmick G, Koduru L, Sen R (2015) Metabolic pathway engineering towards enhancing microalgal lipid biosynthesis for biofuel application—A review. *Renew Sustain Energy Rev* 50:1239–1253. doi: 10.1016/j.rser.2015.04.131
- de Jaeger L, Verbeek RE, Draaisma RB, et al (2014) Superior triacylglycerol (TAG) accumulation in starchless mutants of *Scenedesmus obliquus*: (I) mutant generation and characterization. *Biotechnol Biofuels* 7:69. doi: 10.1186/1754-6834-7-69
- de Vree JH, Bosma R, Janssen M, et al (2015) Comparison of four outdoor pilot-scale photobioreactors. *Biotechnol Biofuels* 8:215. doi: 10.1186/s13068-015-0400-2
- Doan TTY, Sivaloganathan B, Obbard JP (2011) Screening of marine microalgae for biodiesel feedstock. *Biomass and Bioenergy* 35:2534–2544. doi: 10.1016/j.biombioe.2011.02.021
- Doucha J, Lívanský K (2006) Productivity, CO₂/O₂ exchange and hydraulics in outdoor open high density microalgal (*Chlorella* sp.) photobioreactors operated in a Middle and Southern European climate. *J Appl Phycol* 18:811–826. doi: 10.1007/s10811-006-9100-4
- Draaisma RB, Wijffels RH, Slegers PM, et al (2013) Food commodities from microalgae. *Curr Opin Biotechnol* 24:169–177. doi: 10.1016/j.copbio.2012.09.012
- Droop MR (2009) Vitamin B12 and Marine Ecology. IV. The Kinetics of Uptake, Growth and Inhibition in *Monochrysis Lutheri*. *J Mar Biol Assoc United Kingdom* 48:689. doi: 10.1017/S0025315400019238
- Dubois M, Gilles K a, Ton JKH, et al (1956) Colorimetric Method for Determination of Sugars and Related Substances. *Anal Chem* 28:350–356. doi: 10.1021/ac60111a017
- Fábregas J, Masada A, Domínguez A, et al (2002) Changes in the cell composition of the marine microalga, *Nannochloropsis gaditana*, during a light : dark cycle. *Biotechnol Lett* 24:1699–1703.
- Falkowski PG, Owens TG (1980) Light- Shade Adaptation '. *Plant Physiol* 66:592–595. doi: 0032-0889/80/66/0592/04
- Feng P, Deng Z, Hu Z, Fan L (2011) Lipid accumulation and growth of *Chlorella zofingiensis* in flat plate photobioreactors outdoors. *Bioresour Technol* 102:10577–84. doi: 10.1016/j.biortech.2011.08.109
- Fernandes B, Teixeira J, Dragone G, et al (2013) Relationship between starch and lipid accumulation induced by nutrient depletion and replenishment in the microalga *Parachlorella kessleri*. *Bioresour Technol* 144:268–274. doi: 10.1016/j.biortech.2013.06.096
- Fon-Sing S, Borowitzka MA (2015) Isolation and screening of euryhaline *Tetraselmis* spp. suitable for large-scale outdoor culture in hypersaline media for biofuels. *J Appl Phycol* 1–14. doi: 10.1007/s10811-015-0560-2
- Foyer C, Furbank R, Harbinson J, Horton P (1990) The mechanisms contributing to photosynthetic control of electron transport by carbon assimilation in leaves. *Photosynth Res* 25:83–100. doi: 10.1007/BF00035457
- Geider R, Graziano L, McKay RM (1998a) Responses of the photosynthetic apparatus of *Dunaliella tertiolecta* (Chlorophyceae) to nitrogen and phosphorus limitation. *Eur J Phycol* 33:315–332. doi: 10.1080/09670269810001736813
- Geider RJ, Laroche J, Greene RM, Olaizola M (1993) Response of the Photosynthetic Apparatus of *Phaeodactylum-Tricornutum* (Bacillariophyceae) to Nitrate, Phosphate, or Iron Starvation. *J Phycol* 29:755–766. doi: 10.1111/j.0022-3646.1993.00755.x
- Geider RJ, MacIntyre HL, Kana TM (1998b) A dynamic regulatory model of phytoplankton acclimation to light, nutrients, and temperature. *Limnol Oceanogr* 43:679–694. doi: 10.4319/lo.1998.43.4.0679

- German JB (1999) Food processing and lipid oxidation. *Adv Exp Med Biol* 459:23–50.
- Gómez-Pérez CA, Espinosa J, Montenegro Ruiz LC, van Boxtel AJB (2015) CFD simulation for reduced energy costs in tubular photobioreactors using wall turbulence promoters. *Algal Res* 12:1–9. doi: 10.1016/j.algal.2015.07.011
- Griffiths MJ, Harrison STL (2009) Lipid productivity as a key characteristic for choosing algal species for biodiesel production. *J Appl Phycol* 21:493–507. doi: 10.1007/s10811-008-9392-7
- Griffiths MJ, Hille RP, Harrison STL (2011) Lipid productivity, settling potential and fatty acid profile of 11 microalgal species grown under nitrogen replete and limited conditions. *J Appl Phycol* 24:989–1001. doi: 10.1007/s10811-011-9723-y
- Guccione A, Biondi N, Sampietro G, et al (2014) *Chlorella* for protein and biofuels: from strain selection to outdoor cultivation in a Green Wall Panel photobioreactor. *Biotechnol Biofuels* 7:84. doi: 10.1186/1754-6834-7-84
- Han F, Huang J, Li Y, et al (2013) Enhanced lipid productivity of *Chlorella pyrenoidosa* through the culture strategy of semi-continuous cultivation with nitrogen limitation and pH control by CO₂. *Bioresour Technol* 136:418–424. doi: 10.1016/j.biortech.2013.03.017
- Hempel F, Bozarth AS, Lindenkamp N, et al (2011) Microalgae as bioreactors for bioplastic production. *Microb Cell Fact* 10:81. doi: 10.1186/1475-2859-10-81
- Ho S-H, Chang J-S, Lai Y-Y, Chen C-NN (2014a) Achieving high lipid productivity of a thermotolerant microalga *Desmodesmus* sp. F2 by optimizing environmental factors and nutrient conditions. *Bioresour Technol*. doi: 10.1016/j.biortech.2014.01.017
- Ho S-H, Chen C-NN, Lai Y-Y, et al (2014b) Exploring the high lipid production potential of a thermotolerant microalga using statistical optimization and semi-continuous cultivation. *Bioresour Technol* 163:128–35. doi: 10.1016/j.biortech.2014.04.028
- Hu Q, Sommerfeld M, Jarvis E, et al (2008) Microalgal triacylglycerols as feedstocks for biofuel production: perspectives and advances. *Plant J* 54:621–39. doi: 10.1111/j.1365-313X.2008.03492.x
- Jassby AD, Platt T (1976) Mathematical formulation of the relationship between photosynthesis and light for phytoplankton. *Limnol Oceanogr* 21:540–547. doi: 10.4319/lo.1976.21.4.0540
- Jerez CG, Enrique N, Malpartida I, et al (2014) Hydrodynamics and photosynthesis performance of *Chlorella fusca* grown in a Thin-Layer Cascade (TLC) system. *Aquat Biol* 22:111–122. doi: 10.3354/ab00603
- Kandilian R, Pruvost J, Legrand J, Pilon L (2014) Influence of light absorption rate by *Nannochloropsis oculata* on triglyceride production during nitrogen starvation. *Bioresour Technol* 163:308–19. doi: 10.1016/j.biortech.2014.04.045
- Kirst H, Formighieri C, Melis A (2014) Maximizing photosynthetic efficiency and culture productivity in cyanobacteria upon minimizing the phycobilisome light-harvesting antenna size. *Biochim Biophys Acta - Bioenerg* 1837:1653–1664. doi: 10.1016/j.bbabi.2014.07.009
- Kliphuis AMJ, Klok AJ, Martens DE, et al (2012) Metabolic modeling of *Chlamydomonas reinhardtii*: energy requirements for photoautotrophic growth and maintenance. *J Appl Phycol* 24:253–266. doi: 10.1007/s10811-011-9674-3
- Klok AJ, Lamers PP, Martens DE, et al (2014) Edible oils from microalgae: insights in TAG accumulation. *Trends Biotechnol* 32:521 – 528. doi: 10.1016/j.tibtech.2014.07.004
- Klok AJ, Martens DE, Wijffels RH, Lamers PP (2013) Simultaneous growth and neutral lipid accumulation in microalgae. *Bioresour Technol* 134:233–43. doi: 10.1016/j.biortech.2013.02.006
- Li J, Han D, Wang D, et al (2014) Choreography of Transcriptomes and Lipidomes of *Nannochloropsis* Reveals the Mechanisms of Oil Synthesis in Microalgae. *Plant Cell* 26:1645–1665. doi: 10.1105/tpc.113.121418
- Li Y, Han D, Hu G, et al (2010) Inhibition of starch synthesis results in overproduction of lipids in *Chlamydomonas reinhardtii*. *Biotechnol Bioeng* 107:258–68. doi: 10.1002/bit.22807
- Li Y, Horsman M, Wang B, et al (2008) Effects of nitrogen sources on cell growth and lipid accumulation of green alga *Neochloris oleoabundans*. *Appl Microbiol Biotechnol* 81:629–36. doi: 10.1007/s00253-008-1681-1

References

- Lin MT, Occhialini A, Andralojc PJ, et al (2014) A faster Rubisco with potential to increase photosynthesis in crops. *Nature* 513:547–550. doi: 10.1038/nature13776
- Lucas-Salas LM, Castrillo M, Martínez D (2013) Effects of dilution rate and water reuse on biomass and lipid production of *Scenedesmus obliquus* in a two-stage novel photobioreactor. *Bioresour Technol* 143:344–52. doi: 10.1016/j.biortech.2013.06.007
- Malik A, Lenzen M, Ralph PJ, Tamburic B (2015) Hybrid life-cycle assessment of algal biofuel production. *Bioresour Technol* 184:436–443. doi: 10.1016/j.biortech.2014.10.132
- Masojidek J, Kopecký J, Giannelli L, Torzillo G (2011) Productivity correlated to photobiochemical performance of *Chlorella* mass cultures grown outdoors in thin-layer cascades. *J Ind Microbiol Biotechnol* 38:307–317. doi: 10.1007/s10295-010-0774-x
- Mata TM, Martins A a., Caetano NS (2010) Microalgae for biodiesel production and other applications: A review. *Renew Sustain Energy Rev* 14:217–232. doi: 10.1016/j.rser.2009.07.020
- Mayers JJ, Flynn KJ, Shields RJ (2013) Rapid determination of bulk microalgal biochemical composition by Fourier-Transform Infrared spectroscopy. *Bioresour Technol* 148:215–220. doi: 10.1016/j.biortech.2013.08.133
- Melis A (2009) Solar energy conversion efficiencies in photosynthesis: Minimizing the chlorophyll antennae to maximize efficiency. *Plant Sci* 177:272–280. doi: 10.1016/j.plantsci.2009.06.005
- Miglio R, Palmery S, Salvalaggio M, et al (2013) Microalgae triacylglycerols content by FT-IR spectroscopy. *J Appl Phycol* 25:1621–1631. doi: 10.1007/s10811-013-0007-6
- Molina Grima E, Belarbi E-H, Ación Fernández FG, et al (2003) Recovery of microalgal biomass and metabolites: process options and economics. *Biotechnol Adv* 20:491–515.
- Mulders KJM, Janssen JH, Martens DE, et al (2014) Effect of biomass concentration on secondary carotenoids and triacylglycerol (TAG) accumulation in nitrogen-depleted *Chlorella zofingiensis*. *Algal Res* 6:8–16. doi: 10.1016/j.algal.2014.08.006
- Mulders KJM, Lamers PP, Wijffels RH, Martens DE (2015) Dynamics of biomass composition and growth during recovery of nitrogen-starved *Chromochloris zofingiensis*. *Appl Microbiol Biotechnol* 99:1873–1884. doi: DOI 10.1007/s00253-014-6181-x
- Münkel R, Schmid-Staiger U, Werner A, Hirth T (2013) Optimization of outdoor cultivation in flat panel airlift reactors for lipid production by *Chlorella vulgaris*. *Biotechnol Bioeng* 110:2882–93. doi: 10.1002/bit.24948
- Norsker N-H, Barbosa MJ, Vermuë MH, Wijffels RH (2011) Microalgal production—a close look at the economics. *Biotechnol Adv* 29:24–7. doi: 10.1016/j.biotechadv.2010.08.005
- Pal D, Khozin-Goldberg I, Cohen Z, Boussiba S (2011) The effect of light, salinity, and nitrogen availability on lipid production by *Nannochloropsis* sp. *Appl Microbiol Biotechnol* 90:1429–41. doi: 10.1007/s00253-011-3170-1
- Parkhill J, Maillet G, Cullen JJ (2001) Fluorescence-based maximal quantum yield for PSII as a diagnostic of nutrient stress. *J Phycol* 37:517–529. doi: 10.1046/j.1529-8817.2001.037004517.x
- Paul NP, Tseng CK, Borowitzka M (2012) *Aquaculture*. Blackwell Publishing Ltd., West Sussex, UK
- Pienkos P, Darzins A (2009) The promise and challenges of microalgal-derived biofuels. *Biofuels, Bioprod Biorefining* 431–440. doi: 10.1002/bbb
- Posten C (2009) Design principles of photo-bioreactors for cultivation of microalgae. *Eng Life Sci* 9:165–177. doi: 10.1002/elsc.200900003
- Příbyl P, Cepák V, Zachleder V (2013) Production of lipids and formation and mobilization of lipid bodies in *Chlorella vulgaris*. *J Appl Phycol* 25:545–553. doi: 10.1007/s10811-012-9889-y
- Pruvost J, Van Vooren G, Cogne G, Legrand J (2009) Investigation of biomass and lipids production with *Neochloris oleoabundans* in photobioreactor. *Bioresour Technol* 100:5988–95. doi: 10.1016/j.biortech.2009.06.004
- Pruvost J, Van Vooren G, Le Guoic B, et al (2011) Systematic investigation of biomass and lipid productivity by microalgae in photobioreactors for biodiesel application. *Bioresour Technol* 102:150–8. doi: 10.1016/j.biortech.2010.06.153

- Quinn JC, Yates T, Douglas N, et al (2012) Nannochloropsis production metrics in a scalable outdoor photobioreactor for commercial applications. *Bioresour Technol* 117:164–71. doi: 10.1016/j.biortech.2012.04.073
- Ramanna L, Guldhe A, Rawat I, Bux F (2014) The optimization of biomass and lipid yields of *Chlorella sorokiniana* when using wastewater supplemented with different nitrogen sources. *Bioresour Technol* 168:127–35. doi: 10.1016/j.biortech.2014.03.064
- Rodolfi L, Chini Zittelli G, Bassi N, et al (2009) Microalgae for oil: strain selection, induction of lipid synthesis and outdoor mass cultivation in a low-cost photobioreactor. *Biotechnol Bioeng* 102:100–12. doi: 10.1002/bit.22033
- Royal Dutch Shell Group (1983) *The Petroleum Handbook*, Royal Dutc. Elsevier Science Publishing, New York.
- Ruiz J, Olivieri G, de Vree J, Bosma R, Willems P, Reith HJ, Eppink MHM, Kleinegris DMM, Wijffels RH, Barbosa MJ Towards industrial products from microalgae. Manuscript submitted
- Rupilius W, Ahmad S (2007) Palm oil and palm kernel oil as raw materials for basic oleochemicals and biodiesel. *Eur J Lipid Sci Technol* 109:433–439. doi: 10.1002/ejlt.200600291
- San Pedro A, González-López C V, Ación FG, Molina-Grima E (2014) Outdoor pilot-scale production of *Nannochloropsis gaditana*: influence of culture parameters and lipid production rates in tubular photobioreactors. *Bioresour Technol* 169:667–76. doi: 10.1016/j.biortech.2014.07.052
- San Pedro A, González-López C V, Ación FG, Molina-Grima E (2013) Marine microalgae selection and culture conditions optimization for biodiesel production. *Bioresour Technol* 134:353–61. doi: 10.1016/j.biortech.2013.02.032
- Santos a M, Janssen M, Lamers PP, et al (2012) Growth of oil accumulating microalga *Neochloris oleoabundans* under alkaline-saline conditions. *Bioresour Technol* 104:593–9. doi: 10.1016/j.biortech.2011.10.084
- Santos AM, Wijffels RH, Lamers PP (2014) pH-upshock yields more lipids in nitrogen-starved *Neochloris oleoabundans*. *Bioresour Technol* 152:299–306. doi: 10.1016/j.biortech.2013.10.079
- Sauer J, Schreiber U, Schmid R, et al (2001) Nitrogen Starvation-Induced Chlorosis in *Synechococcus* PCC 7942. Low-Level Photosynthesis As a Mechanism of Long-Term Survival. *PLANT Physiol* 126:233–243. doi: 10.1104/pp.126.1.233
- Schenk PM, Thomas-Hall SR, Stephens E, et al (2008) Second Generation Biofuels: High-Efficiency Microalgae for Biodiesel Production. *BioEnergy Res* 1:20–43. doi: 10.1007/s12155-008-9008-8
- Schreiber U, Klughammer C, Kolbowski J (2012) Assessment of wavelength-dependent parameters of photosynthetic electron transport with a new type of multi-color PAM chlorophyll fluorometer. *Photosynth Res* 113:127–44. doi: 10.1007/s11120-012-9758-1
- Siaut M, Cuiñé S, Cagnon C, et al (2011) Oil accumulation in the model green alga *Chlamydomonas reinhardtii*: characterization, variability between common laboratory strains and relationship with starch reserves. *BMC Biotechnol* 11:7. doi: 10.1186/1472-6750-11-7
- Simionato D, Block M a, La Rocca N, et al (2013) The response of *Nannochloropsis gaditana* to nitrogen starvation includes de novo biosynthesis of triacylglycerols, a decrease of chloroplast galactolipids, and reorganization of the photosynthetic apparatus. *Eukaryot Cell* 12:665–76. doi: 10.1128/EC.00363-12
- Solovchenko a. E, Khozin-Goldberg I, Didi-Cohen S, et al (2007) Effects of light intensity and nitrogen starvation on growth, total fatty acids and arachidonic acid in the green microalga *Parietochloris incisa*. *J Appl Phycol* 20:245–251. doi: 10.1007/s10811-007-9233-0
- Solovchenko A, Solovchenko O, Khozin-Goldberg I, et al (2013) Probing the effects of high-light stress on pigment and lipid metabolism in nitrogen-starving microalgae by measuring chlorophyll fluorescence transients: Studies with a $\Delta 5$ desaturase mutant of *Parietochloris incisa* (Chlorophyta, Trebouxiophyceae). *Algal Res* 2:175–182. doi: 10.1016/j.algal.2013.01.010
- Sousa C, de Winter L, Janssen M, et al (2012) Growth of the microalgae *Neochloris oleoabundans* at high partial oxygen pressures and sub-saturating light intensity. *Bioresour Technol* 104:565–70. doi: 10.1016/j.biortech.2011.10.048

References

- Spolaore P, Joannis-Cassan C, Duran E, Isambert A (2006) Commercial applications of microalgae. *J Biosci Bioeng* 101:87–96. doi: 10.1263/jbb.101.87
- Stephenson PG, Moore CM, Terry MJ, et al (2011) Improving photosynthesis for algal biofuels: toward a green revolution. *Trends Biotechnol* 29:615–23. doi: 10.1016/j.tibtech.2011.06.005
- Su CH, Chien LJ, Gomes J, et al (2010) Factors affecting lipid accumulation by *Nannochloropsis oculata* in a two-stage cultivation process. *J Appl Phycol* 23:903–908. doi: 10.1007/s10811-010-9609-4
- Sukenik A, Bennett J, Falkowski P (1987) Light-saturated photosynthesis — Limitation by electron transport or carbon fixation? *Biochim Biophys Acta - Bioenerg* 891:205–215. doi: 10.1016/0005-2728(87)90216-7
- Takache H, Pruvost J, Marec H (2015) Investigation of light/dark cycles effects on the photosynthetic growth of *Chlamydomonas reinhardtii* in conditions representative of photobioreactor cultivation. *Algal Res* 8:192–204. doi: 10.1016/j.algal.2015.02.009
- Taleb A, Pruvost J, Legrand J, et al (2015) Development and validation of a screening procedure of microalgae for biodiesel production: application to the genus of marine microalgae *Nannochloropsis*. *Bioresour Technol* 177:224–32. doi: 10.1016/j.biortech.2014.11.068
- Terigar BG, Theegala CS (2014) Investigating the interdependence between cell density, biomass productivity, and lipid productivity to maximize biofuel feedstock production from outdoor microalgal cultures. *Renew Energy* 64:238–243. doi: 10.1016/j.renene.2013.11.010
- Torzillo G, Sacchi a., Materassi R, Richmond a. (1991) Effect of temperature on yield and night biomass loss in *Spirulina platensis* grown outdoors in tubular photobioreactors. *J Appl Phycol* 3:103–109. doi: 10.1007/BF00003691
- Tredici MR (2010) Photobiology of microalgae mass cultures: understanding the tools for the next green revolution. *Biofuels* 1:143–162. doi: 10.4155/bfs.09.10
- Tredici MR, Biondi N, Ponis E, Rodolfi L (2009) Advances in microalgal culture for aquaculture feed and other uses. In: Burnell G. AG (ed) *New technologies in aquaculture. Improving production efficiency, quality and environmental management*. Woodhead publishing limited, pp 661–676
- Trentacoste EM, Shrestha RP, Smith SR, et al (2013) Metabolic engineering of lipid catabolism increases microalgal lipid accumulation without compromising growth. *Proc Natl Acad Sci U S A* 110:19748–53. doi: 10.1073/pnas.1309299110
- Turpin DH (1991) Effects of inorganic N availability on algal photosynthesis and carbon metabolism. *J Phycol* 27:14 – 20. doi: 10.1111/j.0022-3646.1991.00014.x
- Van Vooren G, Le Grand F, Legrand J, et al (2012) Investigation of fatty acids accumulation in *Nannochloropsis oculata* for biodiesel application. *Bioresour Technol* 124:421–32. doi: 10.1016/j.biortech.2012.08.009
- Vanthoor-Koopmans M, Wijffels RH, Barbosa MJ, Eppink MHM (2013) Biorefinery of microalgae for food and fuel. *Bioresour Technol* 135:142–9. doi: 10.1016/j.biortech.2012.10.135
- Vejrazka C, Janssen M, Benvenuti G, et al (2013) Photosynthetic efficiency and oxygen evolution of *Chlamydomonas reinhardtii* under continuous and flashing light. *Appl Microbiol Biotechnol* 97:1523–1532. doi: 10.1007/s00253-012-4390-8
- Vejrazka C, Janssen M, Streefland M, Wijffels RH (2011) Photosynthetic efficiency of *Chlamydomonas reinhardtii* in flashing light. *Biotechnol Bioeng* 108:2905–13. doi: 10.1002/bit.23270
- Wang G, Wang T (2012) Characterization of lipid components in two microalgae for biofuel application. *JAOCS, J Am Oil Chem Soc* 89:135–143. doi: 10.1007/s11746-011-1879-8
- Wen X, Geng Y, Li Y (2014) Enhanced lipid production in *Chlorella pyrenoidosa* by continuous culture. *Bioresour Technol* 161:297–303. doi: 10.1016/j.biortech.2014.03.077
- White S, Anandraj A, Bux F (2011) PAM fluorometry as a tool to assess microalgal nutrient stress and monitor cellular neutral lipids. *Bioresour Technol* 102:1675–82. doi: 10.1016/j.biortech.2010.09.097
- Wijffels RH, Barbosa MJ (2010) An Outlook on Microalgal Biofuels. *Sci* 329 :796–799. doi: 10.1126/science.1189003

- Wijffels RH, Barbosa MJ, Eppink MH (2010) Microalgae for the production of bulk chemicals and biofuels. *Biofuels Bioprod Biorefining* 4:287–295. doi: 10.1002/bbb
- Young EB, Beardall J (2003) Photosynthetic function in *Dunaliella tertiolecta* (Chlorophyta) during a nitrogen starvation and recovery cycle. *J Phycol* 905:897–905. doi: 10.1046/j.1529-8817.2003.03042.x
- Yu S, Zhao Q, Miao X, Shi J (2013) Enhancement of lipid production in low-starch mutants *Chlamydomonas reinhardtii* by adaptive laboratory evolution. *Bioresour Technol* 147:499–507. doi: 10.1016/j.biortech.2013.08.069
- Zemke PE, Sommerfeld MR, Hu Q (2013) Assessment of key biological and engineering design parameters for production of *Chlorella zofingiensis* (Chlorophyceae) in outdoor photobioreactors. *Appl Microbiol Biotechnol* 97:5645–55. doi: 10.1007/s00253-013-4919-5
- Zemke PE, Wood BD, Dye DJ (2010) Considerations for the maximum production rates of triacylglycerol from microalgae. *Biomass and Bioenergy* 34:145–151. doi: 10.1016/j.biombioe.2009.10.012
- Zijffers J-WF, Schippers KJ, Zheng K, et al (2010) Maximum photosynthetic yield of green microalgae in photobioreactors. *Mar Biotechnol (NY)* 12:708–18. doi: 10.1007/s10126-010-9258-2
- Zittelli GC, Biondi N, Rodolfi L, Tredici MR (2013) *Photobioreactors for Mass Production of Microalgae*. John Wiley & Sons, Ltd, Oxford, UK

Summary

Microalgae have drawn the attention of many industries due to the large variety of commercially relevant products (e.g. pigments, lipids, sugars and proteins) that can be sustainably obtained from microalgae.

The work presented in this thesis focused on the production of triglycerides (TAGs). Microalgal TAGs are promising sources for supplementing or replacing the traditional feedstocks (fossil and vegetable oils) of the food, chemical and biofuel industries. Being cultivated in confined systems such as ponds or closed reactor, microalgae do not require arable lands. Furthermore, they can grow on seawater and higher areal TAG productivities can be achieved with microalgae compared to terrestrial crops (e.g. palm and soy). Nevertheless, microalgal TAGs are not yet economically feasible due to the high production costs. To reduce these costs, TAG productivity needs to be maximized.

The aim of this thesis was to increase microalgal TAG productivity by investigating the effect of biological and engineering parameters (i.e. production strain and operational strategy).

The most common technique to induce TAG accumulation in microalgae is to expose them to nitrogen (N) starvation. As a result of N-starvation, the photosynthetic capacity of the cells is reduced, thus determining a decrease of TAG productivity over time. However, differences between microalgal species in their response to N-starvation are expected.

Chapter 2 aimed at selecting a marine species with high TAG productivity. For this, seven marine species (*Neochloris oleoabundans*, *Chlorococcum littorale*, *Chlorella vulgaris*, *Nannochloropsis oculata*, *Tetraselmis suecica*, *Stichococcus bacillaris* and *Nannochloropsis* sp.) were screened under N-starvation and photosystem II maximum efficiency was followed during the experiment, as proxy for the change in photosynthetic activity of the cells. For some species, such as *Neochloris oleoabundans*, photosynthetic activity dropped almost immediately after N-depletion, whereas other species were able to maintain their photosynthetic activity for longer periods, while accumulating TAGs. *Nannochloropsis* sp. was identified as the most suitable species for lipid production as it retained the highest photosynthetic activity during N-starvation and achieved the highest lipid productivity. *Nannochloropsis* sp. was therefore used in all following studies.

The biomass concentration in the reactor at the onset of N-starvation together with the total irradiance received by the culture (i.e. initial-biomass-specific light availability) is expected to have a large impact on TAG productivity. **Chapter 3** aimed at optimizing TAG productivity in outdoor batch pilot cultivations of *Nannochloropsis* sp. by

investigating the effect of initial-biomass-specific light availability on TAG production in horizontal and vertically stacked tubular reactors, which were simultaneously operated under high and low light conditions. It was found that TAG content increased with increasing initial-biomass-specific light availability, whereas an optimum for TAG productivity was determined for each reactor configuration and light condition. Based on the observed trends of TAG productivity for the Dutch climate conditions, it was concluded that for highest TAG productivities, the vertical reactor should be always operated at an initial biomass concentration of 1.5 g L^{-1} , whereas the horizontal reactor should be operated at 2.5 g L^{-1} and 1.5 g L^{-1} under high and low light conditions, respectively.

The research performed in **chapter 4** aimed at assessing repeated-batch processes (i.e. culture is partly harvested at fixed intervals and the remaining fraction is resupplied with nutrients) to further increase TAG productivity compared to batch processes. Repeated-batch cultivations were tested and compared to batch cultivations both at lab-scale under day/night cycles and in two identical, simultaneously operated, outdoor vertically stacked tubular PBRs over different seasons. Although at lab-scale, batch and repeated-batch cultivations led to similar TAG productivities, outdoor repeated-batch processes were always outcompeted by the batch. It was concluded that repeated-batch processes require further optimization. For this, the dependency of physiological responses on operational strategies and settings should be fully investigated to design an optimal repeated-batch process and perform a fair process comparison.

The dependency of physiological responses on operational strategies and settings was studied in **chapter 5** for lab-scale batch and repeated-batch cultivations subjected to continuous light. The obtained physiological insights were condensed into a mechanistic model that successfully described both production processes. The effect of several biological (maximum photosynthetic rate under nitrogen replete conditions, residual biomass fraction during N-starvation) and process parameters (incident light intensity, N-resupply, cycle duration and harvest volume) was investigated on TAG yield on light. With model simulations, scenarios for optimized TAG yield on light were identified enabling processes comparison. It was concluded that, under continuous light, an optimized batch process would always result in higher TAG yields on light compared to an optimized repeated-batch process. This is mainly because, differently from the batch, repeated-batch cycles start with N-starved cells. Their reduced photosynthetic capacity leads to an inefficient use of light during the regrowth phase, thus resulting in lower TAG yields. Nonetheless, it should be underlined that the physiological responses to N-resupply in repeated-batch cultures might differ for cells that are subjected to day/night cycles.

In **chapter 6** an outlook on the most relevant biology and process driven approaches for increasing TAG productivity is presented. Additionally, a techno-economic analysis for a two-step-continuous TAG production process (i.e. growth reactors are operated in continuous mode such that multiple batch-operated stress reactors are inoculated and sequentially harvested) is performed for a hypothetical 100 ha-scale plant in southern Spain using vertically stacked tubular reactors. Photosynthetic efficiencies based on outdoor pilot data were used as model input. The production costs of TAG-enriched biomass based on both current technology and optimized scenarios were presented.

By optimizing both photosynthetic efficiency and process technology, the production cost could be decreased from 7.4 to 3.0 €·kg⁻¹. However, production costs should be further reduced. Concrete opportunities for cost reduction are offered by cheaper reactor designs (e.g. plastic film flat panels). Finally, we showed that, at the current commodity market values, the cost-effectiveness of microalgal TAGs highly relies on the valorization of the whole biomass.

Altogether, this thesis led to increased insights into the biological and process parameters that determine microalgal TAG productivity and provided a solid basis for assessing the economic potential of microalgae.

We are on the right track to achieve an economically feasible microalgal TAG production.

Acknowledgments

René thank you very much for your guidance. I learned a lot from you. You helped me thinking in a broader way. Your questions were always the most difficult and challenging ones. Sometimes we disagreed but you always gave me the opportunity to defend my point even though your point was actually better than mine!

Maria you are a mentor to me. You were able to pursue ambitious goals while being a mother and an exceptional woman. You do this always with a smile and your positive vibe is contagious. You helped me developing self-awareness, thank you for believing in me!

Rouke thank you for all the help and extraordinary support you gave me. You were always there for me, trying to advice me even when I was screaming or crying. You helped me in designing my experiments and give structure to my work. You gave very good tips for a more effective communication and I will always be grateful to you. You made AlgaePARC an amazing place to work!

Packo even though officially you were not my supervisor you acted as one. You completely changed my approach to scientific problems and you made me dig much more into depth. Your contribution to my work is immensurable. Thank you!

Guido thank you for all your help, without you the modeling work would not have been possible in such a short time. You were always available for me. You taught me a lot and I really enjoyed working with you.

Maria C and **Anne** you were my supervisors for only a short period but I really enjoyed working with you.

Jésus thanks for the help with the techno-economic analysis, you were able to explain the most difficult thing in a very simple way! Thank you and **Almu** for your friendship, you will always have a special place in my heart.

Jeroen, Iago, not only you have been amazing colleagues and great friends, you have become the brothers I never had. Every single minute next to you was special, no matter if it was during an important meeting or at the bar, it was always very intense and fun. The support we gave each other is something I will always carry with me.

Marcel we worked together only for my first paper. Nevertheless you always stimulated and advised me. Thank you!

Carsten in a way it is because of you that I started my PhD. You encouraged me in taking such decision, you taught me a lot during my MSc thesis. It is always nice every time I meet you and **Ana** again.

Acknowledgements

Ji Fang you brought a positive vibe into my project when I needed it the most. You worked hard and in an excellent way, I'll always be grateful to you.

Ana you were my last student, you helped me with finalizing my experimental work. You were very committed and you did a great job! Thank you!

Iliana thank you for the editing of my thesis and the beautiful cover!

Snezana (*mami*), you are the most positive and strongest person I've ever met, thank you for being the way you are!

Thank you **AlgaePARC family!** **Snezana, Pieter, Jesus, Mathijs, Iago, Jeroen, Fred, Rick, Ruud**, being with you almost every day during the last four years was great, it really felt like home.

I'd like to thank all my BPE colleagues and all the friends that throughout the last four years made my life in Wageningen very pleasant, in particular **Joao, Derk, Celine, Catalina, Pauline, Youri, Alex, Carl, Maria C, Angel, Lenny, Anne, Lucille, Michiel, Ellen, Marian, Hans, Giuseppe**.

Rafa, appena ci hanno presentati ho capito che non saresti stato solo un collega per me, sei diventato un amico. L'ultimo anno del PhD non sarebbe stato lo stesso senza di te.

Fabian, dopo quattro anni le nostre vite si sono incrociate di nuovo. Sei stato tu il mio Cicerone, mi hai spiegato come funzionano le cose a Wageningen, sei stato tu a farmi conoscere il Greco. Le serate pazze del kiriki e poi all'International Club le ho fatte con te. Ci siamo ritrovati in Olanda dopo quattro anni, siamo un po' più adulti e magari più noiosi ma l'affetto che ci lega è sempre più forte.

Pavlos (*@nom@lizer*), o filos mou, we never needed many words to express the strong feelings we have for each other, we just know this. Good luck with your new life in Berlin, let's see if you will be able to export the *greekness* also there!

Hanna, my adventure in Wageningen started with you in Dijkgraaf 5C. You were there every time I took the most important decisions. You have always participated with joy and enthusiasm. Thank you!

The dinners in Wageningen have always been special when **Marta M, Natalie, Vasco** and **Fabian** were around.

Marta F sei stata all' AlgaePARC solo per sei mesi ma tra noi è stato amore a prima vista e in poco tempo sei diventata una grande amica.

Teresa, Edo, grazie per l'amicizia incondizionata che ci lega. Grazie per le pizzate (Cola per Edo) e le lunghe chiacchierate su religione, politica, cani, scienza, storia, cavolate, musica, chi più ne ha più ne metta. Siete diventati parte della mia famiglia.

Mario, 'mpare, come dire, sei un pilastro per me, anche quando siamo lontani e non ci sentiamo per un po', niente cambia, basta un secondo al telefono o uno sguardo per capirci, per tornare alle notti passate a casa tua a Firenze a parlare di tutto e un po', o ai momenti di pazzia che ci prendevano ai tempi di statistica. Ti voglio bene ciabbbbbbatta!

David sei nel mio cuore e nella mia anima. Quante ne abbiamo passate insieme, dalle nottate pazze alle chiacchiere seduti sul balcone con prosecco, sigarette e vestaglia di ciniglia. A volte mi dico che è valsa la pena venire a Wageningen solo per incontrare te. Sei unico amico mio.

Thank you **Wageningen**, you are a magic place, you made me discover parts of me I did not know.

Marghe, Laura, Elena, Baldu, Bandi, Pippo, Dani, Giulia C, Giulia M voi ci siete sempre stati e sempre ci sarete. Siamo cresciuti insieme, siamo cambiati, viviamo lontani ma vi sento sempre più vicini.

E poi il **cerchio magico: babbo, mamma, Kikki, Tiski**, insieme siamo una cosa sola. **Kikki** sei il mio punto fermo, la mia piccola grande sorella, la donna che mi sarà sempre accanto. **Mamma, Babbo** grazie per avermi sempre incoraggiato, essermi vicini, capirmi anche senza bisogno di parole, grazie per la fiducia e la libertà che mi avete sempre dato.

Beta, my baby, you are my *cure-all panacea*! I love you so much, so much!

Finally you **Christaki**. You are the oxygen I breathe, my essence. You know the best and the worst of me and, despite all, you have always stood by me. Your love and our dreams kept me going. "Από τό μόνο θέλημα τής αγάπης, μ'ακούς Ανεβάσαμε ολόκληρο νησί" Grazie amore mio.

About the author



Giulia Benvenuti was born in Florence, Italy, on the 4th of March, 1985.

After high school she started in 2005 her biotechnology studies at Florence University. She graduated from her BSc in 2008 on the topic of wastewater treatment by microalgae, which was carried out at the AgroFood and Environmental Sciences Department. Thereafter she worked for one year on the same topic as a researcher. In 2009 she continued with her MSc studies on industrial and environmental biotechnology. In 2011, she carried out her MSc thesis at the Bioprocess Engineering Group of Wageningen University on the effect of flashing light on microalgal photosynthesis. In October 2011, she started her PhD research at the Bioprocess Engineering Group within the AlgaePARC research program working on triglyceride production by microalgae. The results of her PhD research are described in this thesis.

List of publications

Vejrazka C, Janssen M, **Benvenuti G**, Streefland M, Wijffels RH: Photosynthetic efficiency and oxygen evolution of *Chlamydomonas reinhardtii* under continuous and flashing light. *Appl Microbiol Biotechnol* 2013, 97:1523–1532.

Benvenuti G, Bosma R, Cuaresma M: Selecting microalgae with high lipid productivity and photosynthetic activity under nitrogen starvation. *Journal of Applied Phycology* 2014, 27:1425 – 1431.

Benvenuti G, Bosma R, Klok AJ, Ji F, Lamers PP, Barbosa MJ, Wijffels RH: Microalgal triacylglycerides production in outdoor batch-operated tubular PBRs. *Biotechnology for Biofuels* 2015, 8:100.

Giatsis C, Sipkema D, Smidt H, Heilig H, **Benvenuti G**, Verreth J, Verdegem M: The impact of rearing environment on the development of gut microbiota in tilapia larvae. *Scientific Reports* 2015, 5:18206.

Benvenuti G, Lamers PP, Breuer G, Cerar A, Wijffels RH, Barbosa MJ: Microalgal TAG production strategies: why batch beats repeated-batch. Accepted for publication in *Biotechnology for Biofuels*.

Benvenuti G, Bosma R, Ji F, Lamers PP, Barbosa MJ, Wijffels RH: Batch and repeated-batch microalgal TAG production in lab-scale and outdoor photobioreactors. Submitted for publication.

Benvenuti G, Ruiz J, Lamers PP, Bosma R, Wijffels RH, Barbosa MJ: Towards microalgal triglycerides in the commodity markets. Submitted for publication.

Overview of completed training activities



Discipline specific activities

Courses

Advance course bioprocess design (Wageningen, 2014)

Microalgae process design (Wageningen, 2013)

Advanced Course on Microbial Physiology and Fermentation Technology (Delft, 2012)

Symposia

European Algae Biomass Association conference (Lisbon, Portugal, 2015) ¹

5th Congress of the International Society for Applied Phycology (Sidney, Australia, 2014) ²

European Maritime day (Bremen, Germany, 2014) ²

2nd International Young Algaeneers Symposium (Narbonne – Montpellier, France, 2014) ²

1st International Young Algaeneers Symposium (Wageningen, 2012) ¹

General courses

Matlab fundamental (Eindhoven, 2015)

Effective behavior in your professional surroundings (Wageningen, 2014)

Career perspectives (Wageningen, 2014)

Masterclass Biobased Innovation (Wageningen, 2013)

Presentation skills (Wageningen, 2013)

Teaching and supervising thesis student (Wageningen, 2012)

Techniques for writing and presenting a scientific paper (Wageningen, 2012)

Basic statistics (Wageningen, 2012)

Optional

Biosolar cells annual meetings (2012 – 2015)

Bioprocess engineering Brainstorm days (2012 - 2015) ²

Bioprocess engineering PhD excursion Spain (2012) ²

Bioprocess engineering PhD excursion Portugal (2014) ^{1,3}

¹ Poster

² Oral

³ Organization

This study was carried out at the Bioprocess Engineering Group of Wageningen University, Wageningen, the Netherlands. The research described in this thesis was financially supported by the Ministry of Economic Affairs, Agriculture and Innovation and Province of Gelderland, Biosolar Cells, BASF, BioOils, Drie Wilgen Development, DSM, Exxon Mobil, GEA Westfalia Separator, Heliae, Neste, Nijhuis, Paques, Cellulac, Proviron, Roquette, SABIC, Simris Alg, Staatsolie Suriname, Synthetic Genomics, TOTAL and Unilever.

Cover & Layout design: AgileColor Design Studio/Atelier || AgileColor.com
Printed by: GVO drukkers & vormgevers, Ede (NL) || gvo.nl